Aalto University

Pressure management in compartment fires

Final report (Final draft before spell check 28.11.2016)

Simo Hostikka, Rahul Kallada Janardhan

Aalto University

Preface

This project was established to answer the research questions arising from two sources: The fire service had observed a previously unknown situation of fire-induced pressure preventing them from entering a burning apartment. At the same time, the ventilation designers from Stravent Oy had realized that the current norms and practices of ventilation design do not adequately support the pressure management.

The project was started as a collaborative effort of Aalto University, VTT Oy, Stravent Oy, South-West Finland Emergency Services, and Palotekninen Insinööritoimisto Markku Kauriala Oy. The Finnish name of the project was “Paineenhallinta huoneistopaloissa (PAHAHUPA)".

We would like to thank the following people for their contributions, help and support:

Experimental team: Pasi Paloluoma and Knut Lehtinen (South-West Finland Emergency Services), Peter Biström (Stravent Oy), Tomas Fagergren (Brandskyddslaget), Jere Heikkinen and Ville Heikura (VTT Expert Services Ltd).

VTT simulation team: Topi Sikanen, Tuomo Ojanen and Timo Korhonen.

Kauriala simulation team: Jukka Hietaniemi and Gleb Bytskov.

Prison case study experts: Teppo Malm (Senaatti) and Kauko Niemelä (RISE).

Aalto team: Umar Riaz and Mehdi Taebnia.

The project was financially supported by the Finnish Fire Protection Fund (PSR), Ministry of Environment, Hagab AB, and the Criminal Sac-

tions Agency of Finland (RISE). The project was lead by a steering group, whose members were Jarkko Häyrinen (Ministry of Interior, chairman), Jorma Jantunen (Ministry of Environment), Börje Axelsson (Hagab AB), Ari Pakarinen (RISE), Kimmo Vähäkoski (Emergency Service College), Pasi Paloluoma (South-West Finland Emergency Services), Timo Karkulahti (Stravent Oy), Jukka Hietaniemi (Palotekninen Insinööritoimisto Markku Kauriala Oy), Liisa Poussa (VTT Oy, replaced by Eila Lehmus in fall 2016), and Simo Hostikka (Aalto University). The support and guidance from the steering group members is greatly appreciated.

Espoo, November 28, 2016,

Simo Hostikka and Rahul Kallada Janardhan

Contents

1. Introduction

1.1 Background

In early 2014, a group of professional fire fighters from the Southwest Finland Emergency Services, city of Turku, was rehearsing a situation where they ignited a fire inside an apartment of an abandoned building, closed the door and tried to attack the fire after a moment to suppress it. To their surprise, two firemen could not open the inner door of the apartment (many Finnish apartments have double doors to the corridor) due to the high pressure inside the apartment. This led to the questions: What if there was an occupant trying to escape the burning apartment? Can the pressure be high enough to prevent escape?

Thermal expansion of gas during a fire will result in increased pressure if the fire takes place in a relatively closed compartment [1]. The phenomenon has received only little attention in the history of fire science because most studies have been performed in enclosures with large opening to ambient. This has been well-justified from the viewpoint of structural safety, as only a long-lasting fire can cause high temperatures that pose a risk to the fire resistance. Also, the need to ensure the availability of air has affected the experimental design of fire dynamics research. The smoke management calculation typically assume that pressure differences across the vents are dominated by the hydrostatic pressures, order of few tens of Pa at most.

Hägglund et al. [2, 3] have measured the pressures resulting from liquid pool fires in a compartment with only one, relatively small vent to ambient. They reported over- and under-pressure peaks as high as 1200

Pa and 1800 Pa respectively. By adding a mechanical ventilation to the same configuration, the over-pressures were changed to 900 Pa and under-pressures to -1200 Pa. They observed that even the mechanically driven ventilation flows were reverted according to the direction of the pressure. Unfortunately, neither the heat release nor the mass loss rate of the fire were measured, thus limiting the possibility of quantitative analyses, such as a code validation. More recently, the experiments within the OECD PRISME programme have produced detailed information about the development of compartment pressure, ventilation flows and liquid pool fire dynamics in a very air-tight compartment [4]. As high as 3000 Pa over-pressures were observed with fires of about 1 MW [5]. The results from the PRISME project cannot be directly transferred to the residential conditions due to the highly specialized construction, but they have already been used to validate the pressure and ventilation flow simulations of the Fire Dynamics Simulator [6] (FDS) software by Wahlqvist and van Hees [7]. Fourneau et al. [8] used zone modelling to investigate the fire safety differences between traditional and modern air-tight buildings (Passivhaus). They observed a significant difference in pressure rise (10 Pa vs. 450 Pa) and concluded that the high pressure can lead to a reverse flow in the supply ventilation system and possible pollution of other living areas. They did not recognize the pressure rise as a risk for the escape as such.

1.2 Objectives

The main objectives of the current study were to quantify the pressures in fires taking place in closed residential compartments, to evaluate the potential risks for life and property, to validate the FDS for the simulation of such fires, and to evaluate the significance of different ventilation arrangements and building envelope air-tightness levels on the occupant safety in two case studies. The case studies were a modern apartment building with centralized mechanical ventilation and very air-tight envelope, and a prison cell representing a institutional scenario, where the fire compartment is very small, but coupled to other similar compartments through a ventilation system. Finally, we wish to investigate the poten-

tial means for pressure management.

1.3 Methods

To meet the objectives a series of fire experiments were performed in a typical Finnish apartment, measuring the gas temperatures, pressures and gas species concentrations, as well as ventilation flows. The experimental research is summarized in Chapter **??**. More details can be found from Appendix A, and from the MSc thesis of Janardhan [18].

In the simulation part, we first developed the procedures for modelling the building ventilation and envelope leakages using the available information. The simulations were validated using the experimental results of Hägglund et al. [2, 3] and our own experiments, as summarized in Chapter 4. More details are available in Appendix A.

The validated simulation model was used for two case studies. The first case study (Chapter 5 and Appendix B) investigated the role of ventilation arrangement on the smoke spreading and tenability conditions in a prison. The second case study (Chapter 6 and Appendix C) focussed on the modern apartment buildings. The conclusions from research are summarized in Chapter 8 and the needs for further research in Chapter 9.

2. Pressure-induced casualties in Finnish fire statistics

Chapter author: Pasi Paloluoma, South-West Finland Emergency Services

One hypothesis the project was that the high overpressure during the fire growth can prevent an apartment occupant from opening the inwards opening door and escaping from a burning apartment. By examining the fire statistics we wanted to investigate if this hypothesis is supported by the observations in real incidents.

The source of fire incident data was the assignment register of the rescue services (PRONTO)[1]. The search included years 2012-2014 and the first half of 2015 (3.5 years). During this period, the database included 3889 residential fires. Out of those, 1129 fires occurred in buildings assigned to class "Other residential multi-storey building", which contains most of the apartment buildings. Those fires had resulted in 70 fire deaths, 78 severe injuries and 263 non-severe injuries.

The reliability of the results is reduced by the fact that the location of the dead, injured or rescued persons was not stored in all fire incidents. Also, the information about the existence or type of the inwards-opening door was not available from most fire incidents.

Among the all residential fires, there 35 incidents (0.9 %) where a person had been found (dead, injured or rescued) from the region just inside the exit door. 25 of those were in the apartment buildings (2.2 %). These cases represent the fires where the over pressure may have been the cause of unsuccessful escape. The true fraction of potential cases is higher, though, due to the lack of data on the physical location of the person.

[1] https://prontonet.fi/, accessed September 14, 2015

3. Fire experiments

The experiments were conducted in a 1970's apartment building in the city of Kurikka, western Finland. The test apartment included a living room, bedroom, kitchen, bathroom, aisle and a closet (Figure 3.1), and was located in the first floor of the building. The apartment floor area was 58.6 m^2 with a ceiling height of 2.57 m. The apartment had the typical Finnish two door system with the inner door opening inwards and outer door opening towards the staircase. The apartment had three ventilation exhaust vents, one in the bathroom, one in the closet, and one in the kitchen hood. The kitchen hood was closed during the experiments. The bathroom and closet vents were connected to 120 mm diameter ducts leading to the roof of the building. There was a small replacement air vent in the living room to provide make-up air for the ventilation, but this valve was closed tightly during the experiments. Before the fire experiments, the air-tightness of the apartment boundaries was measured using a Blower door test [12]. The determined air permeability q_{50} was 1.7 $m^3h^{-1}m^{-2}$ at underpressure and 2.7 $m^3h^{-1}m^{-2}$ at overpressure.

Thirteen experiments were performed with three different configurations of the two exhaust ducts: *Open* (Tests 1-4), *Normal* (Tests 5-7, 11-13), and *Closed* (Tests 8-10). Photographs of the duct configurations are shown in Fig. 3.2. The experiments were conducted in two phases based on the type of fuel: In the first phase (tests 1-10), 3.0 L of n-Heptane was burned in a 0.7 m x 0.7 m steel pan with a free height of 21 cm. In the second phase, polyurethane foam (PUF) mattress were used. Test 12 was performed in the closet of the apartment, and it was the last test of the campaign. A detailed explanation of the experiments can be found in [18].

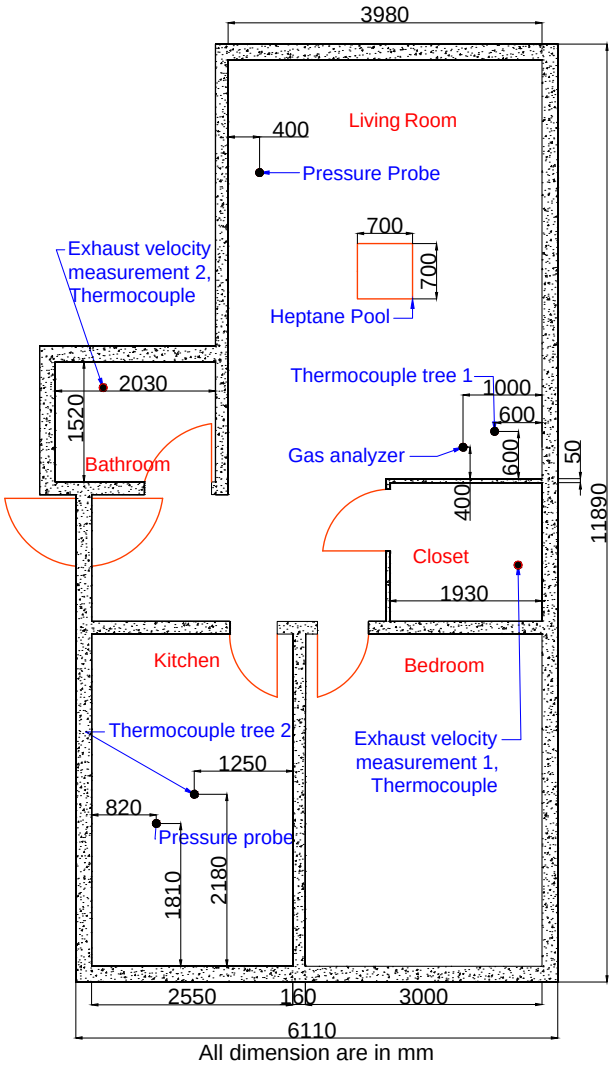

Figure 3.1. Plan drawing of the apartment.

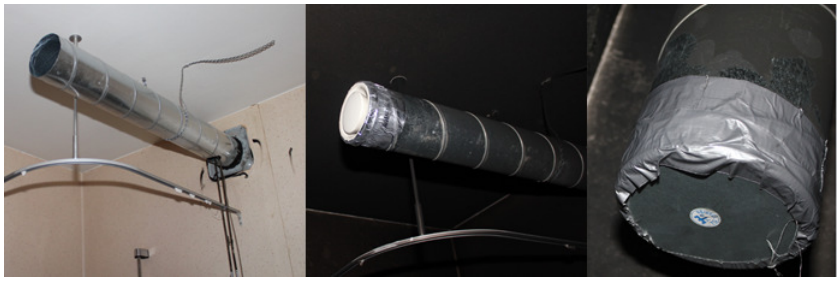

Figure 3.2. Apartment ventilation configuration.

Temperature, pressure, gas concentrations and mass loss rate were measured during the experiments. The peak temperatures under the ceiling were about 300 °C and average peak temperatures of the gas space about 150 °C. The fires were suppressed due to the fuel burnout in about 180 s (heptane) and 100 s (PUF). The recorded pressures in the liquid and solid fuel tests are shown in Fig. 3.3. Fires in relatively closed compartments

were found to produce high over and under pressures. The recorded overpressures were between 300 Pa and 1650 Pa, and they occured in less than 50 s from the ignition. The two experimental parameters, ventilation system configuration and fuel type, were both found to have a significant influence on the pressure magnitude: The peak overpressures of the heptane fires increased from 300 Pa to 600 Pa when the open ducts were equipped with the normal valves, and further to 900 Pa when the ventilation ducts were completely sealed. The heat release rate (HRR) of the PUF fires must have increased faster than the heptane fires' HRR, and therefore the peak overpressures in PUF fires, carried on in normal ventilation conditions, were as high as 1650 Pa.

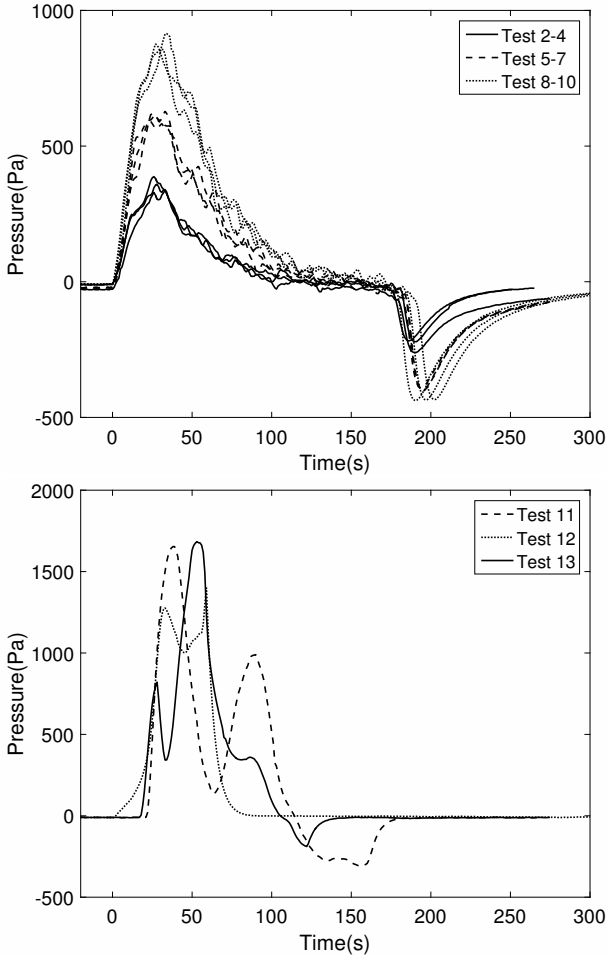

Figure 3.3. Gas pressure in heptane pool fires (top) and PU foam fires (bottom).

The main observations from the experiments were

1. During the overpressure peak, a fireman could not open the inner door

from inside the apartment. Escaping from the apartment in such conditions would not be possible without help from outside.

2. The light-weight wall between the living room and the balcony failed during the PUF fire with a result that the window frame was violently pushed out of the wall (Fig. 3.4). The structural damage was creaged in a pressure range 1400...1650 Pa, being consistent with the 1500 Pa maximum pressure requirement in Sweden.

Figure 3.4. Structural failure of external wall and window frame.

4. FDS modelling

4.1 Modelling the ventilation and leakages

Numerical modelling of leakage and ventilation were the two critical aspects of modelling a compartment fire scenario. These parasmeters affect the pressure rise and gas temperatures in the compartment.

FDS provides two different methods for the leakage modelling: The *Bulk Leakage* -method assigns the leakages onto large segments of the compartment boundaries. For example, in the Kurikka fire simulations, the wall with the window was assigned as the leakage path. The *Localized Leakage* -method assigns the leakages to smaller locations of the boundary, and is suitable if the exact location of the leakages can be identified. In both methods, the leakage flow is calculated by the HVAC solver. For the FOA simulations, a modified form of localized leakage method was applied as a hole connected to a duct needed to be modelled.

The leakage of an envelope is determined using the equation 4.1.

$$\dot{V}_{|\Delta p|} = C_d A_{\text{leak}} \left(\frac{2|\Delta p|}{\rho} \right)^{0.5} \tag{4.1}$$

where $\dot{V}$ is the leakage flow rate at 50 Pa obtained from the leakage tests, C_d is the discharge coefficient, A_{leak} is the leakage area, ρ is the density, and Δp is the pressure difference at which the leakage rate was measured. Assuming C_d = 0.6, ρ = 1.3 kg/m^3 and Δp = 50 Pa, for which $\dot{V} = 0.12$ m^3/s, gives A_{leak} = 0.023 m^2.

HVAC modelling was the next significant aspect in the simulation process. HVAC system was modelled as a combination of ducts, nodes and other components of the HVAC models used in the simulations are nodes,

ducts, and a fan. The other components such as dampers and expansion/contraction fittings are accounted for in the loss terms. Modifications such as combining multiple ducts into a single duct with appropriate loss coefficients were made to simplify the process.

The loss coefficient of the ducts ideally could be estimated by adding up the individual component losses along with the duct friction loss. But complete information regarding the duct layouts was not available for neither FOA experiments nor the Kurikka experiments. Therefore, the loss coefficients used in the simulation were obtained by assigning a duct roughness of 1mm to all ducts and then by adjusting the losses to obtain the known volume flow rates through the ducts. Identical values are used for forward and reverse flow loss coefficients. A detailed explanation reagrding the HVAC and leakage modelling can be found in [19] and [18].

4.2 Model validation

The FDS validation studies are performed using three sets of experiments. The first two sets of validation cases are from the FOA studies conducted by the Swedish-FOA Defence Research Establishment [2, 3]. The third set is from the fire experiments by Aalto University described in Chapter 3.

The simulations were carried out using the FDS version 6.3.2 [15] on a personal computer with a 3.4 GHz Xeon processor and 32 GB ram. The CPU time for a single simulation of 300 s was approximately 8 hours.

The simulation models are based on the apartment layouts shown in figures 3.1 and 4.1. The spatial discretization was made with 0.10 m resolution grid, and the results were not found to be sensitive to the grid resolution. The heat release rate and the fuel pan for the FOA tests are modelled based on the information provided in the [2, 3]. For the KUrikka simulations, fuel pan was modelled as a 0.7 m x 0.7 m burner with a specified mass loss rate (MLR) according to the measurements. The combustion reaction was that of n-Heptane, with soot and CO yields of 3.7 % and 1 %, respectively in all the validation studies except for solid fuel test in Kurikka experiments. The solid fuel heat release rate was inverse modelled based on the recorded flame temperatures [18].

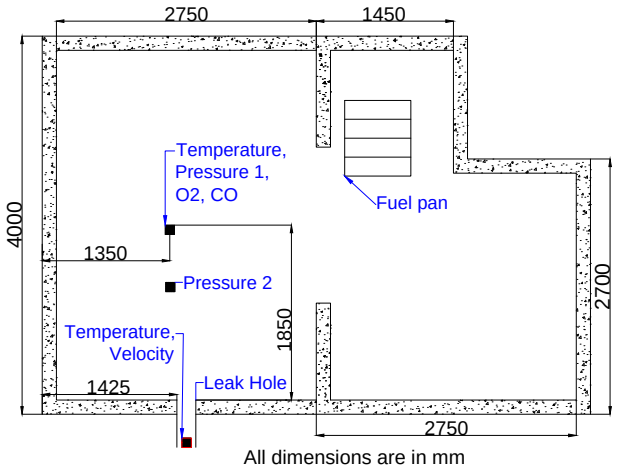

Figure 4.1. Plan drawing of the FOA experiments.

The scatter plots of pressure and temperature for the three sets of validations cases [2, 3, 18] are shown in the Figure 4.2. The first plot shows that the peak drop of oxygen concentrations are underpredicted by 11 % in average, and the model standard deviation is equivalent to the experimental random error. The underprediction (i.e too low consumption of oxygen in combustion) is observed mainly in the FOA test series.

The middle figure summarizes the gas temperature predictions, indicating 11 % overprediction in average and 12 % model standard deviation. These results are similar to the FDS validation results in [16].

The third part of Figure 4.2 summarizes the peak overpressures. FDS is found to underpredict the pressures by 13 % in average, with 19 % model standard deviation.

The validation studies show that FDS can be reliably used for modelling compartment fire scenarios and estimating pressure rise in compartments. The reported uncertainty metrics can be used to make corrections to the model predictions.

The validation simulations are also reported in Appendix C. However, in the manuscript submitted to IAFSS 2017 symposium, the simulations were carried out using bulk leakage method. Figure 4.2 includes results for localized leakage, which was found to be more relevant to the apartment case study.

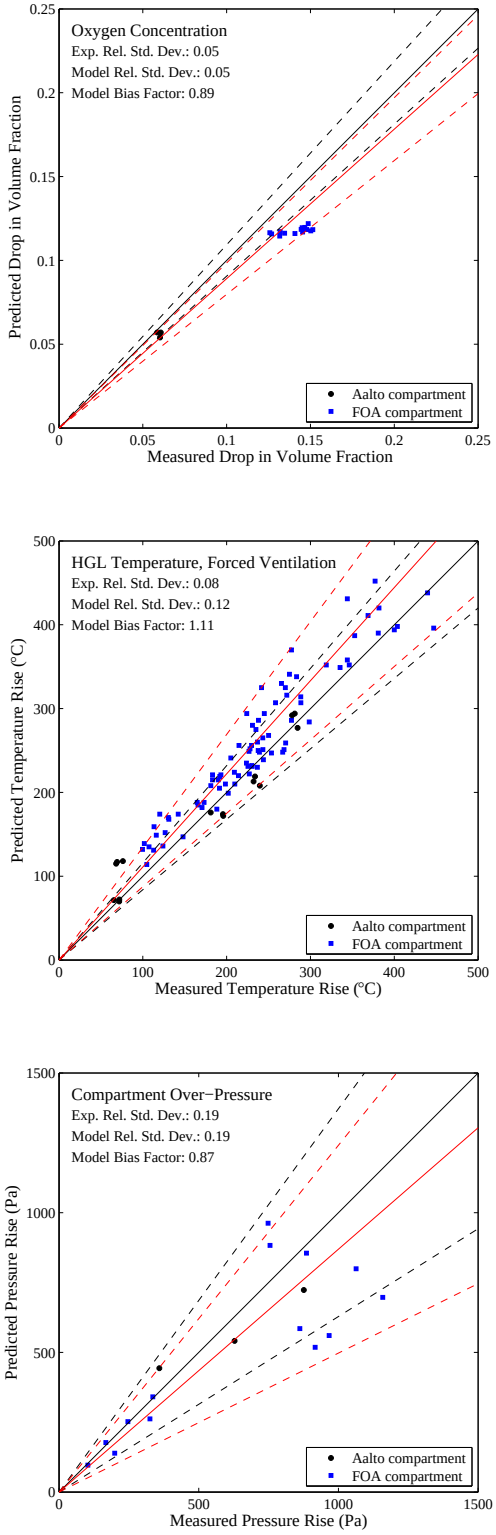

Figure 4.2. FDS Validation Summary plots for oxygen concentration, temperature and overpressure.

5. Case study: Prison cell fire

Gleb Bytskov and Jukka Hietaniemi
Palotekninen insinööritoimisto Markku Kauriala Oy

This case study was conducted to evaluate the effects of the fire-induced pressure on the safety of the occupants of prison cells. This case was of special interest as the occupants of an enclosure in a prison cannot evacuate by their own. Therefore, the fire safety design of such a building should

- provide sufficient time for the staff members to evacuate the occupants of the cell of fire origin,
- provide sufficuent time for staff to evacuate the inmates of other cells before smoke spread is unmanageable,
- enable the staff to safely attack the fire, and
- prevent or limite the spread of smoke and fire.

A detailed spesification and the results of the case study are shown in Appendix B. The prison cell was made of concrete and its dimension were a 5.8m (length) x 2.2m (breadth) x 3m (height). The cells are equipped with mechanical ventilation exhaust and supply providing an air circulation rate of 40 l/s for each cell.

A layout with three cells was adopted for the analysis as shown in Figure 5.1, with the fire cell at the bottom and one cell on top and one cell adjacent to the fire room. The air-permeability q_{50} of the cell structures was assumed to be 1.5 $\mathrm{m^3 m^{-2} h^{-1}}$. The ventilation ducts from the three cells connect the main exhaust duct at the same point. The main duct

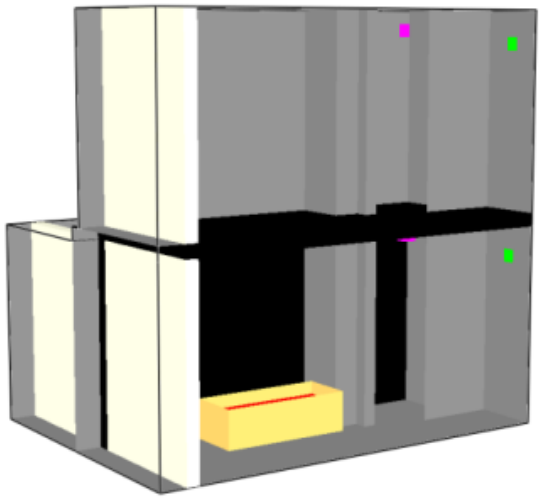

Figure 5.1. Simulation model of prison cells

is equipped with an exhaust/supply fan which has a maximum flow of 130 l/s and a maximum pressure of 400 Pa. Fire dampers are placed in the inlet ducts and their activation was concidered to be either smoke or temperature -based.

Based on the numerical fire simulations of the prison cell fires, the following conclusions were made.

With a realistic fire development, the peak over pressure inside the fire cell will be close to 4000 Pa if both dampers of the fire cell are closed. This means that a mechanical failure of some structure can be expected. If one of the dampers is left open, the fire cell pressures remain below 1000 Pa, and there is no risk of structural damage. With ultra-fast fire development, the observed peak pressures are 3.5 kPa even in the case of open damper, and damages are possible. Since the uncontrolled damages may lead to increased smoke spreading to neighbouring spaces, the full closing of the fire cell should be avoided.

The high overpressures (several hundreds of Pa or more) in the fire cell were found to last for 3 minutes of less. During this period, opening the cell door will result in strong smoke flow to the corridor.

In the cell of fire origin, the life safety criteria are met within 80-130 s from the ignition, depending on the rate of fire growth. However, from the viewpoint of gas temperatures, safe rescue is possible for personnel without protective equipment only during the first 50-90 s from the ignition.

Smoke spreading through the ventilation network was studied by monitoring the toxic concentrations in the neighbouring cells. The main conclusion was that some smoke was observed in all ventilation configurations, except those where both supply and exhaust ducts of the fire cell were closed by a damper. However, the toxic gas concentrations in the neighbouring cells remained at safe level when fire cell's exhaust duct was kept open (the safe situation for pressure), if the ventilation fan was kept on. The operating fan also provides fresh air to the neighbouring cells and dilutes the concentrations when the fire is suppressed.

The smoke spreading to the neighbouring cells was found to be strongest when the ventilation system's fan is off and there are no dampers. In this case, the conditions of the neighbouring cells can become dangerous at 2 m height from the floor, but will remain tolerable closer to the floor.

The simulations investigating the adjacent cells' toxicity conditions were limited to a 2.5 min duration. During this time, the fire heat release rate had reduced significantly due to the lack of oxygen, but the risks of longer exposures in the cases with closed fans cannot be ruled out. Longer simulations are needed to investigate the longer exposures.

6. Case study: Apartment fire

Topi Sikanen, VTT Technical Research Centre of Finland Ltd.
Umar Riaz, Rahul Kallada Janardhan, Simo Hostikka
Aalto University, Tomas Fagergren, Brandskyddslaget

6.1 FDS Modelling

This case study was conducted to study the influence of the envelope airtightness on the fire-induced pressures and smoke spreading through ventilation networks in a modern apartment. Modern apartments are different from the traditional apartment of the fire experiment and pose a larger risk of pressure rise as the envelopes are more air tight. In modern HVAC systems, there are usually separate mechanical supply and exhaust air systems equipped with additional components for heating/cooling, as well as heat recovery and air filtration units. The modern ventilation fans are often equipped with dampers that automatically close the ambient connection when the fan is turned off. In a fire situation, turning off the fan can completely close the ventilation system.

The scientific presentation of the scenario is given in Appendix C, and here we provide a brief summary of the case description and results. The simulation geometry for the hypothetical building consists of a single floor of a multi storey apartment building as shown in Figure 6.1. There were 8 apartments with floor areas of 50 m^2 and 2 apartments with a floor area of 100 m^2. The model does not include a staircase connecting the domain to the other floors of the building.

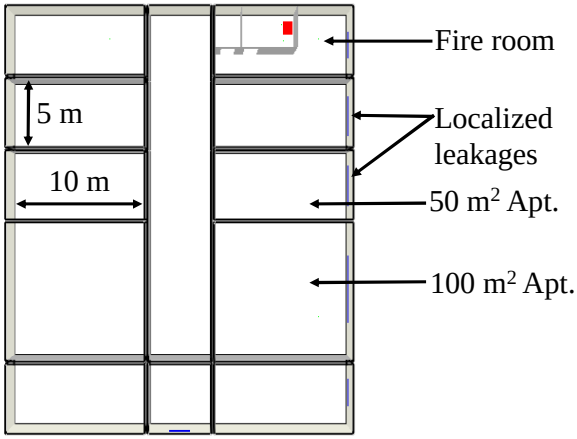

Figure 6.1. Geometry for the apartment case study

The ventilation system consists of independent inlet and exhaust networks, both equipped with a fan with stalling pressure of P_{max} = 550 Pa and a zero-pressure flow rate of V_{max} = 650 l/s. The fan unit model parameters were tuned to produce 150 Pa pressure loss to the flow. Each network consists of a central duct (ϕ=250 mm) and smaller (ϕ=125 mm) ducts for each individual apartment.

Three different levels of the building envelope air-tightness were investigated, corresponding to the traditional, current practice, and the technically possible target state. Three different variations of the fire apartment ventilation were studied, including cases where both ventilation ducts were closed, only inlet was closed, and both ducts remained open. For Fires with three different growth rates were used in the simulations.

The peak overpressures are summarized in Figure 6.2. These results are corrected for the estimated model bias of -13 %. The relative model standard deviation of 19 % is used to draw the 95 % confidence limits around the estimated peak overpressures. The trends in the results are clear and consistent. All the three parameters - fire growth rate, damper configuration and air-tightness - are found to be important for the expected peak pressure. Although not shown here, the results were found to be independent of the fan operation (on or off) and the position of the fan unit's damper. This means that the leakages through the other apartments can compensate for the fan pressure differences and complete closing of the ventilation system.

Assume that the critical over pressure for door opening is 100 Pa, we can observe that the door opening is possible in traditional buildings if the fire

growth rate is only medium. For more air-tight buildings and faster fires, the door opening would be challenging. It is, however, important to notice that these were just the momentary peak pressures, and do not tell much about the time duration when (how soon and how long) the door opening would be difficult.

Challenges for the structural integrity can be expected in fast or ultra-fast fires. If we choose the failure criterion based on our own experimental observation (1500 Pa), the fast fires could pose a risk when the dampers are closed and the envelope is very airtight. In fires that develop even faster, problems would be expected in all modern buildings. In very air-tight buildings, the capacity of the basic ventilation network is not sufficient to relief the pressures even if no dampers are used.

The possibility of smoke spread to the other apartments was investigated by monitoring the smoke concentration in the neighbouring apartments. The results indicate that smoke spreads to the neighbours regardless of the fan operation if dampers are not used at all. Interestingly, the smoke did not spread to other apartments when a damper was used only on the inlet side and the exhaust ventilation fan was kept runningin. Obviously, the cases with both dampers operating can be expected to be safe in this respect.

6.2 PFS Modelling

The PFS (Program Flow System) can calculate almost any static flow system. The flow system is described with a simple sketch, and the media can be air, water, other fluids or compressed gases. The program solves the steady state pressure and flow rates using assumed gas temperature.

PFS program was used to investigate the apartment fires with two growth rates (medium and fast), Near-Zero air tightness (leakage volume flow of 0.036 m^3/s at 50 Pa), assumed gas temperature of 250 °C, and different ventilation configuration. The simulated conditions and results are shown in Appendix D.

The results for the apartment overpressure were significantly higher than what was found using FDS software. For instance, at Medium growth rate and both dampers closed, PFS predicted a pressure of 4673 Pa while

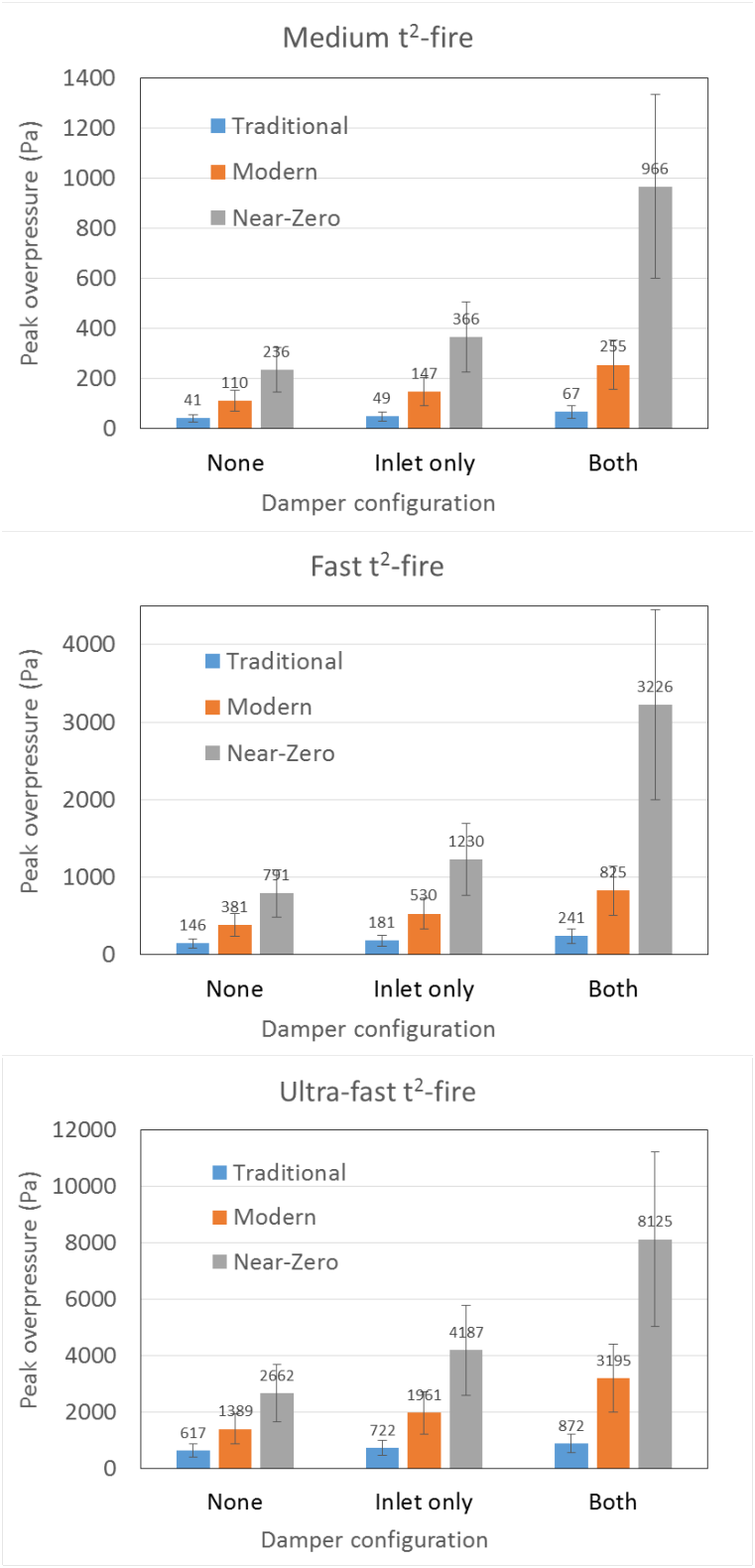

Figure 6.2. FDS predictions for the peak overpressures in the apartment building case study, corrected for the observed bias. The error bars show the 95 % confidence limits.

FDS predicted only 966 $\pm$ 367 Pa overpressure. However, the relative differences between the pressures obtained with different ventilation scenarios were similar between the two programs. Most importantly, the results concerning the smoke spreading were identical, supporting the conclusion that the smoke spreading to the neighbouring apartments can be prevented both closing both apartment ducts or by closing only inlet side and keeping the exhaust open and fan running.

7. Pressure management

Umar Riaz and Simo Hostikka, Aalto University

Numerical simulations were used to investigate the feasibility of pressure management options in the apartment case study. First, an analytical integration formula was developed for the pressure development in order to speed up the computations. The method requires gas temperature as an input. It was validated using both experimental data and FDS simulations[1].

Using model, we calculated the peak pressures in the case of fast t^2 fire development and Near-Zero envelope at different leakage areas (Figure 7.1). Assuming the critical pressure levels for structural damage and door opening to be 1500 Pa and 100 Pa, respectively, we obtain the necessary additional leakages to maintain the peak pressures below these thresholds.

The results are shown in Table 7.1. Maintaining the pressure under 100 Pa in the configuration without dampers requires an additional leakage equivalent to circular hole of 180 mm diameter. Tightening the damper configuration increases the required additional leakage area. Maintaining the pressure below the structural safety threshold in the closed dampers -configuration requires an additional leakage of 67 mm diameter. The limit was not reached in the other damper configurations.

Different technical solutions can be proposed for the implementation of the necessary additional leakages in the energy efficient buildings. The technical details and economical or architectural implications were not

[1]The method, as well as the detailed pressure management results will be reported in the MSc thesis of Umar Riaz in 2017.

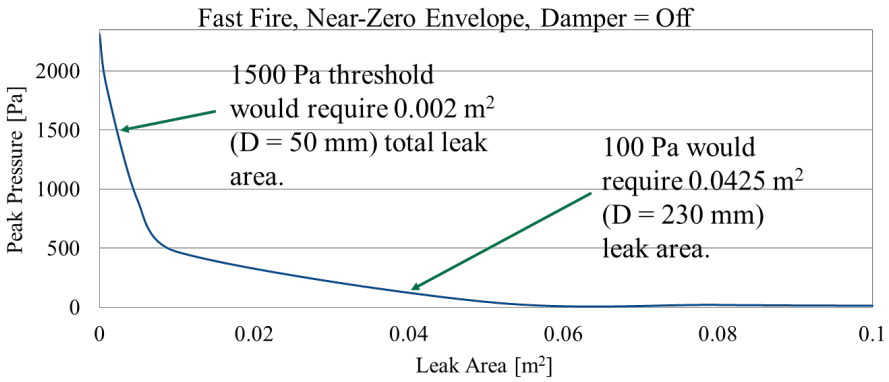

Figure 7.1. Necessary total leakage are for maintaining pressure at desired level in a fast t^2 fire.

studied in the current research. However, one can already observe that the 100 Pa threshold will require significant leakage which can be difficult to implement in real building projects. The 1500 Pa requirement, in turn, can be implemented through ventilation system dimensioning (contradictory to the assumed damper configuration) or small leak path in the building envelope.

Table 7.1. Required leakage areas for pressure management in fast fire within a 50 m2 apartment of a Near-Zero building.

Threshold pressure	Damper configuration [Pa]	Additional leakage [m^2]	Equivalent vent diameter [m]
100	OFF	0.025	180
100	Inlet only	0.029	190
100	ON	0.034	210
1500	ON	0.0036	68

8. Conclusions and recommendations

In this project, we investigated the influence of the building ventilation conditions and envelope air-tightness on the fire-induced pressures, smoke spreading and occupant safety using fire experiments and validated simulations. The experimental part included eleven heptane and polyurethane foam fires in 1970's apartment with three different ventilation conditions. The results indicate that

1. The effect of the ventilation configuration (or effective leakage) on the pressure rise in the compartment is significant and should be taken into account during the building fire safety design process.
2. Fire-induced overpressure can prevent the occupants from escaping from spaces with inward opening doors. This possibility should be taken into account in the building codes and guidelines.
3. Fire-induced pressure can cause severe structural damage and a significant change in fire dynamics through the additional source of air.

The experimental results accompanied by the previous Swedish experiments were used to validate the FDS simulations. The simulations were then used to investigate the pressure conditions, smoke spreading and occupant safety in two mechanically ventilated buildings. The focus of the simulations was on the influence of ventilation arrangements and building envelope air-tightness. Based on the simulations, we can make the following conclusions:

4. The apartment fire simulations can be used to investigate the pressure rise and its consequences during the building fire safety design or fire investigations.

5. The occupant's possibilities to escape from a burning apartment through an inwards-opening door cannot be ensured in new buildings with air-tight envelopes, as the fire pressure will exceed 100 Pa with high probability. Banning the use of inwards-opening doors in such buidings should be seriously considered.
6. The peak over-pressures can become high enough to cause structural damages in mechanically ventilated apartment buildings with very air-tight envelopes. With fast t^2 fires, the peak overpressure was 3200 $\pm$ 1200 Pa if both supply and exhaust dampers were closed, and 1200 $\pm$ 460 Pa if only the inlet damper was closed. With ultra-fast fires and closed dampers, the peak overpressure was 8100 $\pm$ 3000 Pa. Possible consequences of the structural damages would depend on the type of failure: In case of envelope failures, an accelerated fire spread along the building façade could result. In case of the failing internal structure, smoke spreading to an evacuation route could follow, and the evacuation of the entire building could be put in danger.
7. Different technical solutions can be suggested for maintaining the pressure at safe level. On option is to use the ventilation network as a pressure relief path. When doing so, the spreading of smoke from the burning apartment to the neighbouring apartments must be prevented. Both objectives can be reached simultaneously by
   - closing the supply side by smoke damper,
   - keeping the exhaust side open, and
   - designing the exhaust fan strong enough and keeping it operating during the fire.

   The acceptability of this kind of solutions should be ensured in the normative environment.

The current Finnish building code for structural fire safety (E1, 2011) does not recognize the risks of the fire-induced pressure on the safe evacuation and structural integrity. We therefore recommend that a requirement to consider the fire-induced pressure in building design will be added to the building code.

9. Future research

During the research, the following needs for further information were observed:

Air-tightness of internal building parts: In fires, the pressure build-up occurs within a single fire compartment or even smaller enclosure. The current technologies for evaluating and classifying buildings for the energy efficiency provide good information about the entire building envelope, but the effective leakage areas of the internal structures are not known. New research is needed to quantify the performance of internal structures.

Air-tightness at high pressure differences: The standard practice of envelope characterization deals with pressure differences below 100 Pa, and usually in under-pressure rather then over-pressure. Further quantification of building leakages at higher pressure differences would increase the reliability of fire simulations and design.

Ventilation model parameter estimation: Both the model validation and case studies indicated that the real ventilation networks cannot be modelled in FDS using the detailed system layout and component -level information becaue the spesification of all the system properties would be an exhaustive task, and practically impossible in other applications except the design of new buildings, where the HVAC designers could contribute to the modelling. Therefore, new modelling capability is needed for estimating the essential model parameters, such as the fan curve and loss coefficients, from the known design basis.

Acceptability of new management solutions: New solutions are here

proposed for the simultaneous management of pressure and smoke spreading. The general acceptability of these solutions may require further sensitivity studies and discussion of practical implications in HVAC design. For instance, how does the system size/complexity and the relative position of the burning apartment (distance from the fan) affect the pressure levels in the exhaust ventilation system and the fulfilment of smoke compartmentation?

Bibliography

[1] F.W. Mowrer. Enclosure Smoke Filling and Fire-Generated Environmental Conditions. In Hurley, M.J. (ed.) SFPE Handbook of Fire Protection Engineering, Fifth ed., Society of Fire Protection Engineers, Springer, 2016. Pp. 1066-1101. DOI 10.1007/978-1-4939-2565-0

[2] B. Hägglund, K. Nireus and P. Werling. Pressure rise due to fire growth in a closed room. Description of three full-scale tests. FOA Defence Research Establishment, FOA-R-96-00347-2.4-SE, 1996. 27 p.

[3] B. Hägglund, K. Nireus and P. Werling. Pressure rise due to fire growth in a closed room. An experimental study of the smoke spread via ventilation ducts. FOA Defence Research Establishment, FOA-R-98-00870-311-SE, 1998. 97 p.

[4] L. Audouin, L. Rigollet, H. Prétrel, W. Le Saux, and M. Röwekamp. OECD PRISME project: Fires in confined and ventilated nuclear-type multi-compartments - Overview and main experimental results, Fire Safety Journal, 62 B, 2013, 80-101.

[5] L. Audouin, H. Prétrel, W. Le Saux. Overview of the OECD PRISME project – main experimental results, in: 21st International Conference on Structural Mechanics in Reactor Technology (SMiRT 21), 2011.

[6] K.B. McGrattan, R. McDermott, J. Floyd, S. Hostikka, G. Forney, and H. Baum, Computational fluid dynamics modelling of fire. International Journal of Computational Fluid Dynamics, 2012, 1–13.

[7] J. Wahlqvist and P. van Hees. Validation of FDS for large-scale well-confined mechanically ventilated fire scenarios with emphasis on pre-

dicting ventilation system behavior. Fire Safety Journal 62 B, 2013, 102-114.

[8] C. Forneau, N. Cornil, C. Delvosalle, H. Breulet, S. Desmet, and S. Brohez. Comparison of fire hazards in passive and conventional houses, Chemical engineering Transactions, 26, 375-380, 2012. DOI:10.3303/CET/1226063.

[9] S. Bengtson, B. Hägglund, Dslayv, a Helpful Engineering Tool. Journal of Applied Fire Science 1 (1), 1990, 7-21.

[10] S. Bengtson, B. Hägglund, F. Madsen, Comparison between a Simple and a More Complex Zone Model in Fire Engineering. Fire Safety Science, 2 (1989), 471-480.

[11] D. Baroudi. Piecewise least squares fitting technique using finite interval method with Hermite polynomials. VTT Technical Research Centre of Finland, Espoo. VTT Publications, 135, 1993, 27 p.

[12] SFS-EN 13829, Thermal performance of buildings. Determination of air permeability of buildings. Fan pressurization method (ISO 9972:1996, modified). Suomen standardoimisliitto SFS ry. 2000.

[13] R.G. Rehm and H.R. Baum. The Equations of Motion for Thermally Driven, Buoyant Flows. Journal of Research of the NBS, 83:297–308, 1978. 2, 8, 13, 109

[14] K.B. McGrattan, R. McDermott, S. Hostikka, J. Floyd, C. Weinschenk and K. Overholt. Fire Dynamics Simulator (Version 6) User's Guide, (2015)(a). NIST.

[15] K. McGrattan, S. Hostikka, R. McDermott, J. Floyd, C. Weinschenk, and K. Overholt. Fire Dynamics Simulator, Technical Reference Guide, Volume 1: Mathematical Model. National Institute of Standards and Technology, Gaithersburg, Maryland, USA, and VTT Technical Research Centre of Finland, Espoo, Finland, sixth edition, November 2015.

[16] K. McGrattan, S. Hostikka, R. McDermott, J. Floyd, C. Weinschenk, and K. Overholt. Fire Dynamics Simulator, Technical Reference Guide, Volume 1: Validation. National Institute of Standards and Technology,

Gaithersburg, Maryland, USA, and VTT Technical Research Centre of Finland, Espoo, Finland, sixth edition, November 2015.

[17] B.J. McCaffrey, J.G. Quintiere, M.F. Harkleroad, Estimating room fire temperatures and the likelihood of flashover using fire test data correlations. Fire Technology., 17, 2, 1981. 98-119.

[18] R.K. Janardhan, and S. Hostikka. Experiments and numerical simulations of pressure effects in apartment fires, Fire Technology, 2016 submitted for review.

[19] S. Hostikka, R.K. Janardhan, U. Riaz, and T. Sikanen. Fire-induced pressure and smoke spreading in mechanically ventilated buildings with air-tight envelopes. International Association for Fire and Safety Science, 2016.

A. Experiments and numerical simulations of pressure effects in apartment fires

Rahul Kallada Janardhan and Simo Hostikka

Submitted for review in *Fire Technology* journal.

Fire Technology manuscript No.
(will be inserted by the editor)

Experiments and numerical simulations of pressure effects in apartment fires

Received: date / Accepted: date

Abstract We have investigated the development of gas pressure and the resulting flows in compartment fires first experimentally, by burning a series of heptane pool and polyurethane mattress fires inside a real apartment, and then by carrying out numerical simulations of the experiments with the FDS code. The experimental results indicate that the gas pressure in relatively closed apartment can become high enough to revert the flows of the ventilation system, prevent escape through inwards-opening doors, and even break some structures. We also report the FDS validation for this type of simulations and discuss the process of modelling the ventilation system and leakages.

Keywords Pressure · Envelope leakage · FDS · Simulations · Experiments

1 Introduction

In early 2014, a group of professional fire fighters from the Southwest Finland Emergency Services, city of Turku, was rehearsing a situation where they ignited a fire inside an apartment of an abandoned building, closed the door and tried to attack the fire after a moment to suppress it. To their surprise, two firemen could not open the inner door of the apartment (many Finnish apartments have double doors to the corridor) due to the high pressure inside the apartment. This led to the questions: What if there was an occupant trying to escape the burning apartment? Can the pressure be high enough to prevent escape?

Thermal expansion of gas during a fire will result in increased pressure if the fire takes place in a relatively closed compartment [1]. The phenomenon has received only little attention in the history of fire science because most studies have been performed in enclosures with large opening to ambient. This has been well-justified from the viewpoint of structural safety, as only a long-lasting fire can cause high temperatures that pose a risk to the fire resistance. Also, the need to ensure the availability of air has affected the experimental design of fire dynamics

Address(es) of author(s) should be given

research. The smoke management calculation typically assume that pressure differences across the vents are dominated by the hydrostatic pressures, order of few tens of Pa at most.

Hägglund et al. [2,3] have measured the pressures resulting from liquid pool fires in a compartment with only one, relatively small vent to ambient. They reported over and under pressure peaks as high as 1200 Pa and 1800 Pa respectively. By adding a mechanical ventilation to the same configuration, the over pressures were changed to 900 Pa and under pressures to -1200 Pa. They observed that even the mechanically driven ventilation flows were reverted according to the direction of the pressure. Unfortunately, neither the heat release nor the mass loss rate of the fire were measured, thus limiting the possibility of quantitative analyses, such as a code validation. More recently, the experiments within the OECD PRISME programme have produced detailed information about the development of compartment pressure, ventilation flows and liquid pool fire dynamics in a very air-tight compartment [4]. As high as 3000 Pa over pressures were observed with fires of about 1 MW [5]. The results from the PRISME project cannot be directly transferred to the residential conditions due to the highly specialized construction, but they have already been used to validate the pressure and ventilation flow simulations of the Fire Dynamics Simulator [11] (FDS) software by Wahlqvist and van Hees [8]. Fourneau et al. [17] used zone modelling to investigate the influence of the energy efficiency fire safety by comparing the modelling results in traditional and modern air-tight buildings (Passivhaus). They observed a significant difference in pressure rise (10 Pa vs. 450 Pa) and concluded that the high pressure can lead to a reverse flow in the supply ventilation system and possible pollution of other living areas. They did not recognize the pressure rise as a risk for the escape as such.

The main objectives of the current study were to quantify the pressures in fires taking place in closed residential compartments, to evaluate the potential risks for life and property, and to validate the FDS for the simulation of such fires. Through the simulation capability, we will later evaluate the different ventilation arrangements and means for pressure management. By doing so, we want to bring more insight into the potential fire and evacuation safety issues related to the mechanically ventilated, air-tight enclosures that are currently being built due to the energy efficiency requirements and the trend of high-rise construction.

To meet the objectives we performed a series of fire experiments in a typical Finnish apartment, measuring the gas temperatures, pressures and gas species concentrations, as well as ventilation flows. The experimental setup is described in Section 2. The experiments were simulated with FDS, paying attention to the characterization of the building features that have the most influence on the pressure, such as envelope leakage. The simulation model is presented in the third section of this article, and the results reported in the fourth section. As the experiments were performed in a real apartment building, all the experimental uncertainties could not be ruled out, and they are discussed in the end of the article.

2 Experimental study

2.1 Geometry

The experiments were conducted in a 1970's apartment building in the city of Kurikka, Finland. The building had three floors and a basement. The test apartment included a living room, bedroom, kitchen, bathroom, aisle and a closet, and was located in the first floor of the building. The apartment floor area was 58.6 m^2 with a ceiling height of 2.57 m. The envelope area A_{env} was 165 m^2, including the floor and the ceiling. A floor plan is shown in Fig. 1.

The concrete walls that were shared with the adjacent apartments were approximatelly 0.16 m thick. The walls to the exterior were around 0.20 m thick. The walls towards the outside consisted of concrete-insulation elements and three-glass windows. The wall from the living room to the balcony had a light-weight structure with wooden frame. The apartment had the typical Finnish two door system with the inner door opening inwards and outer door opening towards the staircase.

2.2 Ventilation configuration

The apartment had three ventilation exhaust vents, one in the bathroom, one in the closet, and one in the kitchen hood. The kitchen hood was closed during the expriments. The bathroom and closet vents were connected to 160 mm diameter ducts leading to the roof of the building. There was a small replacement air vent in the living room to provide make-up air for the ventilation, but this valve was closed tightly during the experiments to enable accurate characterization of the ventilation flows. The ventilation had originally been designed to be buoyancy-driven, but a roof fan had been installed to the bathroom duct at some point during the building use.

Thirteen experiments were performed with three different configurations of two the exhaust ducts:

1. open duct,
2. normal configuration with the original valves installed on the ducts, and
3. ducts closed with metal foil and tape.

Photographs of the duct conditions are shown in Fig. 2. The ventilation configurations are summarized in Table 1. Test numbering corresponds to the order of the experiments, except for Test 12 which was in fact the last test of the campaign.

The roof fan connected to the bathroom exhaust was operating except for the tests 3, 4 and 10, where it was switched off. The solid fuel tests were performed under the normal operating conditions of the exhaust ducts with the roof fan running and the kitchen duct tightly sealed.

2.3 Leakages

The air-tightness of the apartment boundaries was measured using a Blower door test according to the standard SFS-EN 13829 [10]. A powerfull fan was attached

Table 1 Test configurations. Note that tests 12 and 13 were performed in reverse order.

Test	Fuel	Ducts	Roof fan	Comments
1	heptane 3.2 L	Open	ON	
2	heptane 3.0 L	Open	ON	Repeat of Test 1.
3	heptane 3.0 L	Open	OFF	
4	heptane 3.0 L	Open	OFF	Repeat of Test 3.
5	heptane 3.0 L	Normal	ON	
6	heptane 3.0 L	Normal	ON	
7	heptane 3.0 L	Normal	ON	
8	heptane 3.0 L	Closed	ON	
9	heptane 3.0 L	Closed	ON	
10	heptane 3.0 L	Closed	OFF	
11	PUF 3.82 kg	Normal	ON	
12	PUF 3.82 kg + wood	Normal	ON	Fire in closet. Closet exhaust velocity measurement was removed. Last test of the series.
13	PUF 2.65 kg + 2.60 kg	Normal	ON	

to the door leading from the living room to the balcony, and the other vents of the apartment were closed tightly. The door from the stairway to outside was kept open so that the staircase was at the ambient pressure. The fan was used to create a pressure difference between the apartment and the ambient. The amount of air flow through the fan was measured at different pressure differences. The normal practice in the energy effiency studies is to report the leakage at 50 Pa underpressure in a form of a volumetric flow rate $\dot{V}_{50}$, air permeability q_{50} or air exchange rate n_{50}. The air permeability is calculated by dividing the flow rate with the envelope area ($q_{50} = \dot{V}_{50}/A_{\mathrm{env}}$), and the air exchange rate by dividing the flow rate with volume ($n_{50} = \dot{V}_{50}/V$). In this work, the leakage measurements were made at both under and overpressures in a range 30...70 Pa. The measurement uncertainty for $\dot{V}$ was $\pm$ 0.6 %, and for q_{50} it was $\pm$ 4 %. The apartment temperature at the time of the measurements was only 16°C, as it had been out of use for weeks.

Table 2 Results of the leakage tests

Direction	Δp [Pa]	$\dot{V}_{\lvert\Delta p\rvert}$ [m^3/s]	$q_{\lvert\Delta p\rvert}$ [m^3/hm^2]	$n_{\lvert\Delta p\rvert}$ [1/h]	A_{leak} [m^2]	$A_{\mathrm{leak}}/A_{\mathrm{env}}$
Underpressure	-30	0.047	1.0	1.1	0.011	0.70×10^{-4}
Underpressure	-50	0.078	1.7	1.9	0.015	0.89×10^{-4}
Underpressure	-70	0.10	2.2	2.4	0.016	0.97×10^{-4}
Overpressure	30	0.091	2.0	2.2	0.022	1.4×10^{-4}
Overpressure	50	0.12	2.7	2.9	0.023	1.4×10^{-4}
Overpressure	70	0.15	3.3	3.6	0.024	1.5×10^{-4}

The measured flow rates through the apartment boundaries are shown in Table 2. The measured q_{50} values indicate that the building would comply with the requirements of the Finnish building code (Part D3, 2012) for new buildings ($q_{50} \leq 4$ m^3/hm^2). However, the building is less air tight than the building code's recommended level ($q_{50} \leq 1$ m^3/hm^2)

Another way of characterizing the envelope air tightness is to calculate the effective leakage area. Assuming that the leakage behaves as a flow through a sharp-edged orifice, the leakage area A_{leak} can be solved from the following equation

$$\dot{V}_{|\Delta p|} = C_d A_{\text{leak}} \left(\frac{2|\Delta p|}{\rho} \right)^{0.5} \quad (1)$$

where $\dot{V}$ is the leakage flow rate, C_d is the discharge coefficient, A_{leak} is the leakage area, ρ is the density, and Δp is the pressure difference at which the leakage rate was measured. Assuming $C_d = 0.6$, $\rho = 1.3$ kg/m^3 and $\Delta p = 50$ Pa, for which $\dot{V} = 0.12$ m^3/s, gives $A_{\text{leak}} = 0.023$ m^2. Dividing the leakage area by the apartment envelope area gives the corresponding leakage ratio of 1.4 $\times 10^{-4}$. From the viewpoint of smoke management technologies, the building would be classified to the average class (NFPA 92, 2012, Table A.4.6.1). Comparing the leakage areas obtained at different pressures (Table 2) in the range -70...70 Pa, we can observe that the leakage area is only weakly dependent on the absolute value of the pressure, but the values obtained at under and over pressures were clearly different.

Before the fire experiments, the kitchen and bathroom drains were tightly sealed to avoid the situation where the overpressure would push the water out of the water lock, thus creating an additional, uncontrolled leakage path to the apartment.

2.4 Fire loads

The experiments were conducted in two phases based on the type of fuel: In the first phase (tests 1-10), 3.0 L (3.2 L in Test 1) of n-Heptane was burned in a 0.7 m x 0.7 m steel pan with a free height of 21 cm. The fuel was poured on a water layer to stabilize the burning and to provide uniform thickness of heptane. The position of the pan is shown in Fig. 1. In the second phase, polyurethane foam (PUF) mattress were used. Test 12 was performed in the closet of the apartment, and it was the last test of the campaign.

2.5 Measurements

The quantities that were measured during the experiments were gas pressure, gas temperature, O_2, CO_2 and CO concentrations and the gas velocity and temperatures in the exhaust ducts. The measurement locations are shown in Fig. 1. The pressure difference between the apartment gas space and ambient was measured in two locations (one in living room, other in kitchen) at height 1.8 m using Furness FCO 0508264-9 pressure transmitters and metal ducts connecting them to the measurement positions. The calibration uncertainties of the transmitters were about 1%.

For the exhaust gas velocity measurement, additional 0.5 m sections of the ventilation duct were attached in front of the exhaust vents to facilitate the placement of instruments and to improve the reliability of the velocity measurements. Although the length of the tubes was insufficient for achieving fully developed flow

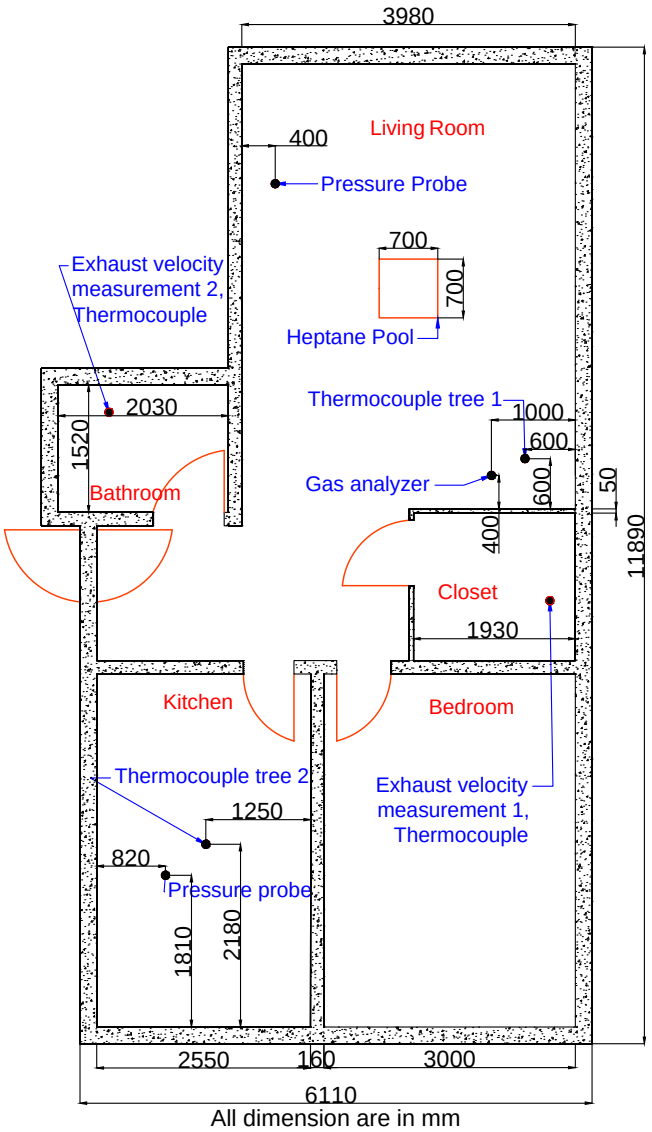

Fig. 1 Floor plan of the test apartment and measurements.

Fig. 2 Apartment ventilation configuration.

profiles, they were expected to make the flow more uniform at the measurement location. Flow velocities were measured using bi-directional probes with calibration uncertainty of about 2%.

Gas temperatures were measured using two trees of five K-type thermocouples (1.5 mm diameter) with 0.5 m vertical separation. One tree of thermocouples was placed in the corner of the fire room, and the other tree in the centre of the kitchen. Thermocouples were also placed in the exhaust ducts for measuring the exhaust gas temperatures.

The gas concentrations were measured through a probe placed 1.7 m from the floor in the living room corner next to the thermocouple tree. The sampling line was lead to the gas analyzers outside thr apartment. The delay due to the length of the line was 16 s. In Test 13, the CO2 and CO levels exceeded the corresponding analyser ranges.

The heptane pan mass was measured using a load cell. The mass loss rate $\dot{m}(t)$ was calculated from the mass data using by piecewise least squares fitting technique using finite interval method [9]. Second order Hermite polynomials were fitted to the mass data, thus providing the mass-loss rate as the first derivative. Heat release rate was calculated from $\dot{m}(t)$ assuming complete combustion of flammable vapors

$$\dot{Q}(t) = \dot{m}(t)\, \Delta H_{\mathrm{c}} \tag{2}$$

where ΔH_{c} is the net heat of combustion of N-Heptane (43.5 MJ/kg).

The mass measurements were not performed in the PUF fires due to the potential risk to the load cell. The HRR curve of Test 11 was estimated from the measured gas temperatures using inverse modelling. According to a classical room fire correlation [16], the temperature rise in a compartment fire is proportional to $\dot{Q}^{2/3}$. The cofficient of proportionality was obtained from the heptane pool fires and then used to obtain a rough estimate of the PUF HRR.

The tests were recorded using video cameras placed inside the fire room and in the balcony.

2.6 Experimental procedure

In the heptane pool fire tests (Tests 1-10), the experiment started by turning on the data loggers and closing the doors of the apartment. A fireman wearing a breathing apparatus poured the heptane into the pool, waited for a few seconds for the mass reading to stabilize, and then ignited the fire using a gas torch. The fireman stayed inside the apartment for the whole duration of the fire.

In the PUF fires, the door was kept open at the time of ignition, and the fireman left the apartment closing the doors behind, except for Test 13, where he stayed inside to test the possibilty of door opening. Test 12 ended to an intentional intervention by the fire brigade.

3 Numerical simulations

3.1 Numerical method

FDS is a Large Eddy Simulation (LES) based Computational Fluid Dynamics sofware which solves the low mach number combustion equations on a rectilinear grid over time [11].

FDS has a dedicated module for modelling Heating, Ventilation and Air-conditioning (HVAC) systems connected to the gas space of the fire simulation. The ventilation network is described as a series of ducts and nodes. The nodes are placed at points where ducts intersect each other or the CFD computational domain. The ducts are uninterrupted domains of fluid flow which can encompass elbows, expansion/contraction fittings and various other fittings. The losses due to friction and various other duct fittings are assigned as dimensionless loss numbers to the ducts. The node losses are attached to the ducts as loss terms only appear in the duct equations [14]. The module does not presently store any mass. Therefore, mass flux into a duct is equal to the mass flux out of the duct. The nodal conservation equations for mass, energy and momentum equations are as follows:

$$\sum_j \rho_j u_j A_j = 0 \tag{3}$$

$$\sum_j \rho_j u_j A_j h_j = 0 \tag{4}$$

$$\rho_j L_j \frac{du}{dt} = (P_i - P_k) + (\rho g \Delta z)_j + \Delta P_j + 0.5 K_j \rho_j |u_j| u_j \tag{5}$$

where ρ is the density, u is the duct velocity, A is the cross sectional area of the duct, h is enthalpy of fluid in the duct, P is the pressure and K is the dimensionless loss coefficient of the duct. The subscripts j indicates the ducts in the calculation, i and k indicate the nodes of the duct [14].

3.2 Simulation model

The simulation model is based on the apartment layout and floor area shown in Fig. 1. The simulation model geometry is shown in Fig. 3. The spatial discretization was made with 0.10 m resolution, and the results were not found to be sensitive to the resolution. The fuel pan was modelled as a 0.7 m x 0.7 m burner with a specified mass loss rate (MLR) according to the measurements. The combustion reaction was that of n-Heptane, with soot and CO yields of 3.7 % and 1 %, respectively.

Leakage modelling was one of the critical aspects of the simulation. FDS provides two different methods for the leakage modelling: The *Bulk Leakage* -method assigns the leakages onto large segments of the compartment boundaries. In our case, entire interior surface was used as a leakage path. The flow is driven by the difference between the background pressures inside and outside the compartment, at floor level. The *Localized Leakage* -method assigns the leakages to smaller locations of the boundary, and is suitable if the exact location of the leakages can be identified. The pressure difference is based on the local pressure averaged over the surface area, and includes the contribution of the perturbation pressure provided

by the hydrodynamic solver. In this work, this method was also used although the exact locations of the leakages were not known. In both methods, the leakage flow is calculated by the HVAC solver.

One challenge of the leakage modelling is that the pressure differences during fires can be an order of magnitude higher than the pressure differences used in the leakage tests. There is no guarantee that the gaps and cracks of the building envelope and the flows through them behave in a similar manner in these two situations. For example, assuming a 1 mm gap size indicates that the flow Reynolds number is less than 1000 at 50 Pa but about 2000 at 500 Pa difference, thus indicating a transition from laminar to turbulent flow. In this situation, both C_d and the exponent of the pressure in Eq. 1 can be different. In addition, the high pressure differences can cause deformations in the structures, thus changing the effective leakage area.

The performance characteristics of the roof fan are not know, and the fan model parameters were estimated based on the duct velocity measurements and expected normal mode operation. A stalling pressure of 200 Pa and a maximum flow rate of 200 L/s were assumed. To avoid spurious pressure fluctuations the time stepping (DT_HVAC) of the HVAC network model was set to 2 seconds.

The ventilation ducts leading from the closet and bathroom to the roof were modelled as systems of two or three duct sections. The first section (length L_1) represents the additional duct fitted in front of the actual duct for measurements. It was assumed to have no flow loss. The second section represents the duct leading from the apartment to the roof. The bathroom duct was connected to a third section which contained the fan, was assumed to be 1 m long and connected to an ambient node. All the ducts had a roughness of 0.001 m. The duct lengths, areas and loss coefficients are listed in Table 3. The loss of the ventilation system was expected to be mainly due to the valve in the node connecting the duct to the room. The valves are adjustable, and the values of K_2 were chosen to reproduce their normal-model operation. In the case of open configuration, very small losses were assumed to the system.

Table 3 HVAC model inputs.

Ventilation configuration	L_1 (m)	L_2 (m)	L_3 (m)	A_1, A_2 (m^2)	A_3 (m^2)	K_1	K_2	K_3
Bathroom duct								
Open	0.4	10	1.0	0.01227	0.049	0	3	1
Normal	0.4	10	1.0	0.01227	0.049	0	38	1
Closet duct								
Open	0.4	10		0.01227		0	2	
Normal	0.4	10		0.01227		0	70	

The thickness of the concrete walls was set to 0.20 m for external walls and 0.16 m for internal walls. The conductivity, specific heat and density of the concrete were set to 0.7 W/(m.K), 0.75 kJ/(kg.K) and 2200 kg/m^3, respectively.

The simulations were carried out using the FDS version 6.3.2 [14] on a personal computer with a 2.8 GHz AMD Phenom II x6 1055T processor and 8 GB ram. The CPU time for a single simulation of 300 s was approximately 36 hours utilizing 6 cores of the computer.

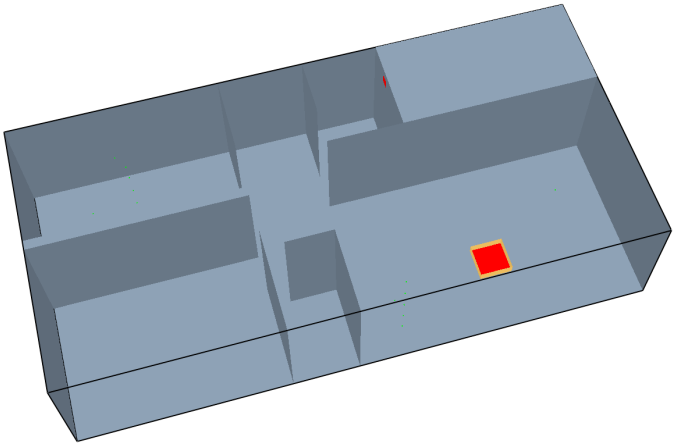

Fig. 3 Simulation model of the apartment.

4 Results and discussion

4.1 General observations

Two main observations are of general interest:

1. In few seconds after the ignition and door closing, the high overpressure inside the apartment was observed as a strong, high-pitch noise. In Test 13, the fireman who stayed inside after igniting the fire with a torch, tried to open the inwards-opening door by pulling the handle. He could not pull the door open using his own force. After a few attempts, the other firemen were able to push and bend the door from the staircase side so that the pressure was reliefed, and the door opening became possible.
2. In Test 12, the light-weight wall between the living room and the balcony failed structurally. The window frame was seen to move already in Test 11 and 13, thus being exposed to about 1650 Pa pressure difference. In Test 12 about 60 s after the ignition, the pressuce, unexpectedly, pushed the window frame out of the wall. At the moment of this structural failure, the pressure difference was about 1400 Pa. (For comparison, the typical wind loads on the envelope are of the same order of magnitude with these pressures.) The event was preceeded by a low squeaky noise heard from outside for about one second. Visual inspection of the structures after the fire showed now sign of thermal damage. The pressure of the apartment was thus reliefed before the possibility to intervene the fire.

4.2 Heat release rates

The heat release rates (HRR) of the liquid pool fires were obtained from the measured mass loss rate curves. The HRR results in three experiments with different ventilation configurations are shown in Fig. 4 as solid lines. As can be seen, the burning behaviour of the pool fire was not affected by the ventilation configuration. Nor were there differences between the tests with nominally identical conditions,

thus indicating a good repeatibility of the experiments. The measured HRR curves were prescribed HRR inputs to the FDS simulations. Figure 4 shows the simulated HRR curves as dashed lines.

As the measured HRR was not available for the PUF fire (Test 11), a rough estimate of the HRR curve was first developed using the inverse method. Then, the HRR curve was manually adjusted to reach a good agreement between measured and simulated gas temperatures. The resulting HRR curve is shown in Fig. 4. These temperature results cannot be used for validating the temperature predictions. However, we will use the pressure results to supplement the heptane pool fire results, but the nature of the validation for Test 11 must be considered qualitative.

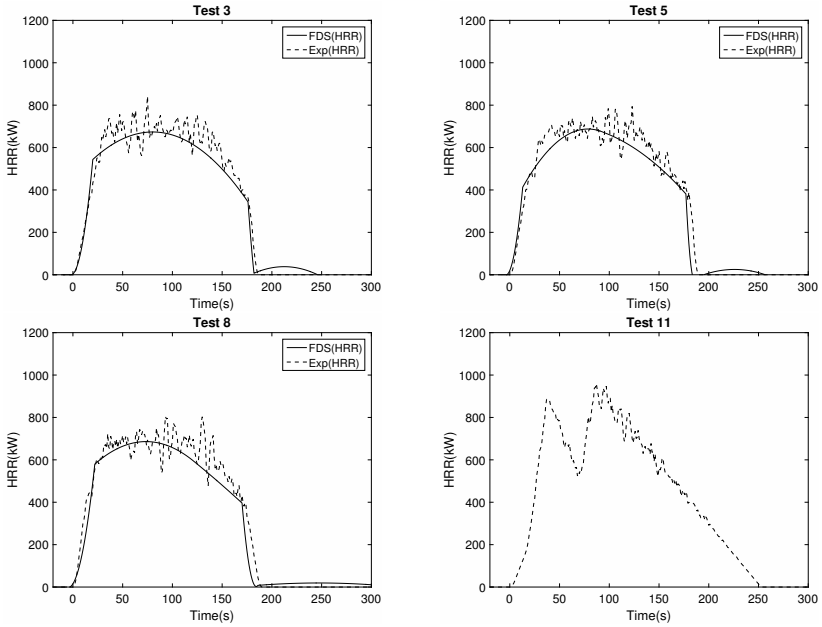

Fig. 4 Comparison of simulated and measured heat release rates .

4.3 Gas temperatures

The gas temperatures measured close to the living room ceiling are shown in Fig. 5. The figure on the left shows the results for three heptane fires with different ventilation arrangements. We can observe that the repeatability of the pool fires is very good, and that the ventilation arrangement has no influence on the gas temperatures inside the burning room. The figure on the right shows the corresponding data for the three PUF fires. Here the repeatatility is not observed, as the fire sources were different. In addition, the fire source of Test 12 was placed in the closet, hence showing a delay in the temperature rise.

Experimental (solid lines) and simulated (dashed lines) temperatures at different heights are compared in Fig. 6. The method of leakage modelling did not have

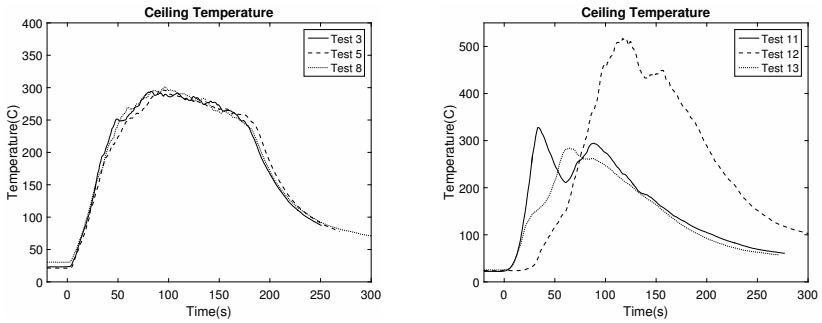

Fig. 5 Gas temperatures in heptane pool fires (left) and PU foam fires (right).

any significant influence on temperature predictions. Hence only the temperatures from the Bulk Leakage method are presented here.

The agreement between the measured and simulated temperatures in the heptane pool fires (Tests 3, 5, and 8) is within the model uncertainty estimated from other similar experiments [15]. The highest overpredictions are observed at 100 cm height from the floor. The experimental results indicate a stronger stratification of the gas temperature profile than the FDS simulations. The results of Test 11 (PUF fire) cannot be considered validation. They are presented for the sake of comparison and to provide basis for further use in pressure validation. The errors in the simulated temperatures in Test 11 are combinations of the true model uncertainties and the HRR input uncertainty.

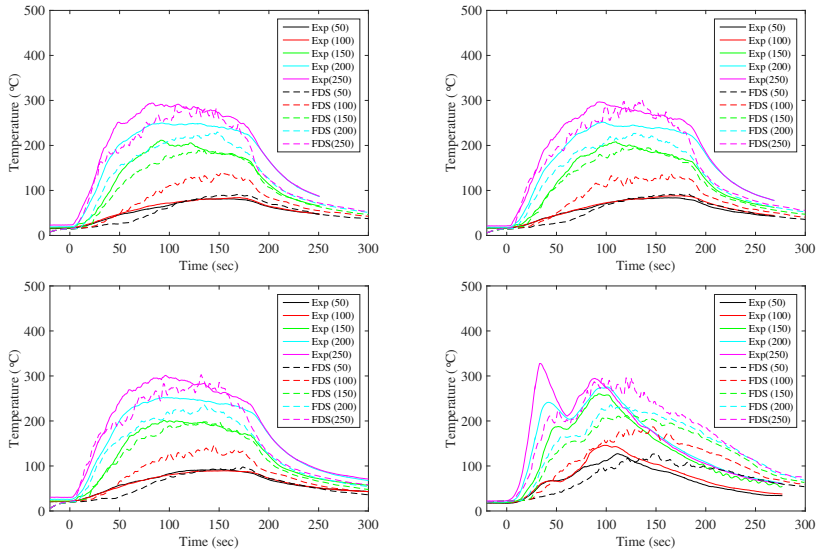

Fig. 6 Comparison of simulated and measured gas temperatures. Top row: Test 3 and Test 5. Bottom row: Test 8 and Test 11.

4.4 Gas concentrations

The measured volume fraction of oxygen in the fire room of the is shown in Fig. 7. The fires are generally well ventilated, and the heptane fire results (left figure) show a good repeatability and independence of the ventilation configuration. This indicates that the ventilation flow rates in Tests 3 and 5 are too small to influence the fire room gas concentrations within the observed time scale. Only Test 12 (closet fire with additional solid fuels) can be considered underventilated. However, the measurements are affected by the window breakage and fire brigade intervention. The significantly different fire development of Test 12 is visible in CO concentrations (Fig. 8) as well. The peak CO concentrations are about 300 ppm in the heptane pool fires and between few hundred and 2000 ppm in the PUF fires. In Test 12, the CO concentration exceeded the analyzer range of 5000 ppm.

The simulated O_2 and CO concentrations are not presented here, but the minimum O_2 concetrations were used to calculate the model uncertainty metrics later in the paper.

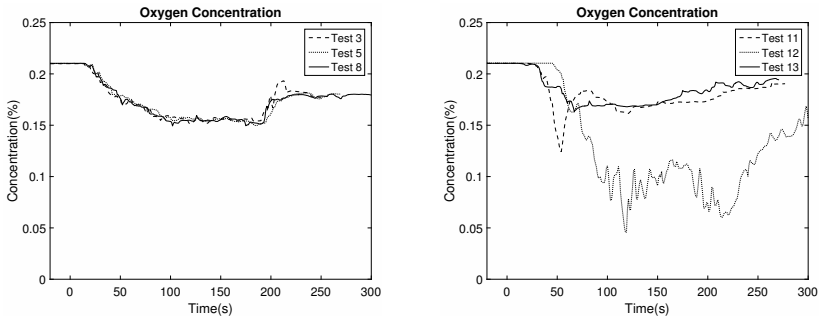

Fig. 7 Oxygen volume fractions in heptane pool fires (left) and PU foam fires (right).

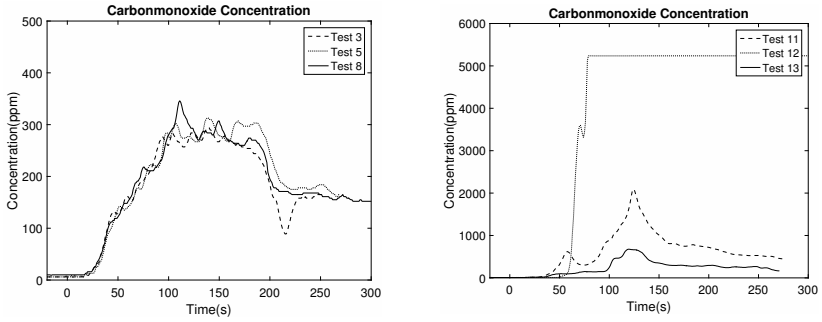

Fig. 8 CO concentrations in heptane pool fires (left) and PU foam fires (right).

4.5 Gas pressures

The recorded pressures in the liquid and solid fuel tests are shown in Fig. 9. The left figure shows the pressures in heptane pool fires for all the three ventilation configurations. The ventilation configuration is shown to have a significant impact on the pressure rise. As the the open ducts (Tets 2-4) were changed to normal dampers (Tests 5-7), the peak overpressures increased from about 300 Pa to 600 Pa. Closing the ducts completely increased the peak pressures further to about 900 Pa. On the other hand, the roof fan position (ON or OFF) does not seem to influence the pressures at all, or the influence is smaller than the measurement uncertainty. After the fuel burnout at 170 s, there is an underpressure peak of -200 to -400 Pa, but the difference between the normal and closed ventilation configurations cannot be observed as in the overpresssures.

In the PUF fires (Fig. 9, right), the overpressures are significantly higher than in the heptane pool fires, ranging from about 1400 Pa in Test 12 to 1650 Pa or Tests 11 and 13. The pressure values follow the fuel burning behaviours and the changes in geometrical conditions. In Test 11, the fire decreased in size after about 40 s but increased again at 60 s as a pool of melt PU was formed on the floor. In Test 13, opening of the door by the firemen is seen as short reduction in pressure at about 30 s. Both tests show a negative peak after fuel burnout. In Test 12, a rapid decay of pressure is shown at 80 s when the external wall was broken, and consequently no negative pressure peak appears.

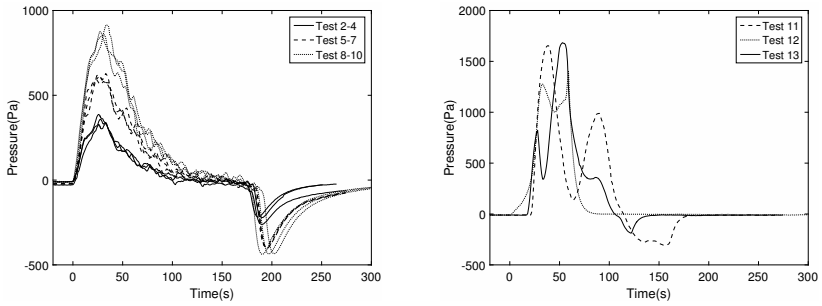

Fig. 9 Gas pressure in heptane pool fires (left) and PU foam fires (right).

The experimental pressures and FDS predictions with the two leakage modelling methods are compared in Fig. 10. The pressure predicted by FDS was smoothed over 5 datapoints using moving average method to remove some noise from the plots. For Test 3 (open ducts), FDS overpredicts the peak overpressures, but for the normal and closed configurations (Tests 5 and 8), the experimental pressure peaks are between the predictions given by the two leakage modelling methods. This indicates that in reality, either the ventilation system of Tests 2-4 has even lower total flow loss than what is expected in the FDS model, or the effective leakage area is higher than what was found in the air-tightness tests. Allocation of the system losses between the exhaust vent valves and the other parts of the systems was based on the very limited knowledge of the system geometry and the expected fan pressure level and normal flow conditions.

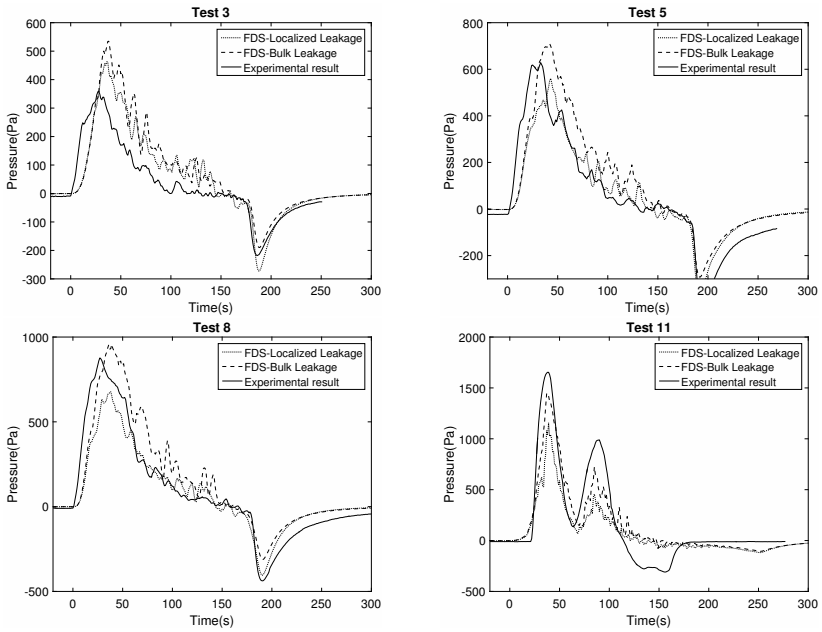

Fig. 10 Comparison of simulated and measured gas pressures.

The localized leakage method gives lower pressure than the bulk leakage modelling method for all four tests shown in Fig. 10. The result can, at least partially, be explained by the fact that the bulk leakage is calculated from the pressure difference measured at the bottom of the pressure zone formed by the simulated compartment, while the localized leakage is based on the local pressure. In local pressure, the hydrostatic effect and the perturbation components can increase the pressure difference, which results in higher leakage and lower overall pressure.

4.6 Ventilation flows

The recorded flow velocities in Test 3 and Test 5 are shown in figures 11 and 12, respectively. The bathroom duct velocities are shown on the left and the closet duct velocities on the right. The FDS predictions with the two leakage methods are also shown in the figures. Positive direction means out of the compartment.

In both tests, flow in the closet's exhaust duct is shown to be initially in inwards direction. In Test 3 (Fan off), also the bathroom duct has initial inwards flow. The negative flow can be caused by two factors: First, the routes of make-up air in the original gravity-based ventilation seem to have been insufficient. Secondly, the cooling of the compartment, heated by the previous tests, before the ignition can cause an initial underpressure. The roles of these and other possible factors cannot be accuratelly confirmed.

The open configuration has clearly higher ventilation speeds than the normal configuration with outlet valve. FDS is shown to capture the shape and magnitude of the outwards flow, but the magnitude of reverse flow after the fire burnout is underestimated by the model.

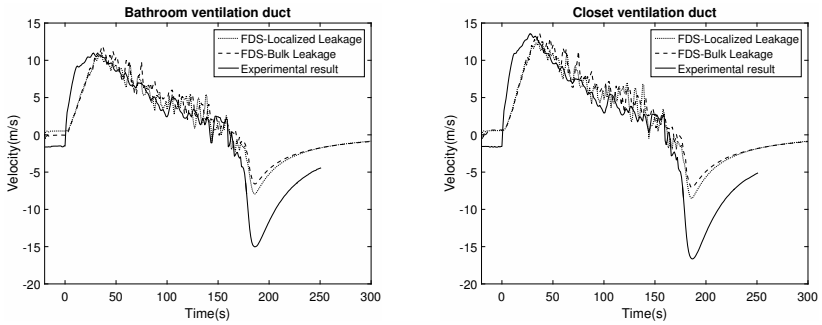

Fig. 11 Ventilation flow speed in Bathroom (left) and Closet (right) exhaust in Test 3.

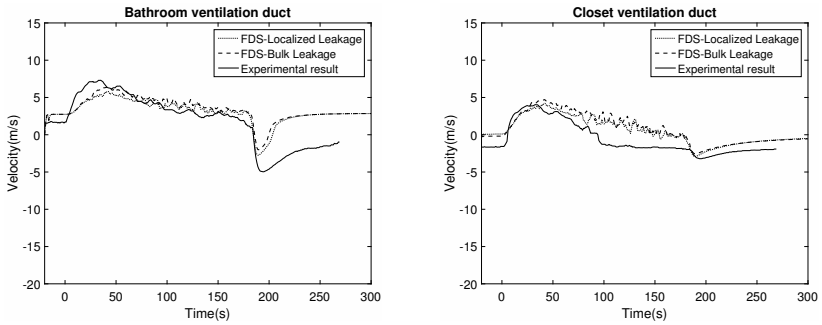

Fig. 12 Ventilation flow speed in Bathroom (left) and Closet (right) exhaust in Test 5.

4.7 Uncertainties and limitations

The main sources of the the experimental uncertainity are the uncertain ventilation system configuration, lack of direct HRR measurement and the problematic quantification of addditional leakage. More precisely:

- The duct sizes and the network layout of the ventilation system were not known precisely. The duct diameters were estimated from the visible sections, but the details behind the structures could not be confirmed. The model geometry was partially based on the standard construction practices during the 1970s. The roof fan characteristics were not known either.
- The HRR was not measured directly in these experiments, but the fuel mass was measured using a load cell and used to calculate HRR. The HRR uncertainty is induced from the polynomial least squares fitting for the MLR and the assumed the yields of incomplete compbustion products.
- The leakage area at 50-70 Pa may not be fully representative to the leakage that occurs at fire pressures. The increase of the leakage area during peak pressure cannot be quantified without a leakage measurement system capable to significantly higher pressures. The direction of the leakage was found to have a significant effect on the leakage area.

The experiments were planned to give insight into the pressures and ventilation flows during apartment fires. The direct utilization of the results in any wider context is limited by at least two aspects of the experiments:

– Both fire types increased in power very quickly after ignition. In fact, they could be classified ultra fast fires in terms of the fire safety engineering design fires. The best way to extrapolate the results to lower growth rates is to use the simulation model which has now been validated.
– In real fires, the high overpressure can push out the water from the water locks of the kitchen and bathroom drains. The influence is difficult to estimate at this stage. Simulations can be used to examine this effect, but it requires hydraulic characterization of the drain systems for air flow.

Due to the observed uncertainty in the estimated leakages, we investigated the sensitivity of the peak pressure predictions to the leakage area using the bulk leakage version of the model. Table 4 compares the experimental values to the predictions using the nominal leakage area and a leakage area increased by 10 %. When the leakage area was increased, the peak pressures decreased 17 % in average, being much closer to the experimental values. However, at the same time the temperatures were reduced as well, indicating that the leakage area cannot be adjusted arbitrarily for better pressure predictions.

Table 4 Peak pressure (Pa) sensitivity to leakage area.

	Experimental	Nominal leakage	1.1 × Nominal leakage
Test 3	359	535	381
Test 5	628	710	616
Test 8	876	957	867

The model uncertainty metrics for three predicted quantities were calculated using the methods proposed in the FDS Validation Guide [15]. The data consisted of three peak values from Tests 3, 5 and 8. The resulting values for the model bias δ and relative standard deviation $\tilde{\sigma}_M$ are reported in Table 5. The table also lists the relative standard deviations of the experimental values $\tilde{\sigma}_E$, both as a-priori expected values and as resulting from the current data. The expected experimental errors are combinations of the corresponding measurement errors and the propagated input uncertainty. They are higher than the values used in [15] because the HRR was not directly measured, and due to the previously mentioned leakage uncertainties. In case of gas temperature, the data indicates a similar uncertainty as what we expected. For oxygen concentration and pressure, however, the data suggest that the errors are in fact smaller than our uncertainty estimates.

Table 5 Uncertainty metrics of computed quantities of Tests 3, 5 and 8.

	$\tilde{\sigma}_E$			
Quantity	(Expect)	(Data)	$\tilde{\sigma}_M$	Model Bias, δ
Peak gas Temperature, Bulk Leakage	0.08	0.08	0.17	1.04
Peak gas Temperature, Localized Leakage	0.08	0.08	0.17	1.04
Min. O_2 concentration, Bulk Leakage	0.1	0.01	0.01	0.97
Min. O_2 concentration, Localized Leakage	0.1	0.03	0.03	0.94
Peak pressure, Bulk leakage	0.2	0.09	0.09	1.21
Peak pressure, Localized leakage	0.2	0.14	0.14	0.96

Despite the small number of data points, these uncertaity metrics can be used to evaluate the quality of the validation with respect to the published FDS validation data [15]. For the peak temperatures, the model bias in the current simulations is smaller than in the large body of validation cases in [15]. For the minimum oxygen concentration, the biases are slighly greater (here 0.94 and 0.97 vs. 0.99 in [15]) but satisfactory, considering the uncertainty in HRR spesification. Indeed, the low biases of temperature and oxygen concentration indicate that the HRR has been reliably estimated. For the peak pressure, the biases of the current simulations (1.21 for the bulk leakage and 0.96 for the localized leakage) are greater than in [15], where the bias of the similar simulations is only 1.02.

The two leakage methods were found to produce quite different pressures. Given the simplicity of the bulk leakage method and the fact that the predictions were in all cases equal or higher than the measured pressure, it can be considered a recommended method for this type of application. It would still be possible to model individual, known leakages such as window or door cracks using the localized method.

The conditions after the fire burnout were not in the focus of this study, and the relatiely higher uncertainties of the negative pressure peaks have not been investigated.

5 Conclusions

A set of fire experiments was conducted in an apartment building under different ventilation conditions to understand the pressure rise in compartments and its effects on the ventilation flows. The main finding was that the heptaine pool and polyurethane foam fires in relatively closed compartments can lead to very high over and under pressures. The recorded overpressures were between 100 Pa and 1650 Pa, and they occured in less than 50 s from the ignition. The two experimental parameters, ventilation system configuration and fuel type, were both found to have a significant influence on the pressure magnitude. We demonstrated that during the period of high overpressure, it is impossible to open an inwards-opening door of the apartment by pulling from inside. In addition, we observed that the pressure resulting from a polyurethane foam fire can cause structural damage to the building.

The experimental campaign was followed by the FDS simulations of the experiments to validate the predictive capability and the process of modelling the leakages and simple ventilation systems. The uncertainties of the numerical simulations in reproducing the thermal, chemical and pressure conditions within the apartment were estimated. For gas temperature and oxygen concentrations, the uncertainties were found to be close to the previously published validations under similar fire conditions. For the peak overpressure, the simulations using the Bulk leakage method resulted in values that were 21 % too high in average. When the Localized leakage method was used, the peak pressures were underpredicted by 4 %, but the scattering of the results was more pronounced. The predicted ventilation flows were in a good qualitative agreement with the experimental results.

Based on the experimental and simulation results, we can conclude that

1. The effect of the ventilation configuration (or effective leakage) on the pressure rise in the compartment is significant and should be taken into account during the fire safety design process.
2. Fire-induced overpressure can prevent the occupants from escaping from spaces with inward opening doors. This possibility should be taken into account in the building codes and recommendations.
3. Fire-induced pressure can cause severe structural damage and a significant change in fire dynamics through the additional source of air. The fire spread along the building facade can be accelerated due to the envelope failures. In case of the failing internal structure, such as the wall between the burning apartment and the building's evacuation route, the smoke spread to the evacuation route would follow and the whole evacuation of the building occupants put in danger.
4. The apartment fire simulations can be used to investigate the pressure rise and its consequences during the fire safety design or fire investigations. More work is needed to quantify the uncertainties of the ventilation flows, but the current simulations were able to capture the qualitative flow behaviour. For performing such simulations, it is important to characterize the envelope leakage and the ventilation configuration.

Further experimental research is needed to investigate the following aspects of the topic:

- The effects of the negative pressure on the ventilation flows, evacuation and the structural stability.
- Leakages are usually known only for the building envelope (if at all) and not for individual apartments of the building. The internal leakages between apartments and the common spaces are not controlled or regulated for the scenarios with high pressure differences.
- The sensitivity of the pressure on the parameters of real ventilation systems should be studied.

The usability and reliability of the simulations in modern buildings requires that the capability of the HVAC module to simulate different ventilation system components shall be examined. In addition, the engineering methods to determine the model input parameters from the possible sources of information should be developed and disseminated. But already now, the simulations were shown to be sufficiently reliable for investigating the topical needs of the fire engineering, such as:

- Implications of the building envelope's air tightness to the fire pressure and ventilation flows, providing more insight to the fire safety effects of the energy efficient and tall construction.
- Risks of structural damage and delayed escape need to be quantified. For instance, it will possible to investigate the likelihood of hazardous conditions at fire growth rates that are closer to the expected residential fire scenarios.

Acknowledgement

We would like to thank the experimental team: Pasi Paloluoma and Knut Lehtinen (South-West Finland Emergency Services), Peter Biström (Stravent Oy), Tomas

Fagergren (Brandskyddslaget), Jere Heikkinen and Ville Heikura (VTT). The research project was funded by the Finnish Fire Protection Fund (PSR), Ministry of Environment, Hagab AB, and the Criminal Sactions Agency of Finland. The work was also partially supported by the Academy of Finland under grant no. 289037.

References

1. F.W. Mowrer. Enclosure Smoke Filling and Fire-Generated Environmental Conditions. In Hurley, M.J. (ed.) SFPE Handbook of Fire Protection Engineering, Fifth ed., Society of Fire Protection Engineers, Springer, 2016. Pp. 1066-1101. DOI 10.1007/978-1-4939-2565-0
2. B. Hägglund, K. Nireus and P. Werling. Pressure rise due to fire growth in a closed room. Description of three full-scale tests. FOA Defence Research Establishment, FOA-R-96-00347-2.4-SE, 1996. 27 p.
3. B. Hägglund, K. Nireus and P. Werling. Pressure rise due to fire growth in a closed room. An experimental study of the smoke spread via ventilation ducts. FOA Defence Research Establishment, FOA-R-98-00870-311-SE, 1998. 97 p.
4. L. Audouin, L. Rigollet, H. Prétrel, W. Le Saux, and M. Röwekamp. OECD PRISME project: Fires in confined and ventilated nuclear-type multi-compartments - Overview and main experimental results, Fire Safety Journal, 62 B, 2013, 80-101.
5. L. Audouin, H. Prétrel, W. Le Saux. Overview of the OECD PRISME project – main experimental results, in: 21st International Conference on Structural Mechanics in Reactor Technology (SMiRT 21), 2011.
6. S. Bengtson, B. Hägglund, Dslayv, a Helpful Engineering Tool. Journal of Applied Fire Science 1 (1), 1990, 7-21.
7. S. Bengtson, B. Hägglund, F. Madsen, Comparison between a Simple and a More Complex Zone Model in Fire Engineering. Fire Safety Science, 2 (1989), 471-480.
8. J. Wahlqvist and P. van Hees. Validation of FDS for large-scale well-confined mechanically ventilated fire scenarios with emphasis on predicting ventilation system behavior. Fire Safety Journal 62 B, 2013, 102-114.
9. D. Baroudi. Piecewise least squares fitting technique using finite interval method with Hermite polynomials. VTT Technical Research Centre of Finland, Espoo. VTT Publications, 135, 1993, 27 p.
10. SFS-EN 13829, Thermal performance of buildings. Determination of air permeability of buildings. Fan pressurization method (ISO 9972:1996, modified). Suomen standardoimisliitto SFS ry. 2000.
11. K.B. McGrattan, R. McDermott, J. Floyd, S. Hostikka, G. Forney, and H. Baum, Computational fluid dynamics modelling of fire. International Journal of Computational Fluid Dynamics, 2012, 1–13.
12. R.G. Rehm and H.R. Baum. The Equations of Motion for Thermally Driven, Buoyant Flows. Journal of Research of the NBS, 83:297–308, 1978. 2, 8, 13, 109
13. K.B. McGrattan, R. McDermott, S. Hostikka, J. Floyd, C. Weinschenk and K. Overholt. Fire Dynamics Simulator (Version 6) User's Guide, (2015)(a). NIST.
14. K. McGrattan, S. Hostikka, R. McDermott, J. Floyd, C. Weinschenk, and K. Overholt. Fire Dynamics Simulator, Technical Reference Guide, Volume 1: Mathematical Model. National Institute of Standards and Technology, Gaithersburg, Maryland, USA, and VTT Technical Research Centre of Finland, Espoo, Finland, sixth edition, November 2015.
15. K. McGrattan, S. Hostikka, R. McDermott, J. Floyd, C. Weinschenk, and K. Overholt. Fire Dynamics Simulator, Technical Reference Guide, Volume 1: Validation. National Institute of Standards and Technology, Gaithersburg, Maryland, USA, and VTT Technical Research Centre of Finland, Espoo, Finland, sixth edition, November 2015.
16. B.J. McCaffrey, J.G. Quintiere, M.F. Harkleroad, Estimating room fire temperatures and the likelihood of flashover using fire test data correlations. Fire Technology., 17, 2, 1981. 98-119.
17. Forneau C., Cornil N., Delvosalle C., Breulet H., Desmet S. and Brohez S. Comparison of fire hazards in passive and conventional houses, Chemical engineering Transactions, 26, 375-380, 2012. DOI:10.3303/CET/1226063.

B. Prison case study report

Gleb Bytskov and Jukka Hietaniemi
Palotekninen Insinööritoimisto Markku Kauriala Oy

PAHAHUPA
CASE STUDIES

PRISON CELL VENTILATION IN FIRE SITUATION

November 28th 2016

Gleb Bytskov
Jukka Hietaniemi

PALOTEKNINEN INSINÖÖRITOIMISTO MARKKU KAURIALA Oy
Radiomiehenkatu 3 B, 20320 TURKU
Puh. 02-254 6000, fax 02-239 2490
Piispantilankuja 6C, 02240 Espoo
Puh. +358 45 7750 3099
Krno: 527.152
Kotipaikka: Turku
LY 0869061-6
ALV. REK.

CONTENT

1 INTRODUCTION

This report describes numerical simulations of pressure development and its consequences in a fire in a tight enclosure.

The enclosure considered is a prison cell, which is connected to two other cells via the HVAC system. The most fundamental fire safety aspect in the building design is to provide means for safe evacuation of the occupants in case of fire. In buildings such as prisons, this goal may be problematic to achieve. Therefore, the prison cell system was chosen as the subject study in this report.

As the persons locked in cells cannot evacuate by themselves, fire safety design shall consider the following issues:

- Provide sufficient time for staff to evacuate the occupants in the cell of fire origin.
- Provide sufficient time for staff to evacuate inmates from cells not involved in the fire.
- Enable staff to safely attack the fire.
- Prevent the spread of smoke and fire.

The aim of this research is to provide a deeper understanding of how pressure and its effects develop in a tightly closed enclosure fire. The pressure rise may have other consequences such as smoke spreading to adjacent cells, or difficulties when opening the door. These are the main fire safety issues analysed in this work.

The study comprises the following three main parts:

1. Simulations using the fire development based on the compartment fire experiments carried out in the PAHAHUPA research project in Kurikka in autumn 2015 [1].
2. Simulations using the fire development based on typical fire load of a prison cell.
3. Assessment of the impact of smoke dampers on the safety in the adjacent cells.

The first two parts, presented in Chapters 4 and 5, focus on the conditions inside the cell of fire ignition. These parts differ in the fire development rate. The heat release rate (HRR) based on the Kurikka experiments grows very fast while the HRR based on typical prison-cell fire load exhibits more moderate fire development.

In addition, the first part investigates different scenarios regarding fire positions and ventilation setups in order to identify the most hazardous ones. The different ventilation setups include variations in the supply and exhaust fan operations, activated or deactivated, as well as supply duct conditions, with or without dampers.

The first part includes also a sensitivity study of the model.

The third part, Chapter 6, presents a further analysis of the influence of smoke damper with emphasis on the safety of persons in the adjacent cells. These studies include the both fire developments.

Chapter 7 is the discussion. This chapter also outlines the major differencies in the results obtained with the two different fire development modes.

The prison cells and the HVAC system are described in Chapter 2. The simulations are carried out by using the Fire Dynamics Simulator software version 6.4.0 as explained in Chapter 3.

Table of simulated cases is presented in Appendix A.

2 CELL AND HVAC SYSTEM

The geometry of the cell examined in this study is presented in Figure 1. The length of enclosure is about 5.8 m, width – 2.2 m and height – 3 m. Cell constructions i.e. walls, floor and ceiling are made of concrete. Enclosure consists of main compartment (living room/bedroom) and lavatory. These rooms are not separated by door (empty door opening). Prison cell has also small wardrobe. Among the regular furniture are bed, table and chair. There is only one outdoor in prison cell, which is usually locked. Prison cell has a window with bars on the opposite side of the door.

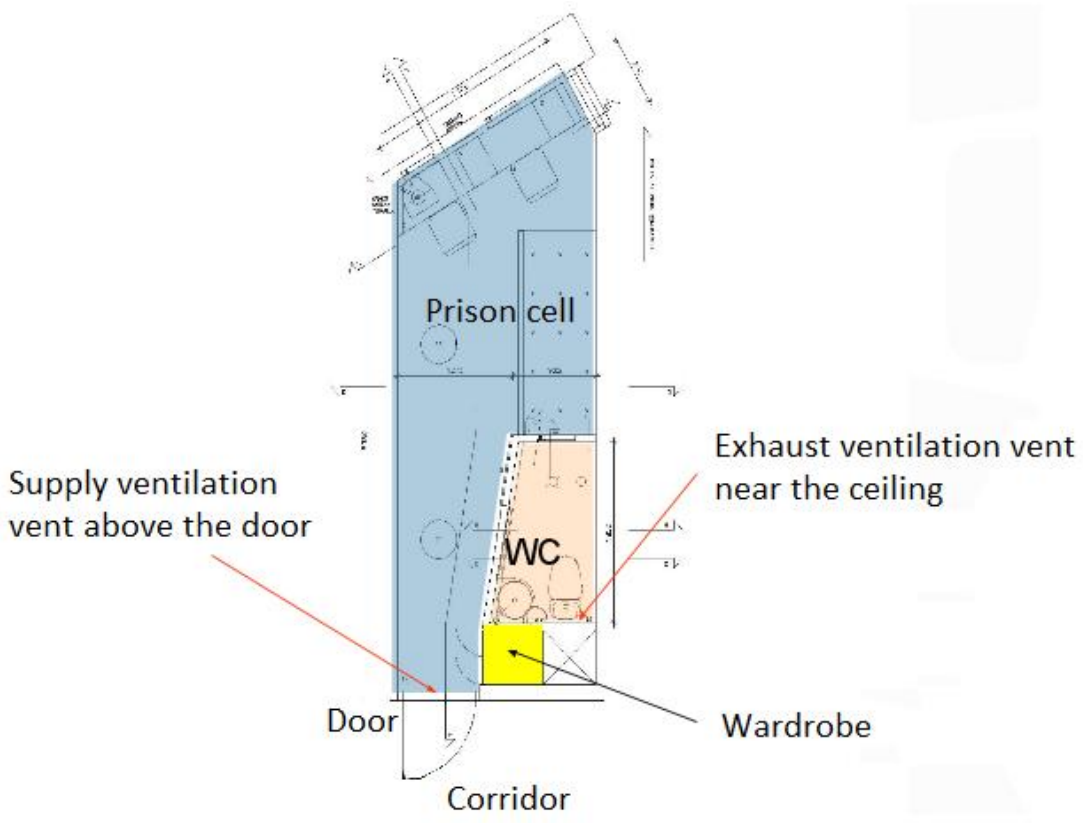

Figure 1. Plan of cell

Cell has a mechanical ventilation. Exhaust ventilation vent is placed in WC room. Supply ventilation vent is located in main room above the door. Ventilation provide air circulation of 40 l/s.

Ventilation system consists of circular pipes with two different size. Small-diameter pipes are directly connected to the prison cells. Cross-sectional area of these pipes is about 200 cm^2 (pipe diameter is 160 mm).

The main pipe leading to the fan has cross-sectional area of 490 cm^2 (circular pipe with diameter of 225 mm).

In reality, compartments are not fully sealed. Leakage occurs through windows, door and cracks. Leakage air flow may decrease the pressure during compartment fire, therefore it should be taken into the account. The following equations and corresponding calculation show the leakage flow from the rooms:

Normal leak rate q_{50} = 1.5 m^3/m^2h. This corresponds to modern buildings with no particular envelope airtightness. Leakage volume flow is:

$$Q_{leak} = q_{50}S \quad (1)$$

where q_{50} is leak rate and S is total envelope area of one room. Total envelope area for this case is about 73.5 m^2. Leakage volume flow at 50 Pa can be calculated using equation:

$$Q_{leak} = c_d A_{leak} \left(\frac{2\Delta p}{\rho}\right)^{0.5} \quad (2)$$

where c_d is discharge coefficient, ρ is air density. Using c_d=0.6 and ρ=1.2 kg/m^3, this would give a leakage area of 0.005593 m^2. Leakage area parameter was implemented to three walls (white walls in Figure 2b).

3 SIMULATION MODEL

Simulations of the fire are carried out by the Fire Dynamics Simulator (FDS) version 6.4.0. FDS6 is a well-validated and verified calculation tool for modelling and simulating fire scenarios, such as those analysed in this report [2, 3, 4, 5]. Ecpecially, development of pressure in enclosure fire was investigated and validated in Aalto University in Master's thesis work with title ''Fire Induced Flows in Building Ventilation Systems'' [1].

For FDS, the prison cell is modelled as an enclosure of dimensions 2.2 × 5.8 × 3 m (width × lenght × height), shown in Figure 2a. Mesh size of models 20 × 20 cm.

The FDS model consisting of three prison cells is shown in Fig. 2b. The cell fire origin is located on the lower level. The second cell is placed next to the cell fire origin and the third cell is located above it. Cells are connected via ventilation system. Green squares in Figure 2b depict the vent of supply ventilation ducts and magenta squares – vent of the exhaust ventilations.

a)

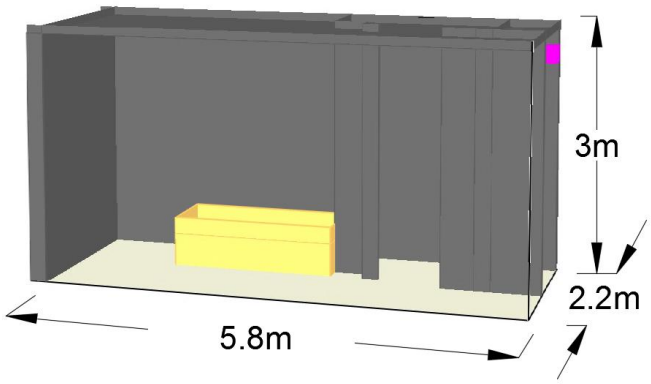

b)

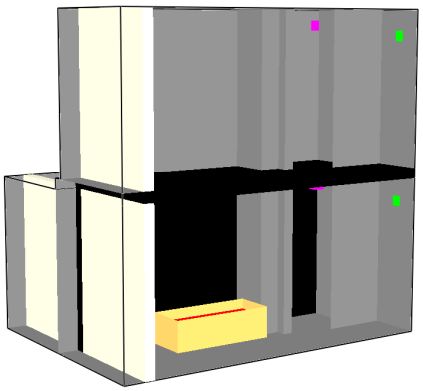

Figure 2. FDS models: a) the cells of fire origin and b) the three cells considered in this study.

Modelled ventilation system scheme is presented in Figure 3. Ducts from three modelled cells connect each together in one point (Figure 3). Fire dampers are assumed to activate at 72 °C in ducts, where they are installed. Dampers cut off only inlet ducts. Dampers don't leak.

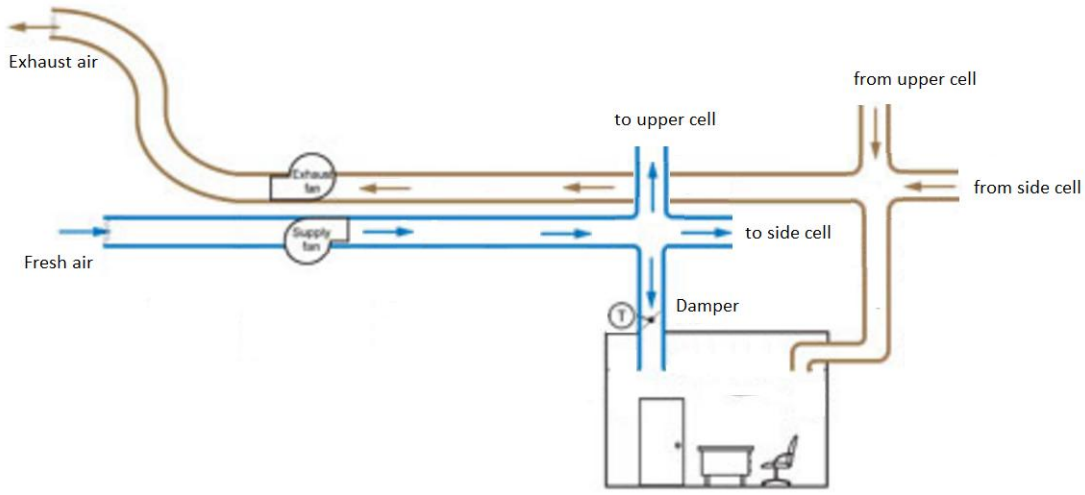

Figure 3. Modelled ventilation system.

The model of ventilation was verified by ensuring volume conservation in the HVAC network, as shown in Appendix B.

Summary of the main conditions assumed for modelling of this case are:

- Each cell is formed a different pressure zone.
- Leakage factor q_{50} = 1.5 m^3/m^2h (airtightness of modern buildings).
- Floor, ceiling and walls of cells are made from concrete with conductivity of 1 W/(mK) [6].
- Fire source origin and HRR is based on the solid fuel test results from Kurikka experiments and typical Finish prison cell fire load.
- Fans have a quadratic fan model with parameters: maximum flow 130 l/s and maximum pressure 400 Pa.
- Air supply and exhaust systems provide air flow into the cells of 40 l/s.
- Nodes losses in ventilation system are assumed to be a zero.
- Dampers activate at 72 °C.

4 SIMULATIONS BASED ON THE FIRE DEVELOPMENT OF THE KURIKKA EXPERIMENTS

4.1 HEAT RELEASE RATE

HRR curve corresponds to Test 11 of Kurikka experiments [1].
The main characteristics of fire source are:

- Maximum HRR 900 kW (Curve HRR RAMP in Figure 4).
- Smoke production fraction is 0,07 kg /kg.
- The highest HRR growth rate is 36 kW/s (time interval from 30th to 50th second), or, expressed in terms of the t-squared HRR-growth model, the growth time is t_g » 40 s (UltraFast fire).
- Heat of combustion is 27.1 MJ/kg, total heat is 125 MJ.

Two different scenarios were investigated with fire ignition in main room and with fire ignition in lavatory.

In Figure 4, HRR RAMP curve corresponds to Test II of Kurikka experiments [1], others curves correspond to FDS simulation results with different setup. The simulated curves deviate from the prescribed HRR after 100 s, because of lack of oxygen, which in its turn caused by small volume of prison cell (about 40 m^3).

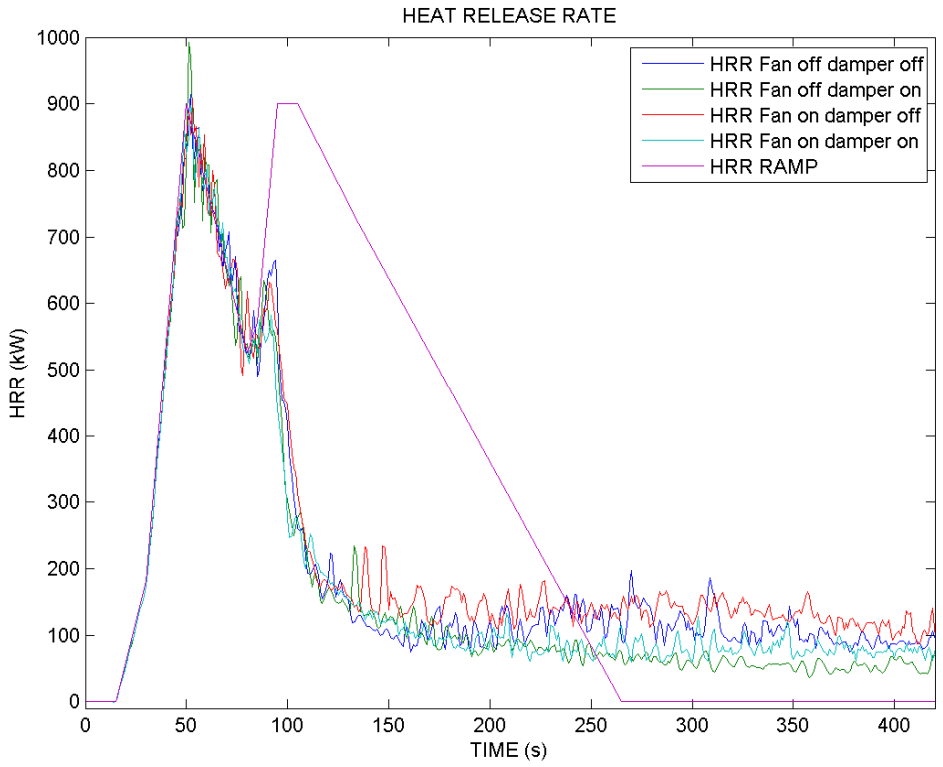

Figure 4. Heat release rate (HRR) from simulations (FIRE IN THE ROOM CASE)

4.2 RESULTS ON PRESSURE AND FLOW RATES

Results presented in this chapter are derived from the simulation model with following parameters:

- Mesh size 20 x 20 cm
- Gas concentrations were mapped on cutted surface on distance of 1 m from wall with imaginary door opening.

Damper activation time has not varied a lot in different cases with damper in supply duct. Times of damper activation are presented in Table 1.

Table 1. Damper activation times.

Case	Time from ignition (s)
Fan off Damper on Room fire	36
Fan on Damper on Room fire	39
Fan off Damper on WC fire	33
Fan on Damper on WC fire	39

4.2.1 Pressure

Figure 5 shows the pressure development in the prison cell with ignition source. The sudden rise of pressure follows after 30 seconds from ignition. It reaches a peak at about 50 seconds time. The hightest pressure rise is observed in simulation case with fans disabled and damper in inlet duct. The lowest pressure rise is observed in simulation with fans enabled and no dampers. Simulations with position of fire in main room shows higher pressure rises as compared with the same simulations with fire in WC.

a)

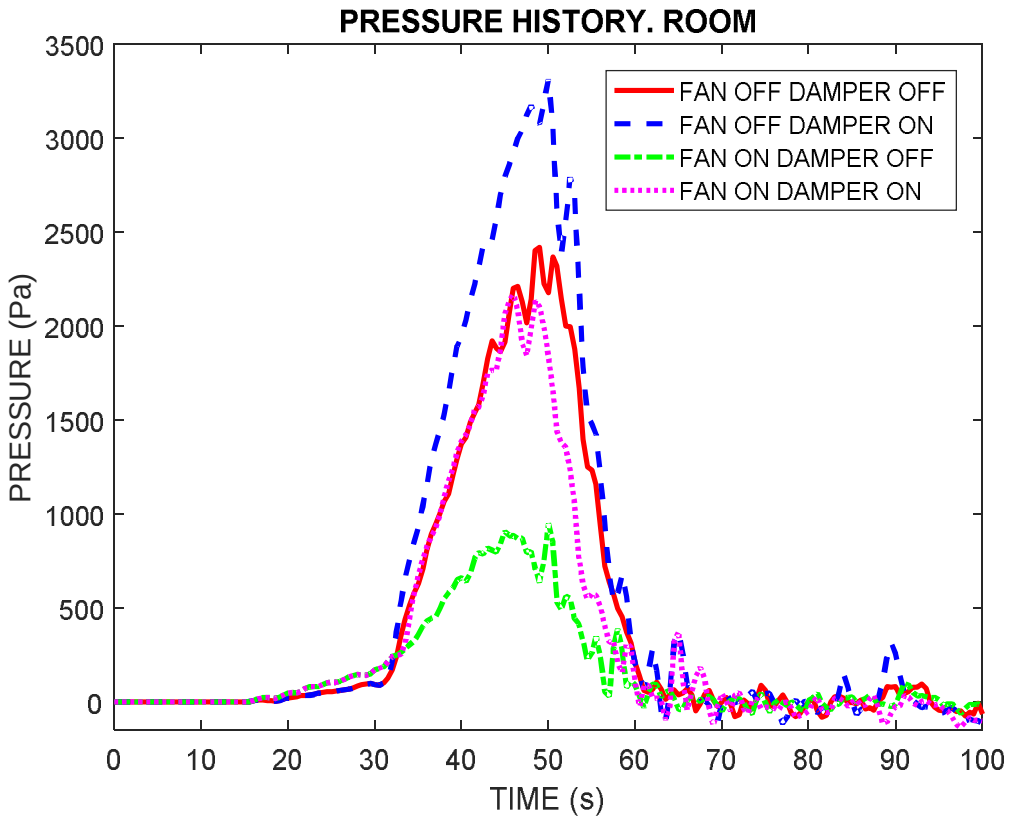

b)

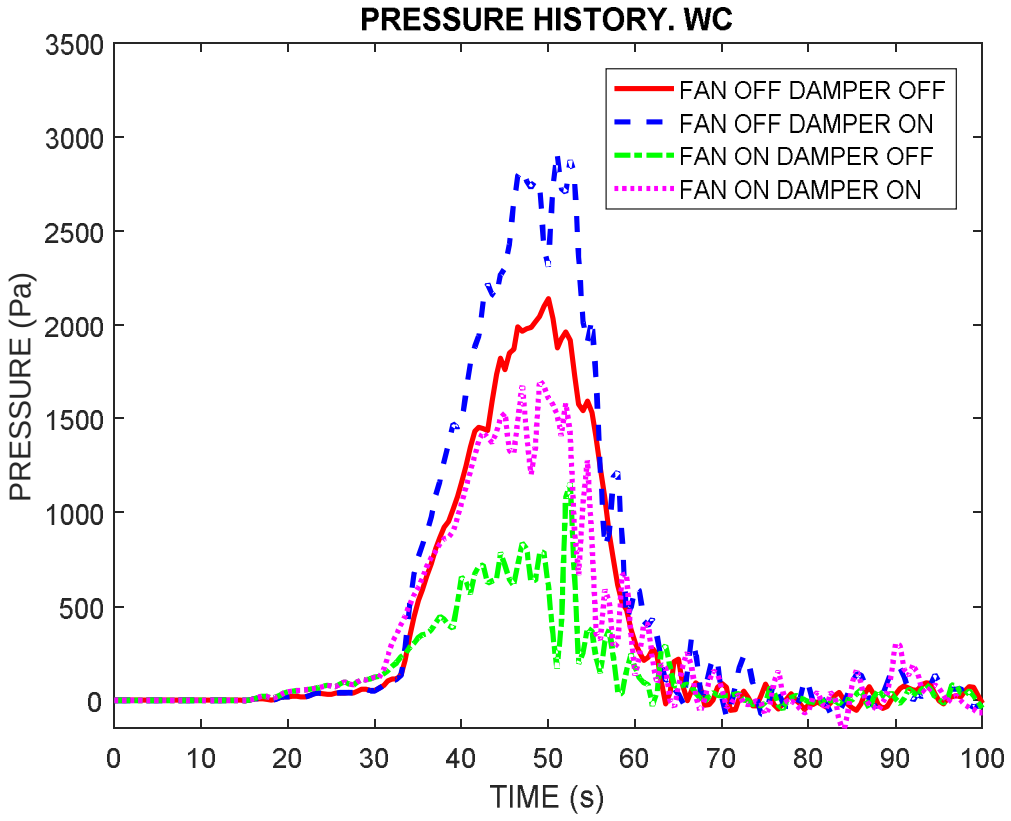

Figure 5. *Pressure history (in Pascals), a) Room, b) WC*

The results can be summarized as follows:

FAN ON/OFF	Pressure graphs shows that the same cases with fan turned on/off differ from each other. 'FAN OFF'-simulations are performed with damper in place of fan. Pressure in FAN OFF case is visibly larger than in FAN ON case. Difference between these two cases is approximately 1500 Pa.
DAMPER ON/OFF	The cases with supply-side dampers indicate about 1000 Pa higher peak pressure than cases without supply ventilation dampers.
POSITION ROOM/WC	Position of burner has a moderate effect to the pressure in the studied cases. Maximum of pressure in scenarios where fire is in the room is constantly higher compared to the scenarios where fire is in the WC (rest rooms). The maximum pressure in the Room-Fire scenarios is approximately 15% larger in WC-Fire scenarios.

4.2.2 Leakage

Leakages caused by pressure differential between sealed appartments and environment are presented in Figure 6.

a)

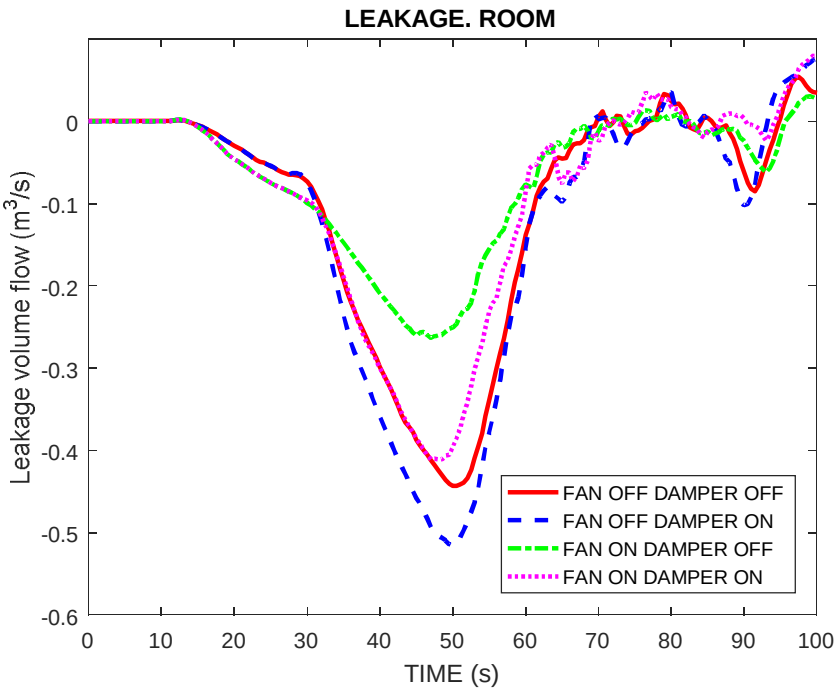

b)

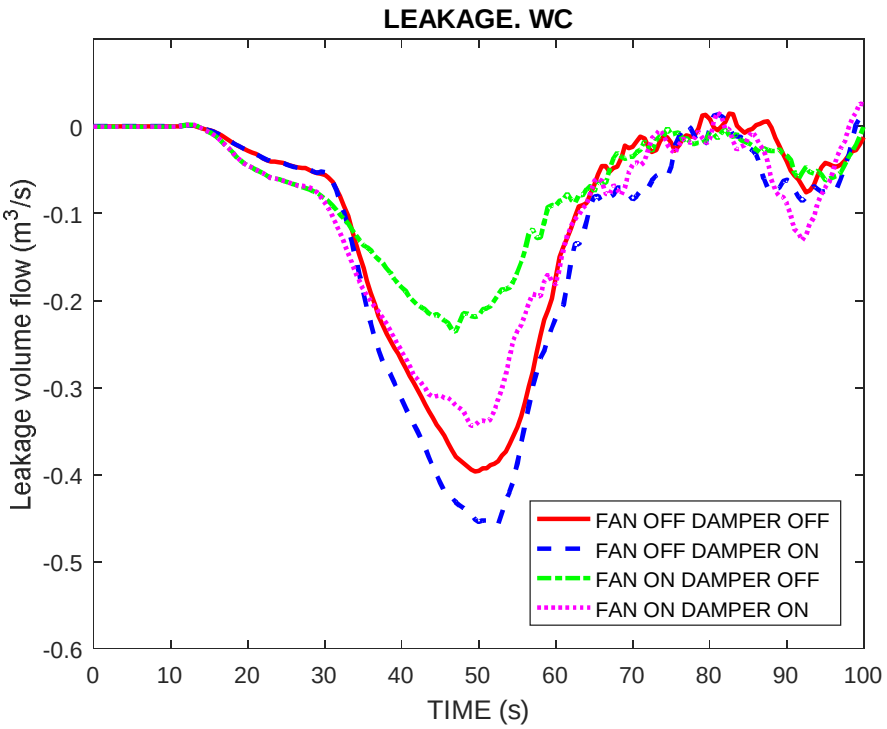

Figure 6. *Leakage (in m^3/s), a) Room, b) WC.*

Leakage is on its maximum, when the pressure reaches the peak. Leakage volume flowes are larger in cases with larger increasing of pressure.

4.2.3 Air volume flow in ducts

Volume flows in ventilation ducts were measured. Results for the supply ducts flows are presented in Figure 7.; For the exhaust ducts in Figure 8.

a)

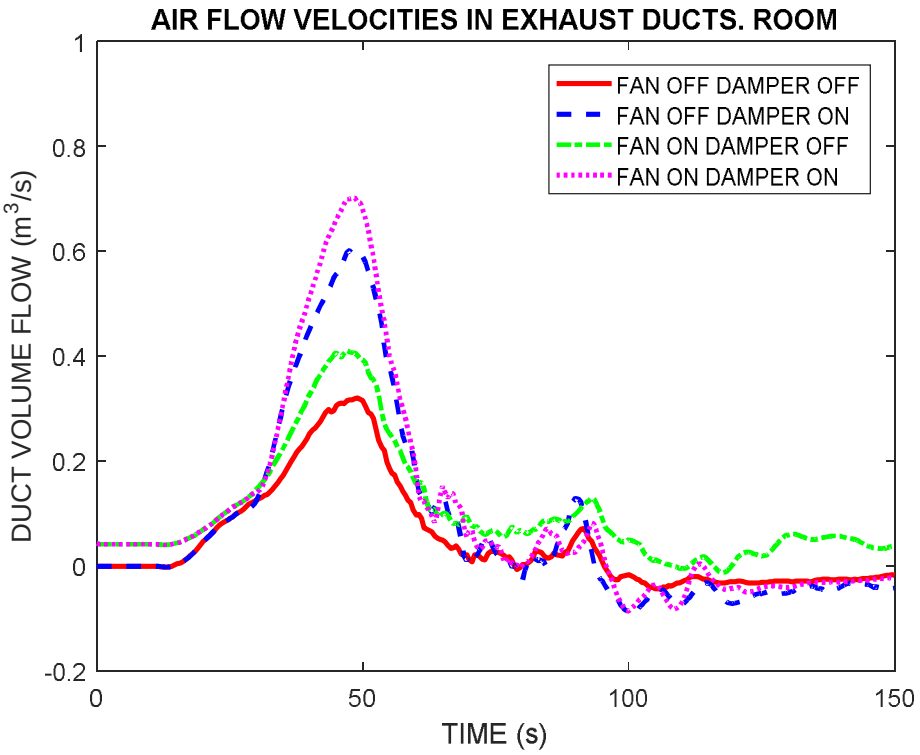

b)

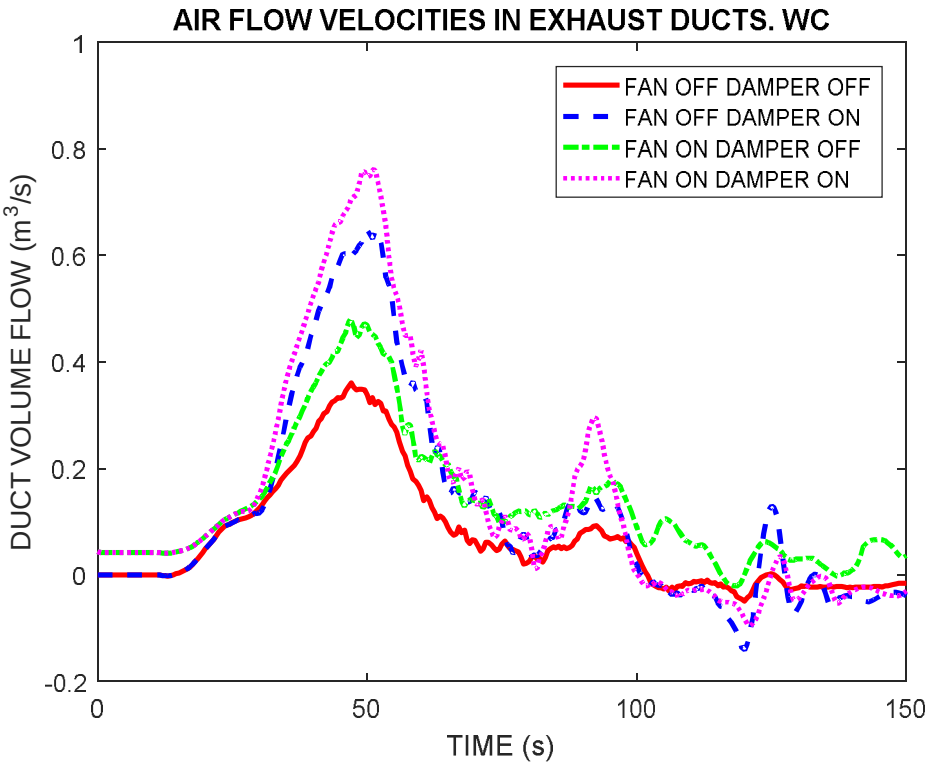

Figure 7. *Airflow in exhaust ducts (in m^3/s), a) Room, b) WC.*

a)

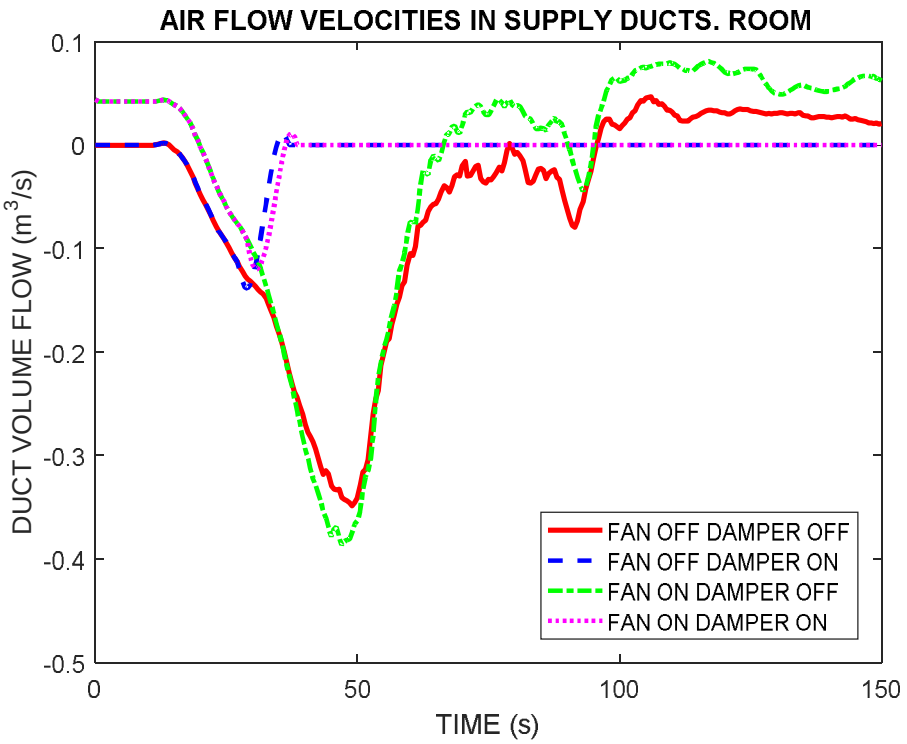

b)

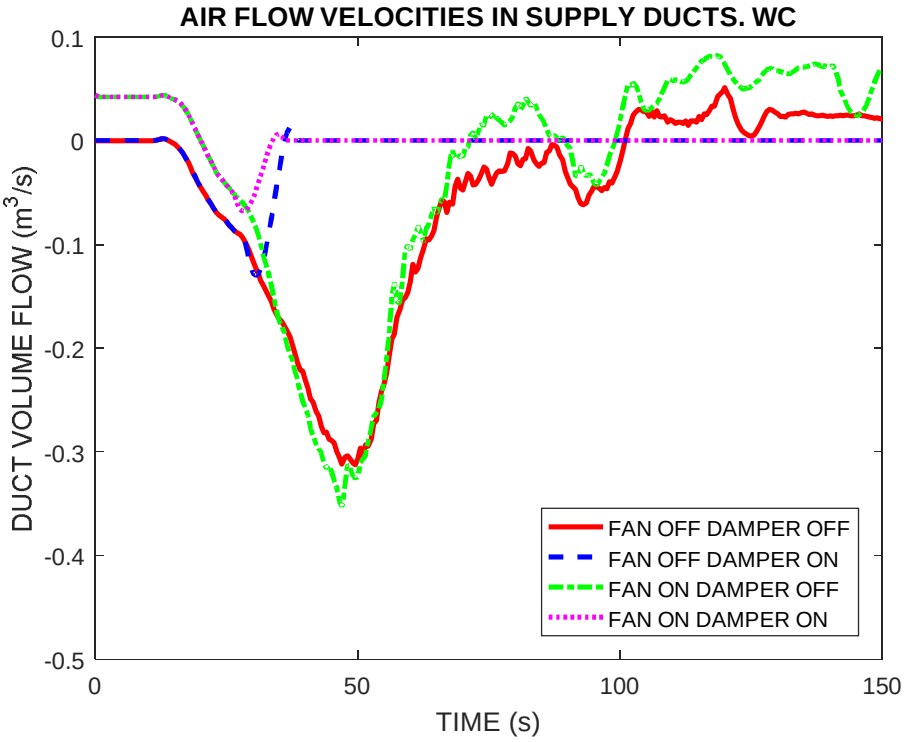

Figure 8. *Airflow in supply ducts (in m^3/s).*

In Figures 8a and 8b the some of supply duct air flows go to zero level after the activation of damper at 35-40 s time from the fire ignition.

4.3 GAS TOXICITY AND TEMPERATURE IN THE CELL OF FIRE ORIGIN

In this section we present the simulation results of

a) carbon monoxide concentration (mol/mol)
b) carbon dioxide concentration (mol/mol)
c) oxygen concentration (mol/mol)
d) Fractional Effective Dose (FED) value
e) temperature (°C)

in the cell of fire origin.

Maximum concentration levels reached in simulations do not differ from each other for room in fire. Maximum concentration of gases during all simulation time are collected in Table 2.

Table 2. Gas concentrations. (FIRE IN THE ROOM CASE. KURIKKA HRR).

Parameter	Maximum value in cell with fire (sim)
CO	n. 12800 ppm
CO_2	n. 0.073 mol/mol
0_2	n. 0.094 kg/kg

For example, according to NKB 1994:07 – directive, in case of poor visibility (less than 1 dB/m), people are considered to be exposed to toxic gases. In this case, the critical conditions of the limit values with respect to personal safety are as follows (Table 3) [7]:

Table 3. NKB 1994:07's limit gas concentrations.

Critical limit	
	ppm
Carbon monoxide (CO)	<2000
Carbon dioxide (CO_2)	<5%
Oxygen (O_2)	>15%

For the room of fire origin, gas concentrations were measured at 0.5m level above the floor. Results for carbon dioxide, oxygen and carbon monoxide are presented in following figures.

a)

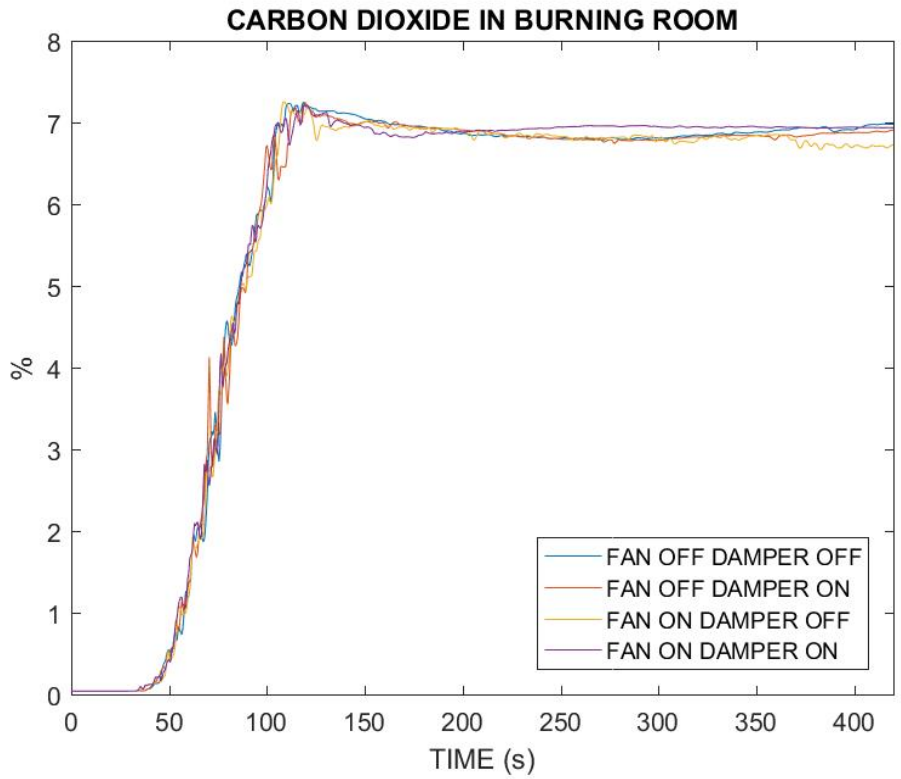
CARBON DIOXIDE IN BURNING ROOM
%
TIME (s)
FAN OFF DAMPER OFF
FAN OFF DAMPER ON
FAN ON DAMPER OFF
FAN ON DAMPER ON

b)

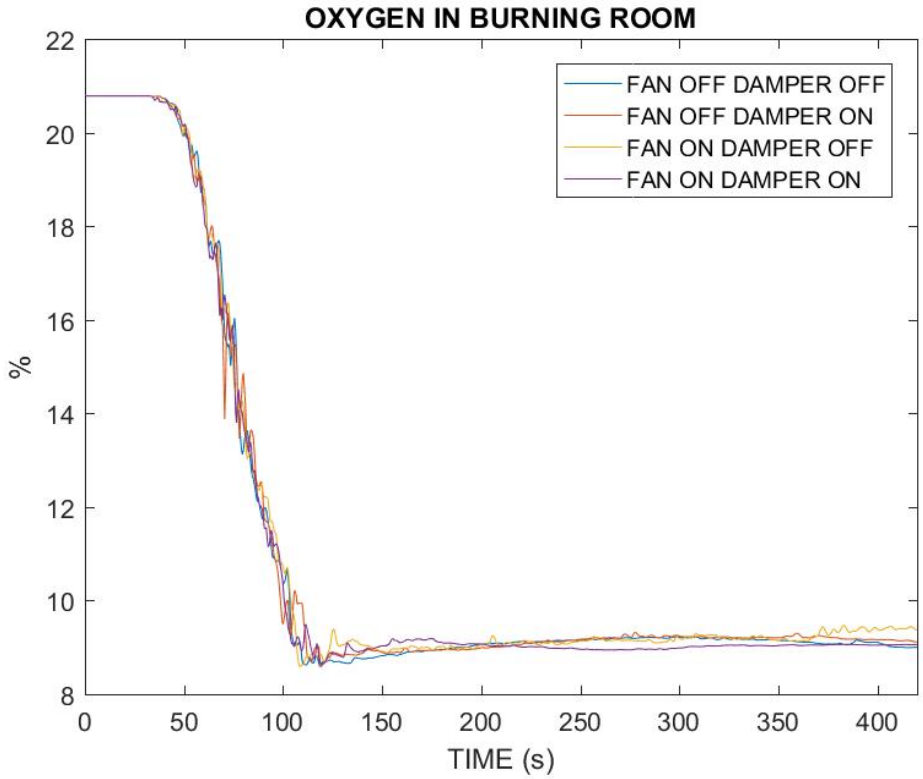
OXYGEN IN BURNING ROOM
%
TIME (s)
FAN OFF DAMPER OFF
FAN OFF DAMPER ON
FAN ON DAMPER OFF
FAN ON DAMPER ON

c)

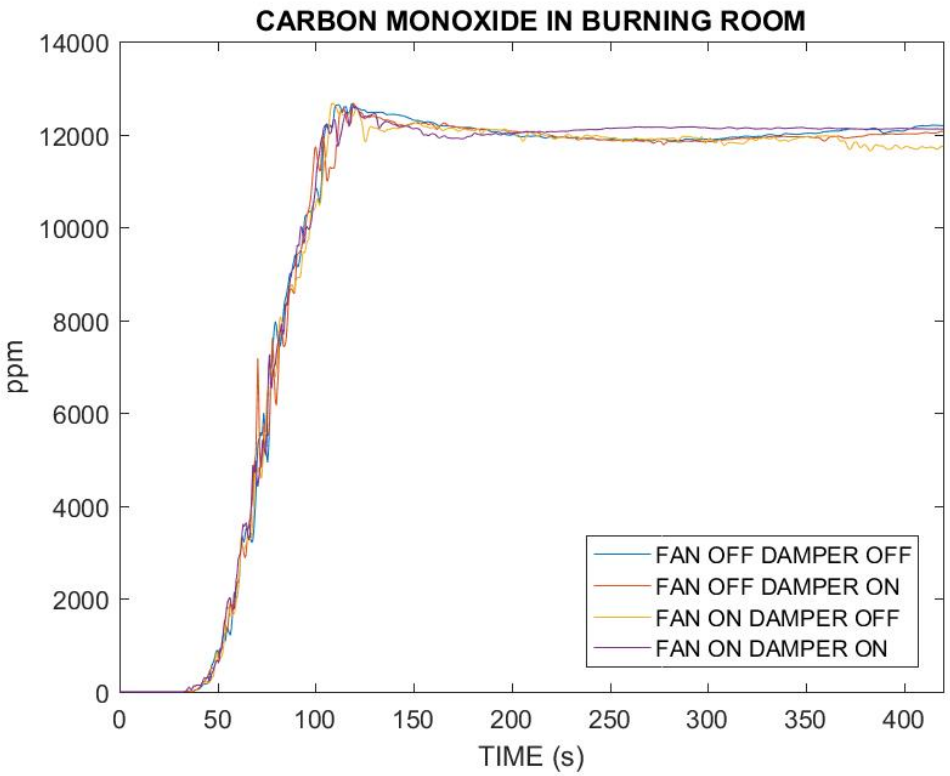

Figure 9. *Gas concentrations a) Carbon Dioxide, b) Oxygen, c) Carbon Monoxide.*

Figure 9 shows the air conditions in fire room. The carbon dioxide volume concentration goes over 5% in about 80 s. Oxygen concentration falls below 15% in approximately same time. Carbon monoxide increase over 2000 ppm faster, this time is about 60 s.

4.4 MODEL SENSITIVITY TO MESH SIZE

Same model was tested with different mesh sizes. In this chapter the results for models with 10 mm and 20 mm mesh size are presented.

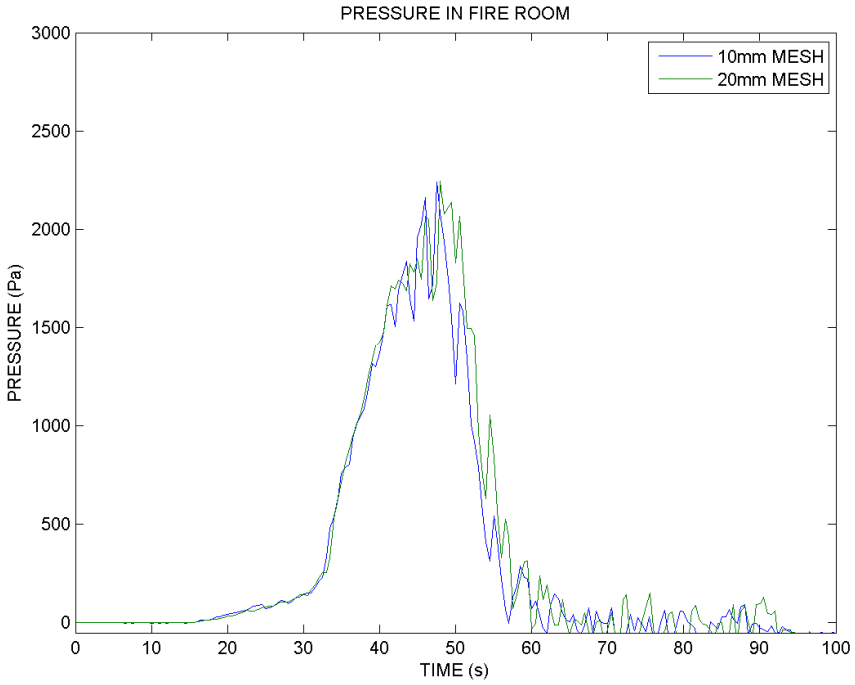

Figure 10. Pressure history (FIRE IN THE ROOM CASE Fan activated Damper activated).

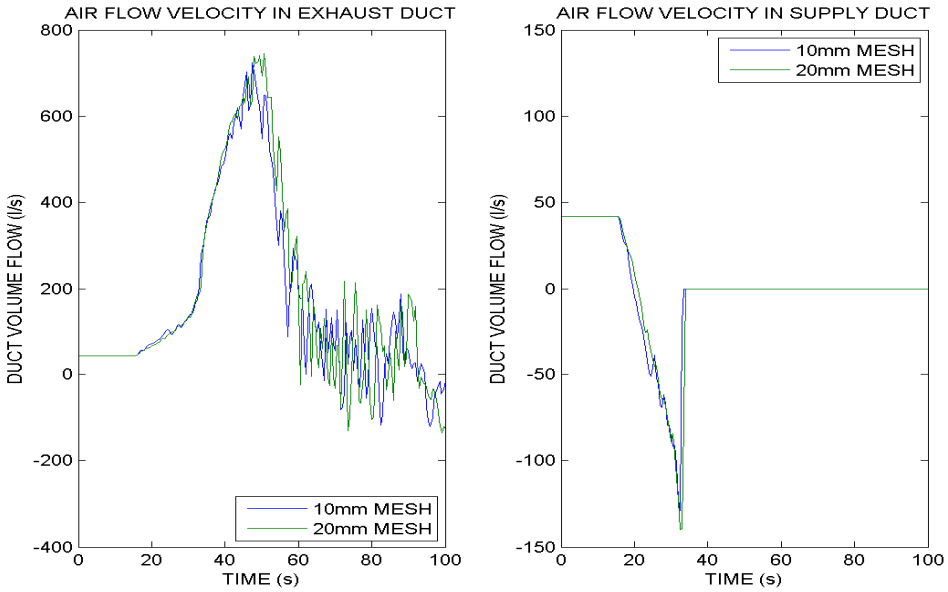

Figure 11. Airflow in ducts (FIRE IN THE ROOM CASE Fan activated Damper activated).

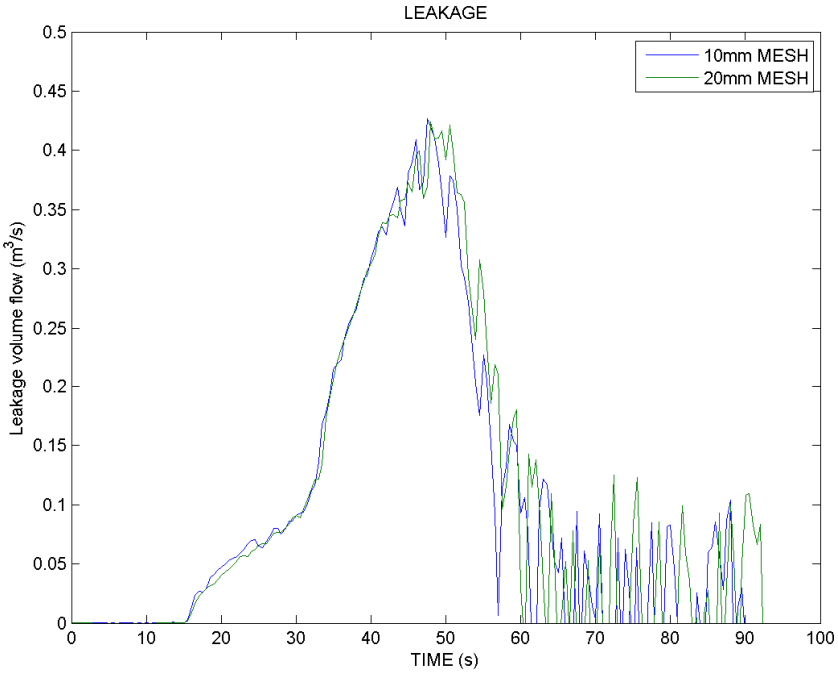

Figure 12. Leakage (FIRE IN THE ROOM CASE Fan activated Damper activated).

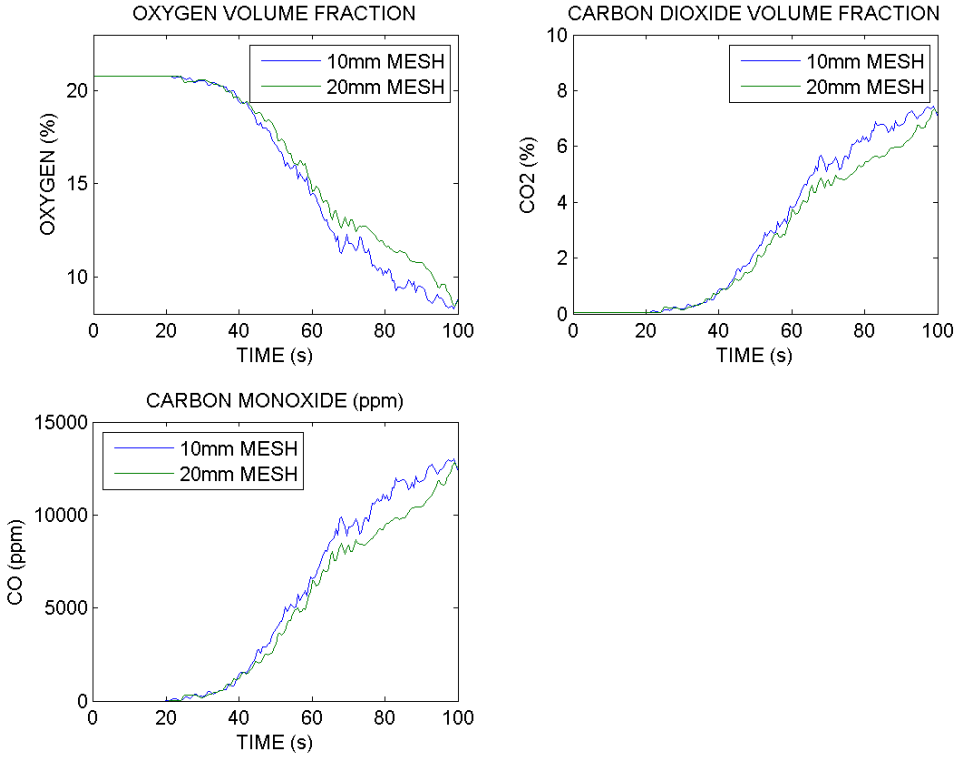

Figure 13. Gas concentrations (FIRE IN THE ROOM CASE Fan activated Damper activated).

5 SIMULATIONS BASED ON ESTIMATED PRISON-CELL FIRE DEVELOPMENT

5.1 HEAT RELEASE RATE

The model of prison cell was also tested with different HRR curves simulating a fire involving the fire load typical of Finnish prisons [8].

The information on the prison cell fire load is presented as a generic description of the fire-load items and the number of the items. This semi-quantitative information was quantified in three steps:

- First, the items were assigned estimates of their weight.
- Second, the items were characterised by an effective heat of combustion [MJ/kg] that converts the mass load [kg] to fire load [MJ] (Figure 14a).
- Third, an estimate of the heat release rate HRR [kW] the fire load was formed on the basis of data of relevant fire experiments (Figures 14b and 14c) [9,10].

All steps and hence also the results involve uncertainties. There were taken into account and modelled by using the Monte Carlo technique developed by VTT as a practical tool for fire-safety engineering analysis. [11,12,13,14,15,16,17,18].

a)

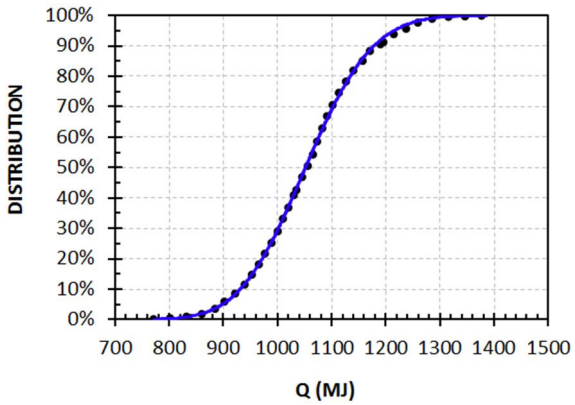

b)

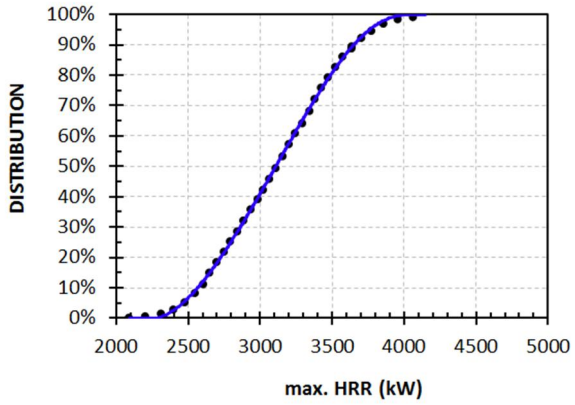

c)
HRR growing time to 1 MW
$t_{g\ high}$ = 100 s
$t_{g\ med}$ = 115 s
$t_{g\ low}$ = 130 s

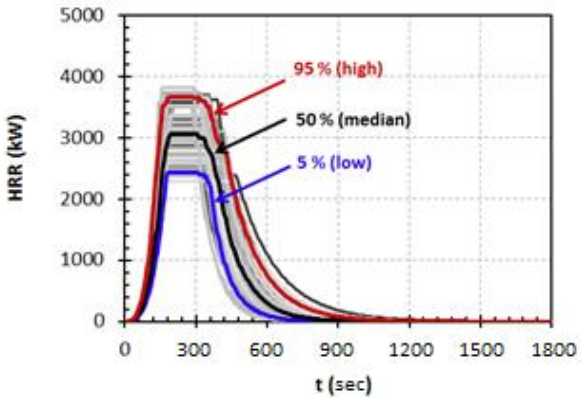

Figure 14. Distributions of a) the fire load and b) the maximum HRR, and, c) a sample of HRR curves of which three design HRR curves were selected representing fires of low, high and medium intensities.

Heat release rates from simulations are presented in Figure 15. Presented results are for cases with no dampers and fan turned off.

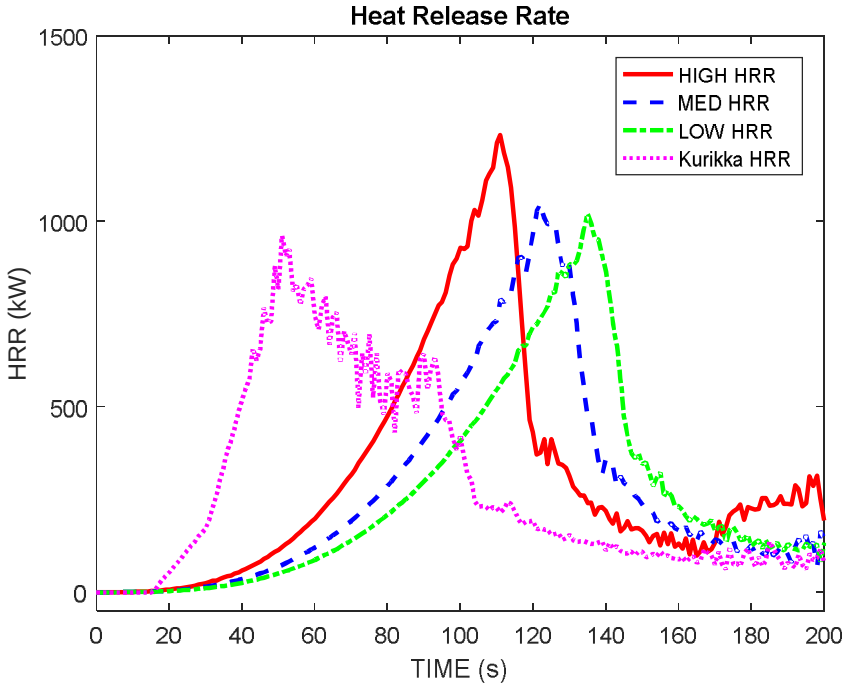

Figure 15. HRR during simulations HIGH, MED, LOW and Kurikka HRR (FAN OFF DAMPER OFF. ROOM)

In Figure 15, ultrafast growing fire HRR (Kurikka) is compared to the fires with estimated HRR. Peak of HRR in simulations do not differ a lot in 4 different cases. Heats of released energy (integral of HRR function with respect to time) are look alike.

5.2 RESULTS ON PRESSURE AND FLOW RATES

5.2.1 Pressure

Pressure in the cell of fire origin was measured at all simulation time. The peak pressure in FAN OFF DAMPER OFF case at high, medium and low HRR are 900, 600 and 500 Pa, respectively.

a)

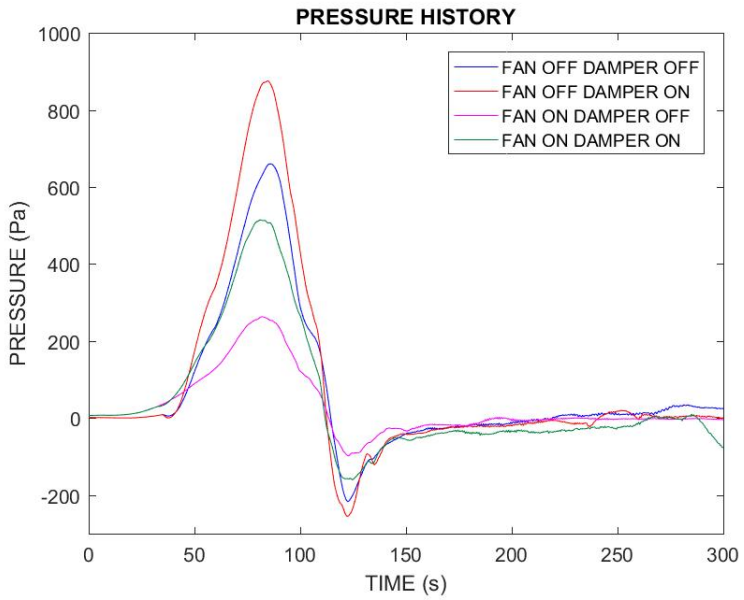

b)

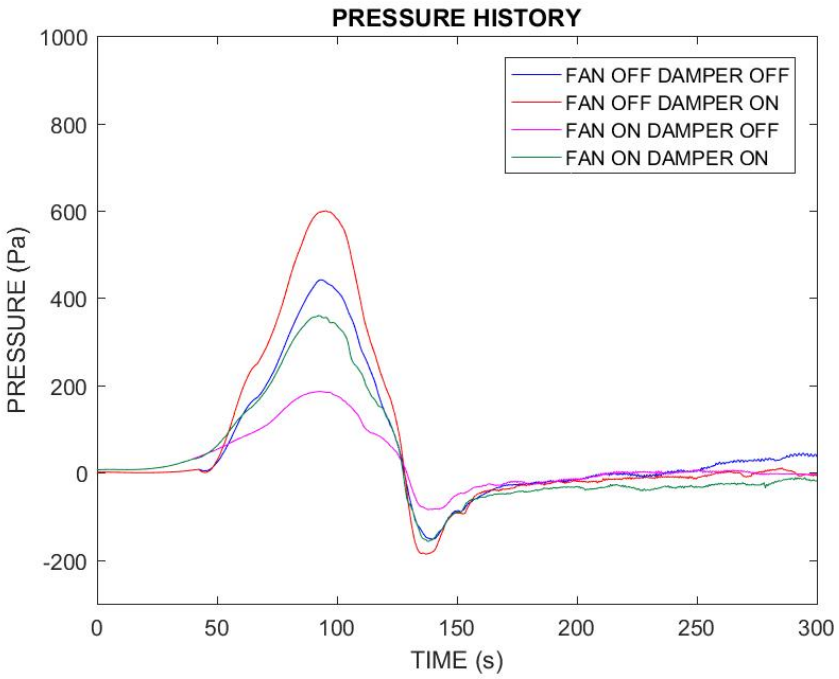

c)

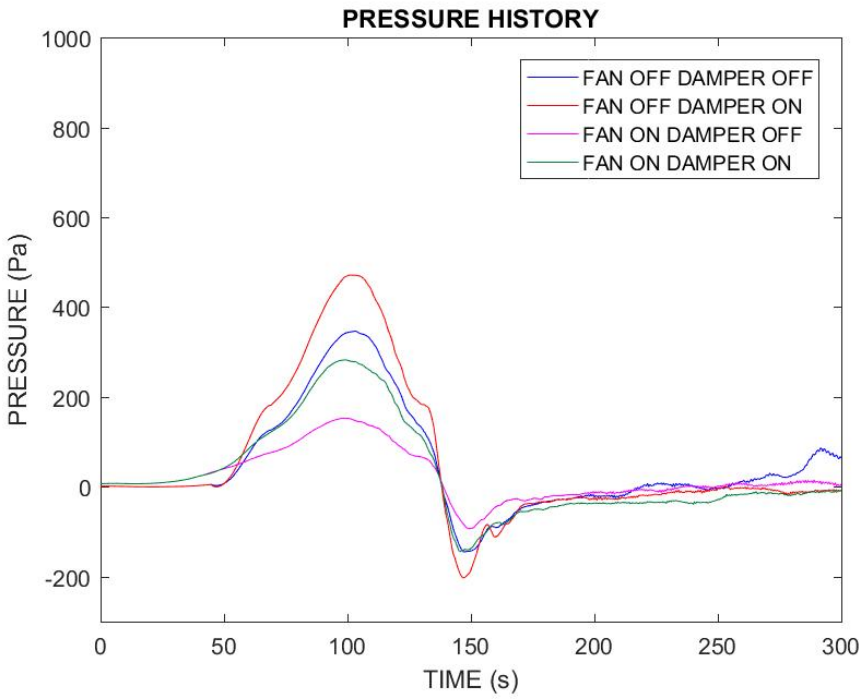

Figure 16. Pressure history. a) HIGH, b) MED, c) LOW HRR.

5.2.2 Leakage

Leakages caused by pressure differential between sealed appartments and environment are presented in Figure 17. Small differences in initial leakages can be explained by that exhaust fan turned off and supply fan turned create a small pressure rise that is compensated by minor leakages.

a)

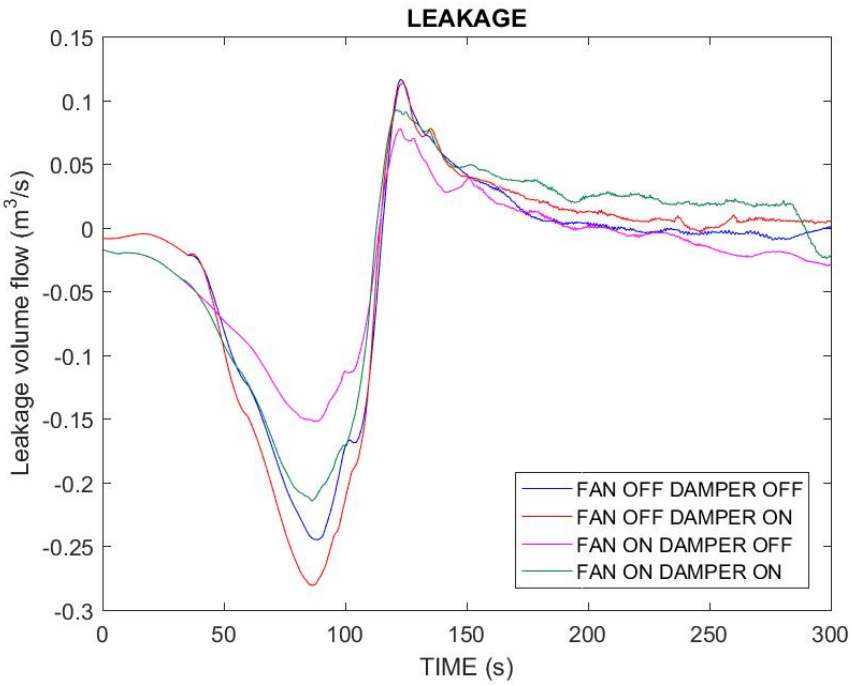
LEAKAGE
Leakage volume flow (m3/s)
TIME (s)
FAN OFF DAMPER OFF
FAN OFF DAMPER ON
FAN ON DAMPER OFF
FAN ON DAMPER ON

b)

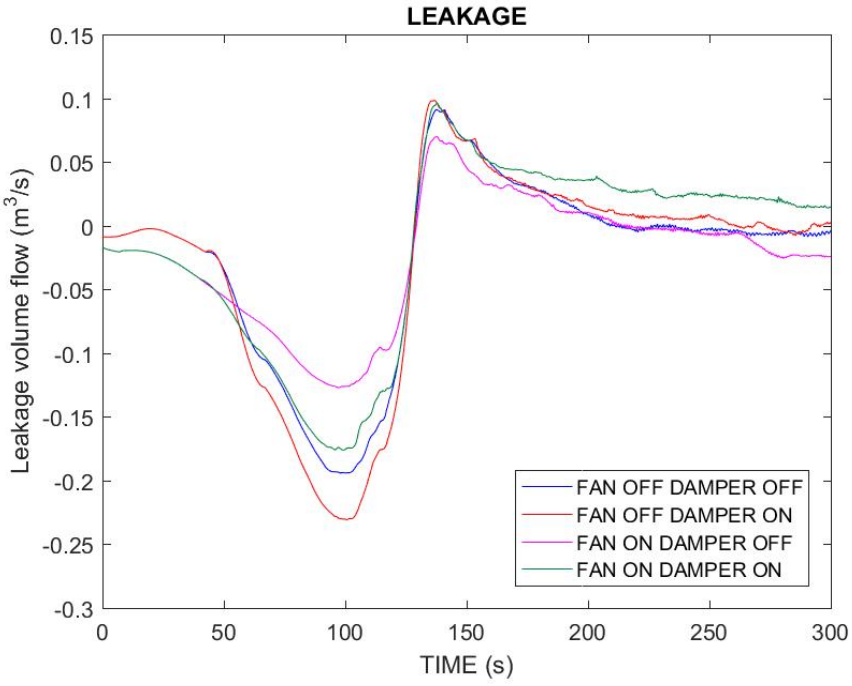
LEAKAGE
Leakage volume flow (m3/s)
TIME (s)
FAN OFF DAMPER OFF
FAN OFF DAMPER ON
FAN ON DAMPER OFF
FAN ON DAMPER ON

c)

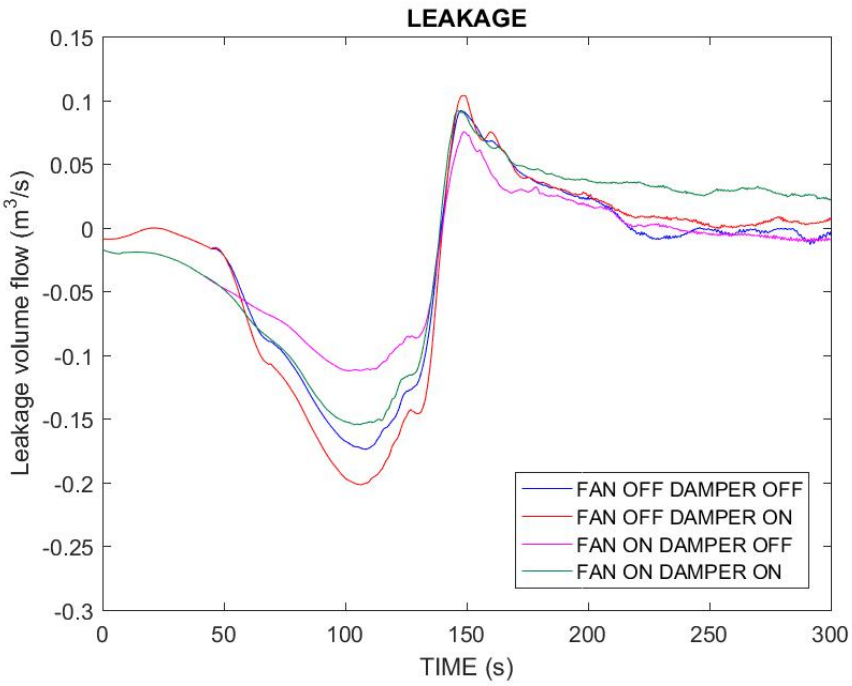

Figure 17. Leakage (in m^3/s). a) HIGH, b) MED, c) LOW HRR.

5.2.3 Air volume flow in ducts

Volume flows in ventilation ducts are presented in following figures. Results for the supply ducts flows are presented in Figure 18.; For the exhaust ducts in Figure 19.

a)

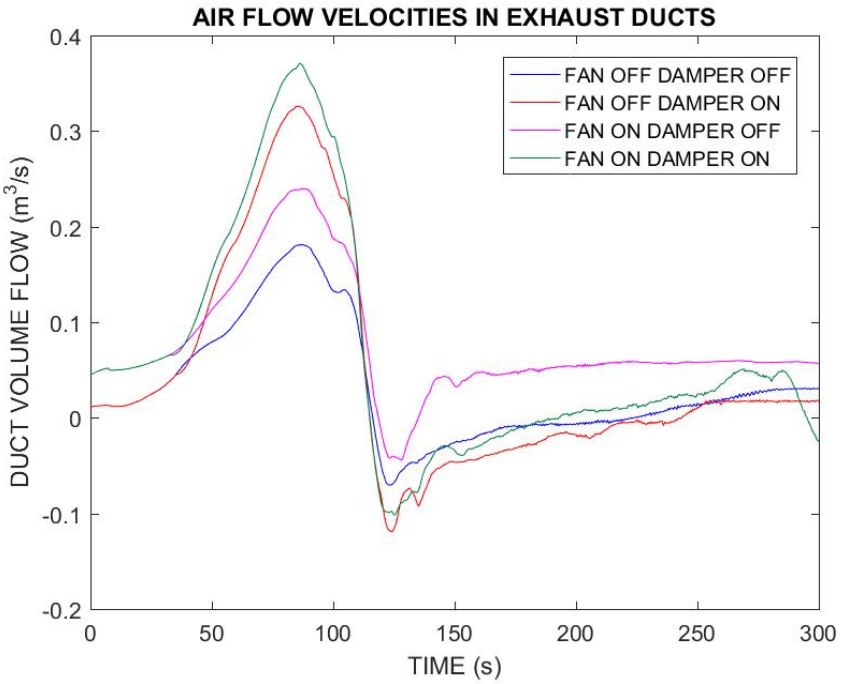

b)

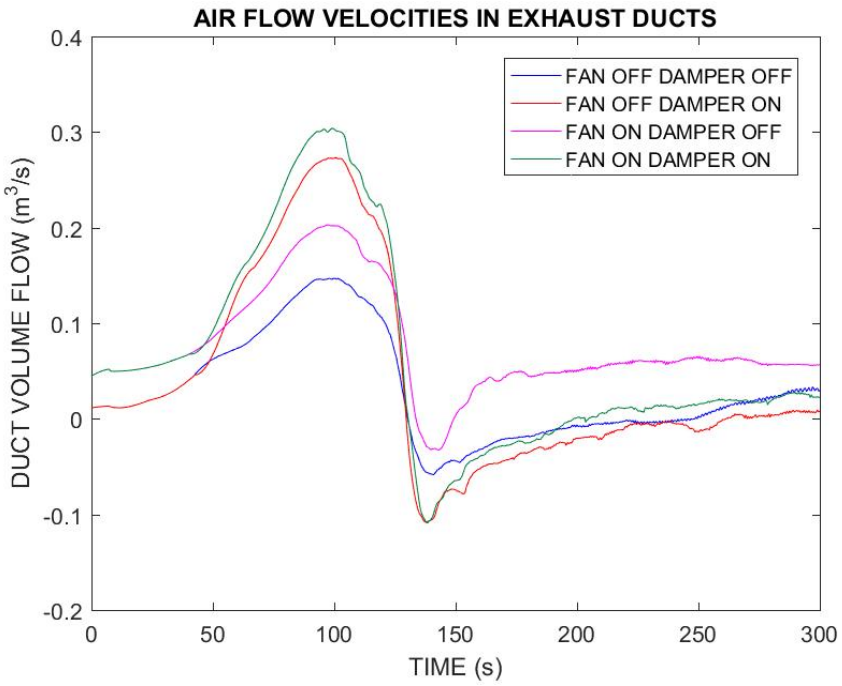

c)

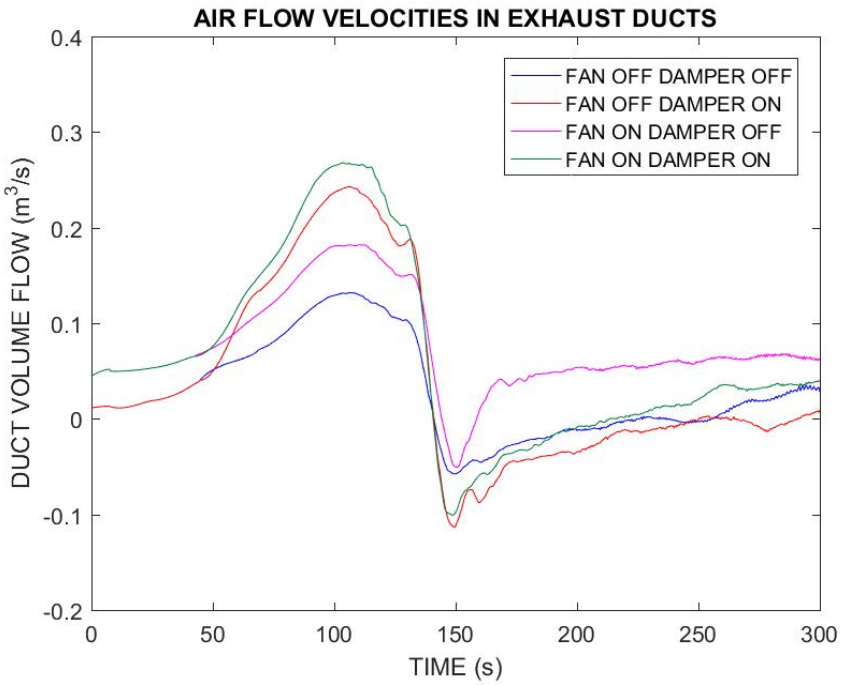

Figure 18. Airflow in exhaust ducts (in m^3/s). a) HIGH, b) MED, c) LOW HRR.

a)

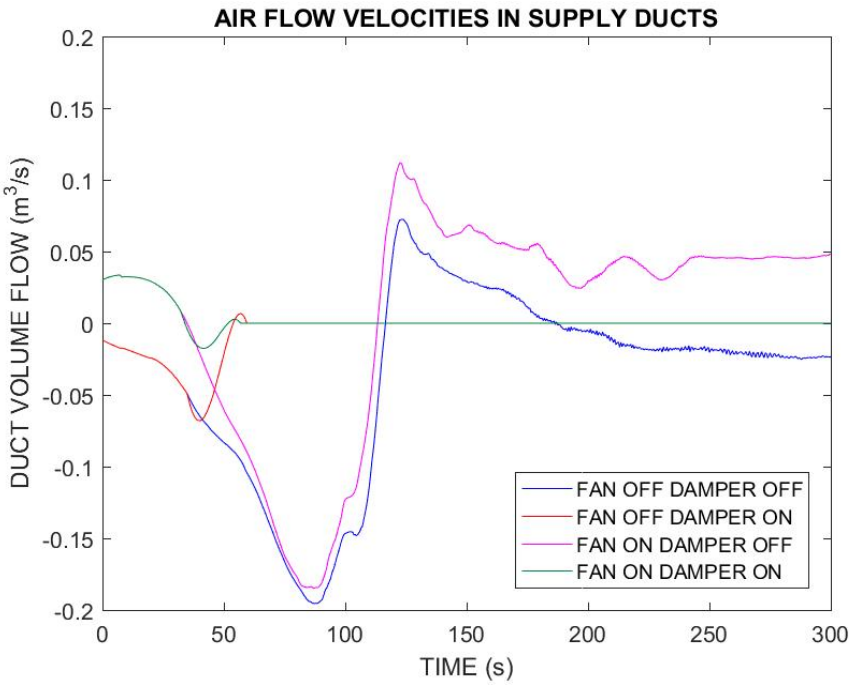
AIR FLOW VELOCITIES IN SUPPLY DUCTS
DUCT VOLUME FLOW (m3/s)
TIME (s)
FAN OFF DAMPER OFF
FAN OFF DAMPER ON
FAN ON DAMPER OFF
FAN ON DAMPER ON

b)

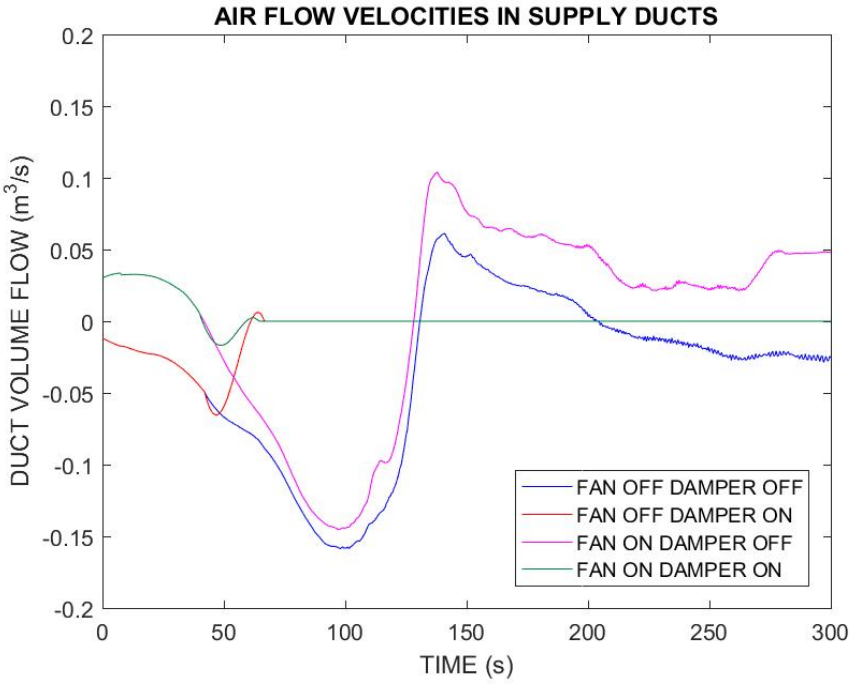
AIR FLOW VELOCITIES IN SUPPLY DUCTS
DUCT VOLUME FLOW (m3/s)
TIME (s)
FAN OFF DAMPER OFF
FAN OFF DAMPER ON
FAN ON DAMPER OFF
FAN ON DAMPER ON

c)

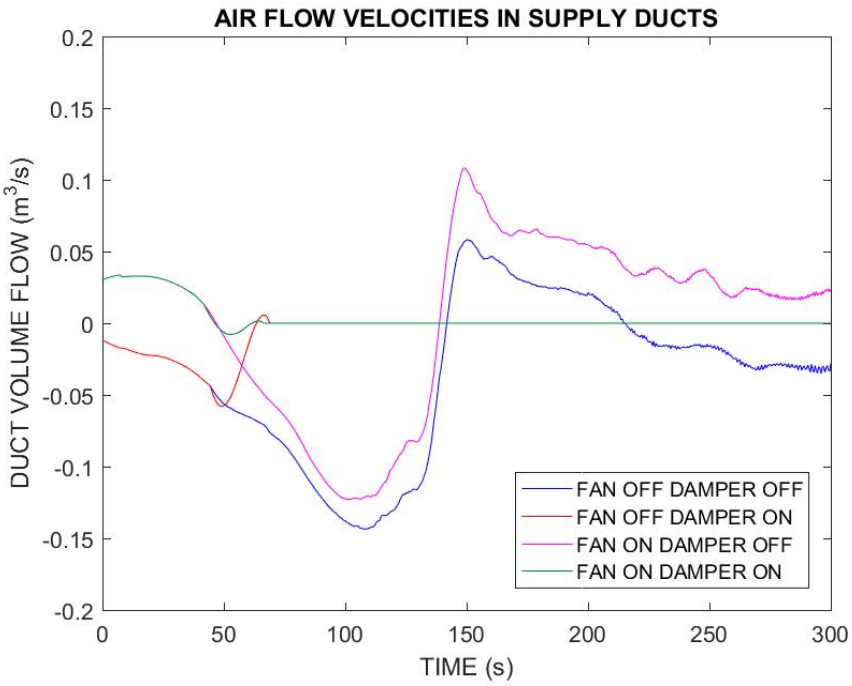

Figure 19. Airflow in supply ducts (in m^3/s). a) HIGH, b) MED, c) LOW HRR.

Figure 19 shows that in cases with dampers after the damper activation air flow through the supply duct stopes. The negative sign of supply ducts air flows can be explained that air flow revers its direction to the opposite when the fire pressure is increased enough to overpower fan action.

Curves that respond to the simulations with disactivated fan, do not start from 40 l/s flow in supply duct. It is because in case of fan disabled, the duct leading to the fan is closed by damper all simulation time.

6 ASSESSMENT OF THE IMPACT OF SMOKE DAMPERS ON THE SAFETY IN THE ADJACENT CELLS

Influence of fire to adjacent prison cells is under investigation in this part. Simulations were performed with ultrafast HRR (Kurikka) and fast growing HRR. Fast HRR is about 2 times less than ultrafast HRR from Kurikka experiments. Slower HRR has a growth rate t_g = 130 s. This means that after 130 s from fire ignition, HRR reashes 1 MW value.

The list of simulated cases is:

- BOTH DAMPERS
  - dampers activate after 10 sec of simulation (smoke dampers).
  - dampers locate on supply and exhaust ducts.
- FAN OFF DAMPER OFF
  - no dampers in supply and exhaust ducts of cell.
  - fans are deactivated (dampers are used instead of fans), closed by metal plate.
- FAN OFF DAMPER
  - dampers are located in supply ducts of cells.
  - fans are turned off, closed by plate.
- FAN ON DAMPER OFF
  - fans are active.
  - no dampers at all.
- FAN ON DAMPER ON
  - fans are active.
  - dampers in supply air ducts of cells.

Table 4 shows the maximum gas concentration on the height of 2m above the floor in adjacent enclosure during the first 2.5 min of simulation. The most severe conditions in adjacent cell were obtained in case with fan turned off and no dampers in ventilation system.

Table 4. Conditions in adjacent prison cell (Examined time is 2.5 min from ignition).

		Limit value after 150 s from fire ignition (adjacent cell)					
		Simulated case.	O2	CO2	CO	Temperature	FED
			mol/mol	mol/mol	ppm	°C	-
2 m height above the floor	KURIKKA HRR (UltraFast)	BOTH DAMPERS	0.21	0.00039	0	20	0
		FAN OFF DAMPER OFF	0.195333	0.00777	1296.480	42.756	0.034
		FAN OFF DAMPER ON	0.199812	0.00512	830.598	39.532	0.021
		FAN ON DAMPER OFF	0.204628	0.00226	329.599	34.655	0.011
		FAN ON DAMPER ON	0.207178	0.00075	64.385	23.645	0.001
	FAST HRR	BOTH DAMPERS	0.21	0.00039	0	20	0
		FAN OFF DAMPER OFF	0.199443	0.00533	868.980	45.262	0.016
		FAN OFF DAMPER ON	0.203537	0.00291	443.166	35.241	0.008
		FAN ON DAMPER OFF	0.204978	0.00206	293.257	30.392	0.006
		FAN ON DAMPER ON	0.207797	0.00039	0.003	20.424	0.000
0.5 m height above the floor	KURIKKA HRR (UltraFast)	BOTH DAMPERS	0.21	0.00039	0	20	0
		FAN OFF DAMPER OFF	0.207794	0.00039	0.370	21.921	0.000
		FAN OFF DAMPER ON	0.207789	0.00039	0.804	21.419	0.000
		FAN ON DAMPER OFF	0.207765	0.00041	3.305	20.497	0.000
		FAN ON DAMPER ON	0.207785	0.00039	1.273	20.434	0.000
	FAST HRR	BOTH DAMPERS	0.21	0.00039	0	20	0
		FAN OFF DAMPER OFF	0.207797	0.00039	0.000	20.715	0.000
		FAN OFF DAMPER ON	0.207797	0.00039	0.016	20.633	0.000
		FAN ON DAMPER OFF	0.207796	0.00039	0.083	20.456	0.000
		FAN ON DAMPER ON	0.207797	0.00039	0.000	20.424	0.000
		CRITICAL VALUE (NKB 1994:07)	>0.15	<0.05	<2000	<80	<0.3

According to the results we can obtain that the limit values of adjacent cell conditions in Kurikka simulation values are higher than respective values in simulation with slower HRR. It can be explained that the higher pressure forces the more air to move from cell of fire ignition to adjacent cells. In Table 4 is presented the highest values in 2.5 min time from ignition, but It should be noted that oxygen is burned out in this time and pressure in the burning room decreased to the initial level.

7 DISCUSSION

Different fire simulations were carried out to show a sudden rise of pressure in an enclosure and caused by pressure smoke spreading via ventilation. Prison cell and its connection to the other cells via ventilation was modelled, and three different scenarios, based on empirical studies, were analysed. The influence of the following parameters was studied: position of the fire source, supply ventilation damper on/off, exhaust ventilation fan on/off. Effect of these parameters is summarized in Table 5. (more detailed information can be found from Chapters 4.2 and 5.2).

Table 5. Influnce of the factors to the pressure rise in fire room with ventilation and to the adjacent cell condition.

	Fire cell pressure		Adjacent cell conditions
Parameter	Type	Magnitude	Type
FAN ON/OFF	Lower/Higher	Strong	Better/Worse
DAMPER ON/OFF	Higher/Lower	Strong	Better/Worse
POSITION ROOM/WC	Higher/Lower	Moderate	-

The effect of the fire growth rate to pressure in burning room and leakage is presented in Figures 20 and 21.

a)

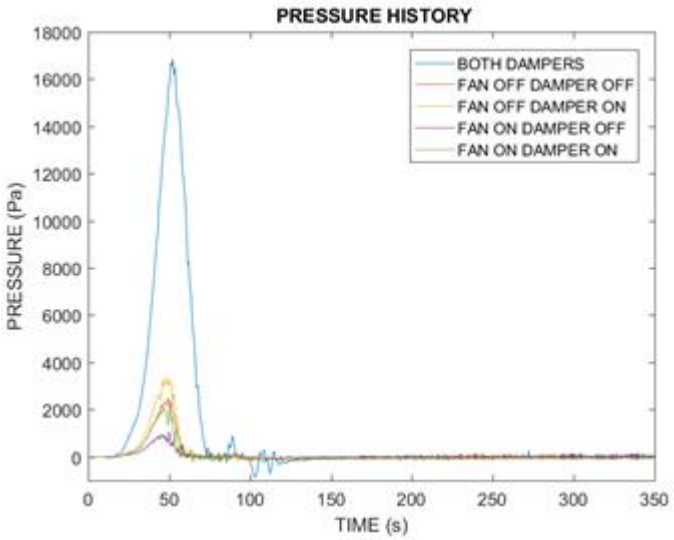

b)

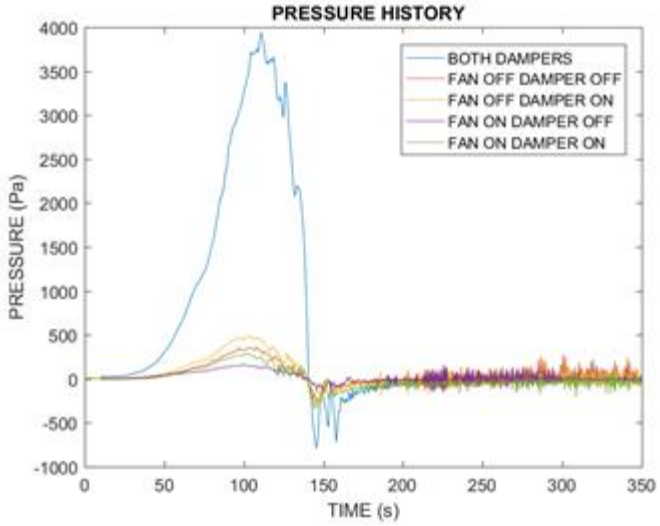

Figure 20. Pressure in burning room (in Pa). a) UltraFast, b) Fast HRR.

a)

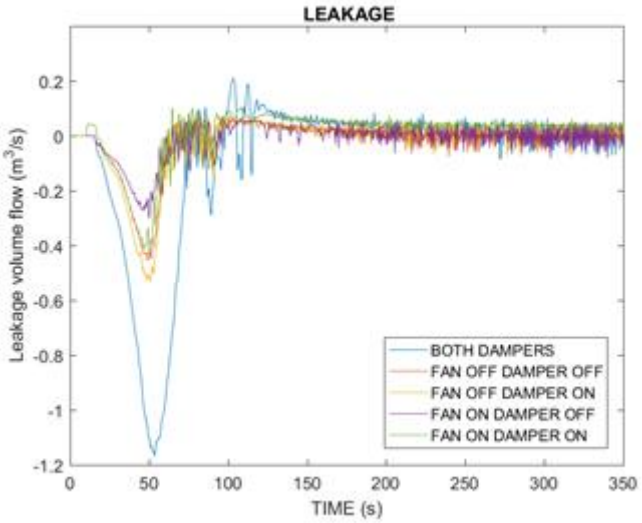

b)

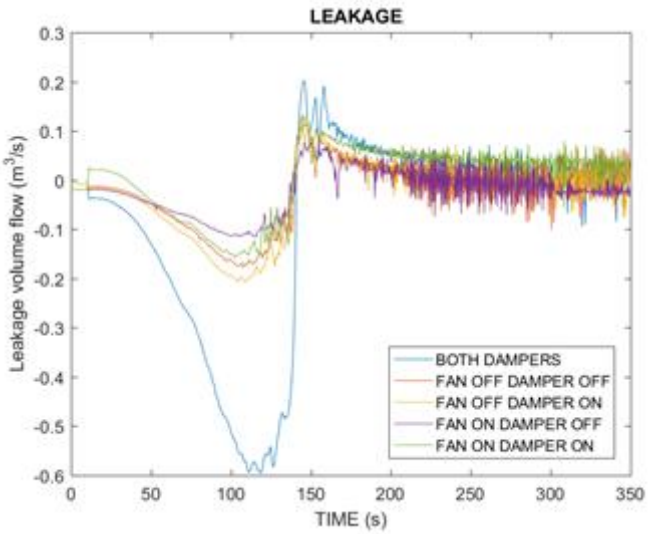

Figure 21. Leakage in burning room (in Pa). a) UltraFast, b) Fast HRR.

In case of ultrafast growing HRR, pressure rise is higher than in case of fast growing HRR. Higher pressure rise causes higher leakage from burning room (Figure 20 and 21).

In case of ultrafast HRR, the personnel have about 80 s time to rescue the prisoner of the ignition cell before the level of FED increases over 0.3 at 0.5 m above the floor. In case of the slower growing HRR the rescue time is about 130 s.

The safe rescuing of the prisoners requires less that the gas temperature is less than 120 ^{o}C. This temperature is achieved as follows:

- In case of ultrafast HRR, temperature at ceiling level reaches 120 ^{o}C in 35 s, at 2 meters above the floor – in 40 s. After 50 s whole room temperature is above 120 ^{o}C.

- In case of fast HRR, ceiling level reaches 120 ^{o}C in 65 s, at 2 meters above the floor – in 75 s. After 90 s whole room temperature is above 120 ^{o}C.

The concentrations at 2 m level in adjacent cell are lower than the critical concentrations during the 2.5 period from the ignition. At that time, the fire is extinguished due to the lack of oxygen, and the concentrations of toxic species start to decrease. This means that the prisoner of the adjacent cells not at great risk during such a fire. Conditions at 0.5 m height in the adjacent cells remain clearly safe for at least 2.5 min from the ignition.
(NOTE: The peak of pressure in simulations varies in range 0 – 2.5 min time from fire ignition).

According to the Table 4, the best results for the adjacent cell air conditions can be reached with activated exhaust fan and smoke damper in supply duct of combustion room. The slower growing HRR case with fan and damper options mentioned above shows that air conditions in adjacent room do not change even at 2 m height above the floor for at least 2.5 min from fire ignition. In addition, the operating fans make sure that the possible smoke in the neighbouring cells will be diluted as soon as the smoke production ends.

8 CONCLUSIONS

Based on the numerical fire simulations of the prison cell fires, we can draw the following conclusions.

With a realistic fire development, the peak over pressures will be close to 4000 Pa if both dampers of the fire cell are closed. This means that a mechanical failure of some structure can be expected. If one of the dampers is left open, the fire cell pressures remain below 1000 Pa, and there is no risk of structural damage. With ultrafast fire development, the observed peak pressures are 3.5 kPa even in the case of open damper, and damages are possible. Since the uncontrolled damages may lead to increased smoke spreading to neighbouring spaces, the full closing of the fire cell should be avoided.

The high overpressures (several hundreds of Pa or more) in the fire cell were found to last for 3 minutes of less. During this period, opening the cell door will result in strong smoke flow to the corridor.

In the cell of fire origin, the life safety criteria are met within 80...130 s from the ignition, depending on the rate of fire growth. However, from the viewpoint of gas temperatures, safe rescue is possible for personnel without protective equipment only during the first 50-90 s from the ignition.

Smoke spreading through the ventilation network was studied by monitoring the toxic concentrations in the neighbouring cells. The main conclusion was that some smoke was observed in all ventilation configurations, except those where both supply and exhaust ducts of the fire cell were closed by a damper. However, the toxic gas concentrations in the neighbouring cells remained at safe level when fire cell's exhaust duct was kept open (the safe situation for pressure), if the ventilation fan was kept on. The operating fan also provides fresh air to the neighbouring cells and dilutes the concentrations when the fire is suppressed.

The smoke spreading to the neighbouring cells was found to be strongest when the ventilation system's fan is off and there are no dampers. In this case, the conditions of the neighbouring cells can become dangerous at 2 m height from the floor, but will remain tolerable closer to the floor.

The simulations investigating the adjacent cells' toxicity conditions were limited to a 2.5 min duration. During this time, the fire heat release rate had reduced significantly due to the lack of oxygen, but the risks of longer exposures in the cases with closed fans cannot be ruled out. Longer simulations are needed to investigate the longer exposures.

APPENDIX A Table of simulated cases.

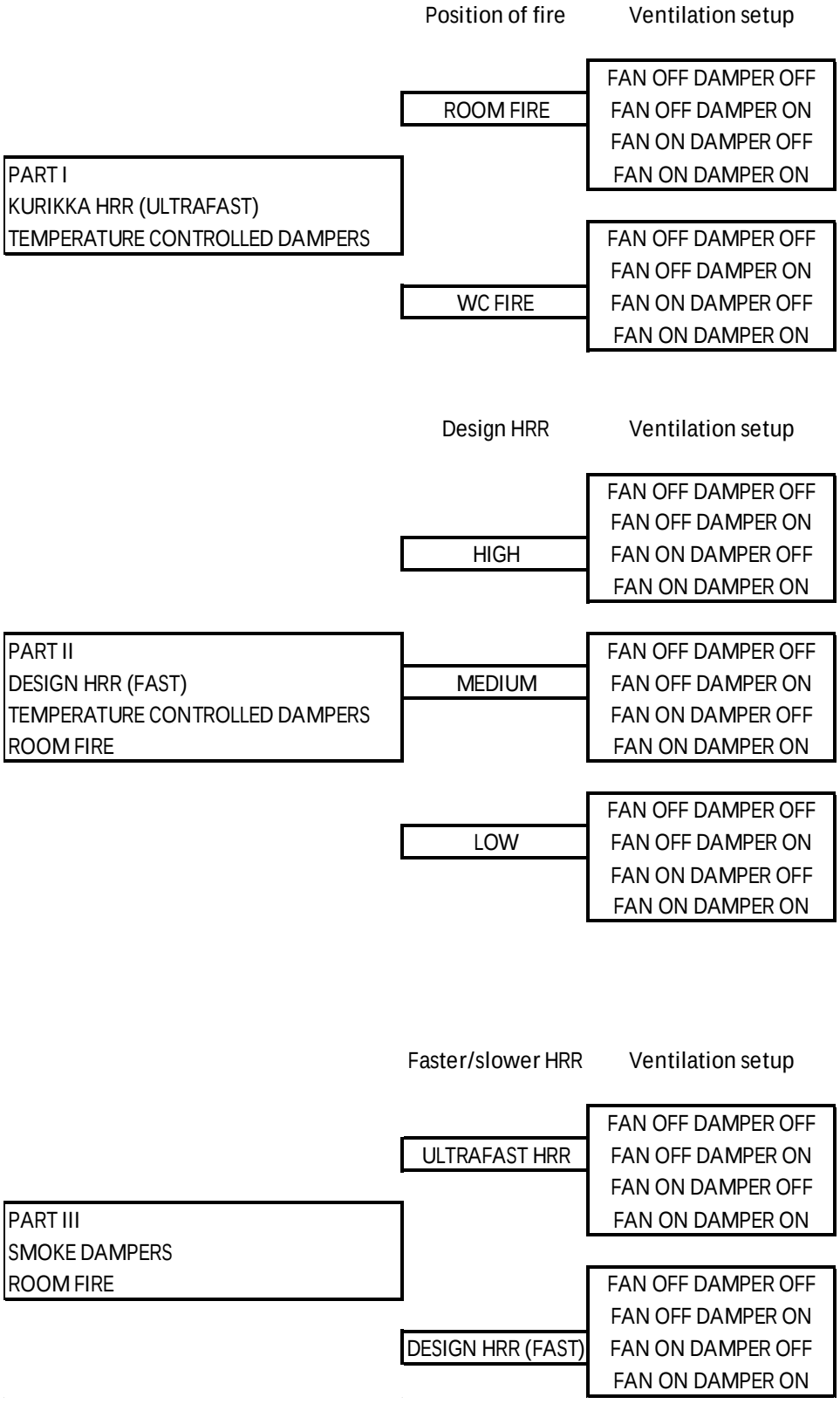

APPENDIX B. Verification of ventilation system.

To be sure that model is made correctly, ventilation system was revised separately. For this task temperature rise in enclosure was measured on vertical plane every 20 cm. On the basis of this data, average gases temperature in burning room was calculated. Average gas temperature in enclosure was also measured using FDS statictical tool. Simulations were performed on one series of 'FAN OFF DAMPER OFF' tests.

For this slightly rough test, burning can be assumed as an isobaric process. Previous tests show that actual pressure increasing can be at the most about 3500 Pa. From point of air thermal expansion and produced by this air flows in the ducts, changes in pressure can be neglected. Within the pressure 3.5 kPa is small value compared with atmospheric pressure, which is approximately equal to 101 kPa. Using ideal gas equation and assuming that process is isobaric, we get that the rate of volume changing affected by increasing of temperature is equal to sum of air outflows.

Rate of volume increasing compared to the sum of measured outflows is presented in next figure. Sum of outflows consists from leakage from the cell, supply and exhaust ducts airflows.

Simulation starts from negative time point which means ventilation works normally before the ignition at 0 sec time. Supply and exhaust fan's volume flows are about 120 l/s at the begining of the simulation. Both fans close at 10 sec. Figure 1B-a shows the ventilation system scheme for supply or exhaust ventilation system.

a)

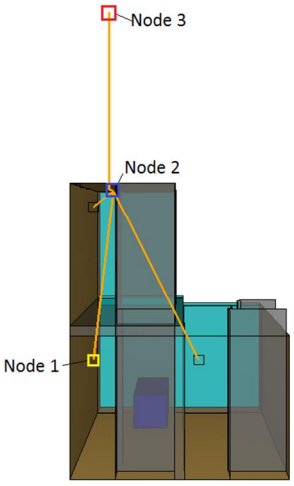

b)

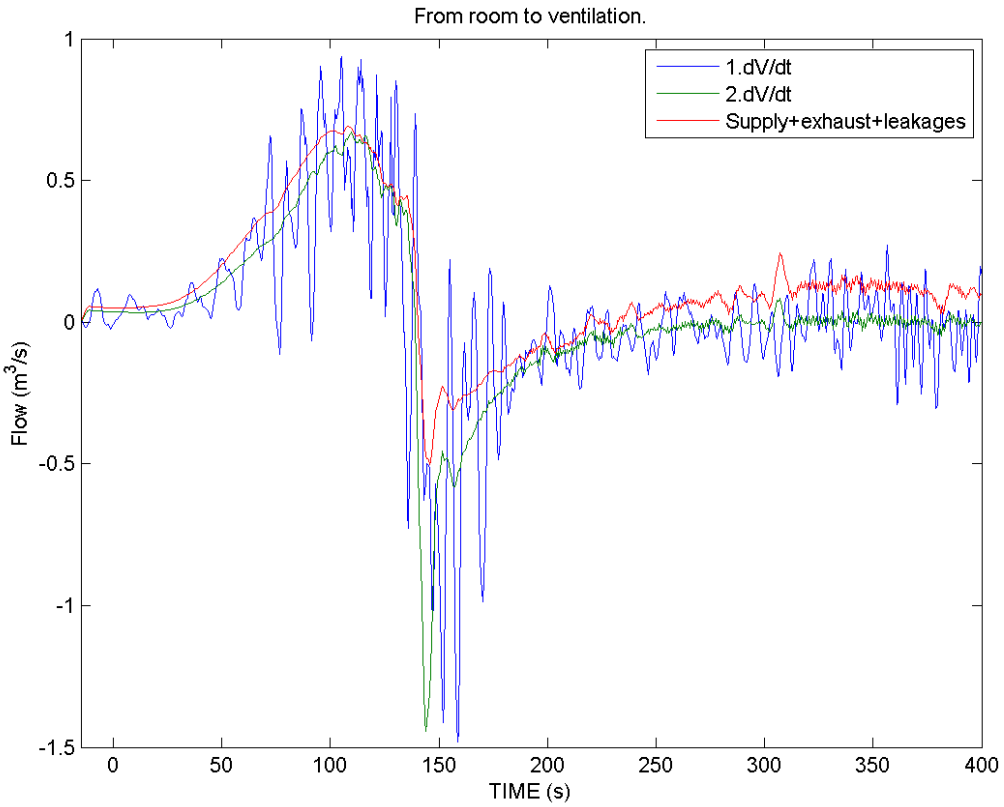

Figure 1B. a) Ventilation system scheme, b) Volume thermal expansion rate vs. outflows due to ventilation and leakage.

In Figure 1B, curve 1.dV/dt responds to volume changing calculated using the average temperature of thermometers placed on the vertical plane. Curve 2 dV/dt responds to volume changing calculated by average temperature of whole combustion room. The last curve means summary of airflows from the combustion room through inlet, oulet and leakages.

a)

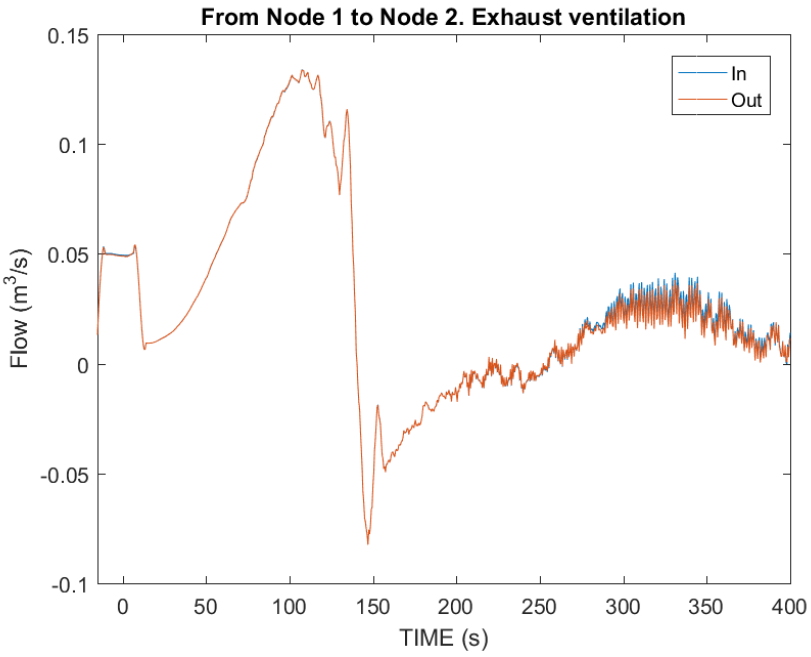

b)

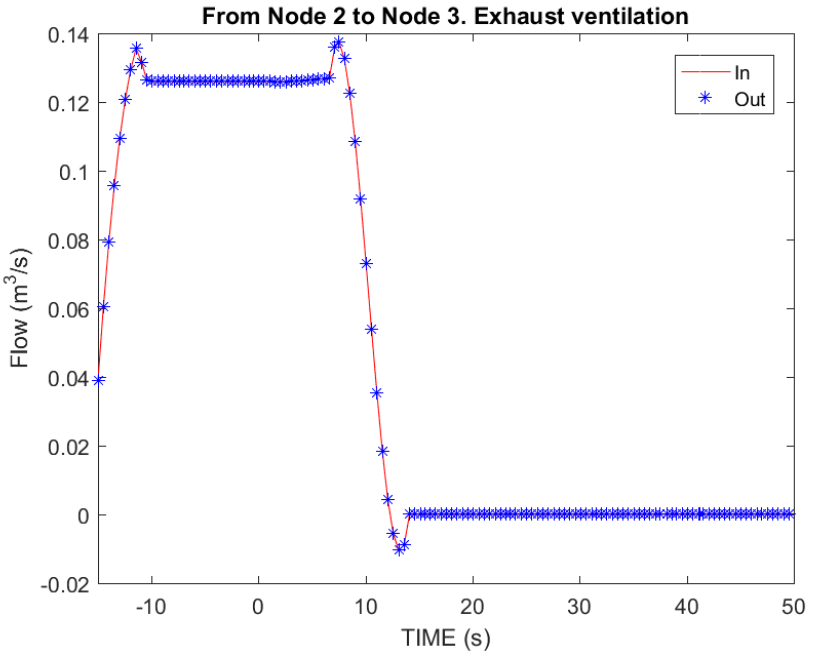

Figure 2B. *a) Exhaust duct flow from Node 1 to Node 2. b) from Node 2 to Node 3.*

Figures 2A and 2B show the airflows in exhaust ventilation during simulation of fire. Fire ignites at 0 s time point, while simulation starts 15 s earlier that time point. The airflow from the combustion room at first 25 s is 40 l/s. After that time fan closes and airflow goes down to the zero (Figure 2B a). At about 20 s time point airflow starts to increase due to pressure in burning room (Figure 2B b).

a)

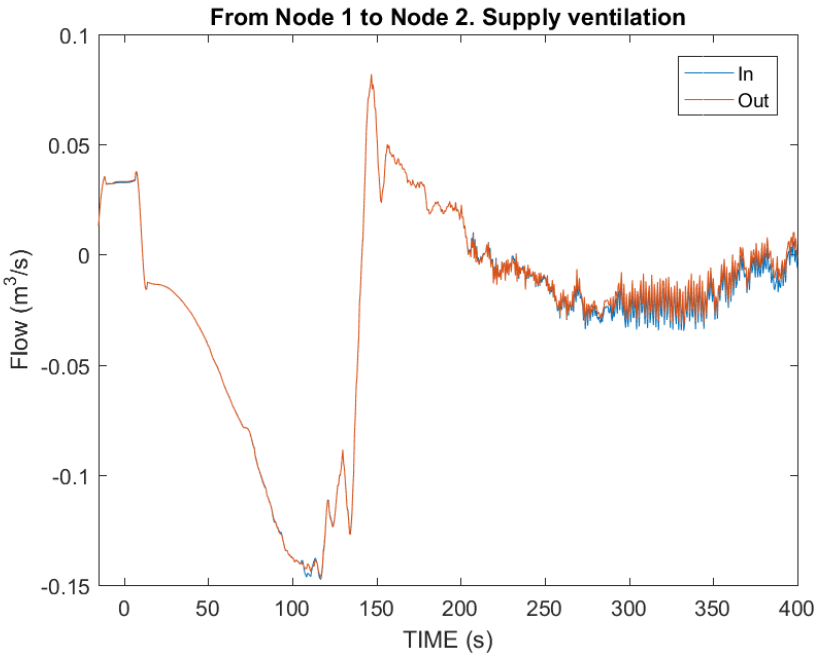

b)

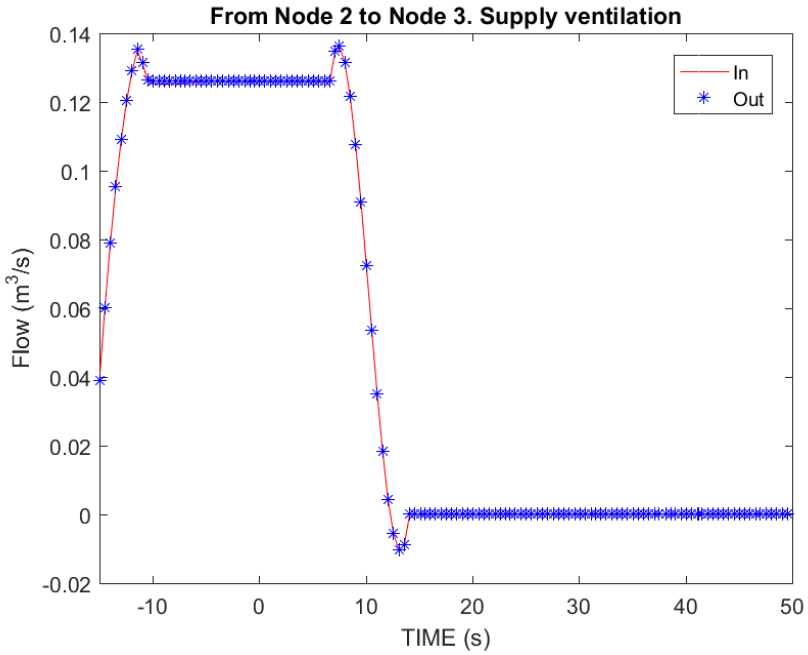

Figure 3B. a) *Supply duct flow from Node 1 to Node 2. b) from Node 2 to Node 3.*

Figures 3A and 3B show the airflows in supply ventilation. At the first seconds of simulation airflow in supply ventilation duct connected to the burning room is 40 l/s. Airflow in supply ventilation duct from node 2 to node 3 is about 120 l/s, because the model consists from 3 ventilated prison cells. When the fan is disactivated and closed, the airflows goes to the zero (Figure 3B b). When the fire causes the pressure rise, airflows reverse it direction with respect to initial direction (Figure 3B a).

APPENDIX C Example of FDS INPUT. Case: room fire, fan on, damper on.

```
&HEAD CHID='FANONDAMPERONROOM'/

MISC RESTART=.TRUE./

&TIME T_END=420.0, T_BEGIN= -5.0 /
&MESH ID='MESH1', IJK=12,29,16, XB=0.0,2.4,0.0,5.8,0.0,3.2/
&MESH ID='MESH2', IJK=11,29,15, XB=2.4,4.6,0.0,5.8,0.0,3.0/
&MESH ID='MESH3', IJK=11,29,15, XB=0.0,2.2,0.0,5.8,3.2,6.2/

&MESH ID='MESH4', IJK=12,3,16, XB=0.0,2.4,5.8,6.4,0.0,3.2/
&VENT MB='YMAX',SURF_ID='OPEN',MESH_ID='MESH4', TRANSPARENCY=0.1/

&MESH ID='MESH5', IJK=11,3,15, XB=2.4,4.6,5.8,6.4,0.0,3.0/
&VENT MB='YMAX',SURF_ID='OPEN',MESH_ID='MESH5', TRANSPARENCY=0.1/

&MESH ID='MESH6', IJK=11,3,15, XB=0.0,2.2,5.8,6.4,3.2,6.2/
&VENT MB='YMAX',SURF_ID='OPEN',MESH_ID='MESH6', TRANSPARENCY=0.1/

&DUMP               SMOKE3D = .TRUE.,
                                  NFRAMES = 100,
                                  DT_PART = 1.0,
                                  DT_HRR  = 1.0,
                                  DT_DEVC = 0.5,
                                  DT_SLCF = 1.0,
                                  DT_BNDF = 1000000,
                                  DT_PL3D = 1000000,
                                  DT_ISOF = 1000000,
                                  DT_RESTART = 50./
&PRES               MAX_PRESSURE_ITERATIONS = 50,
                                  VELOCITY_TOLERANCE = 0.001,
                                  CHECK_POISSON=.TRUE.,
                                  RELAXATION_FACTOR = 1 /

&REAC ID='POLYURETHANE',
    FYI='NFPA Babrauskas',
    C=25,
    H=42,
    O=6,
    N=2,
    SOOT_YIELD=0.07
                    CO_YIELD=0.2,  /   CFT is not used. It can improve the O2 consumption curve.

&MATL ID='PUR',
                                  EMISSIVITY=0.9,
                                  DENSITY = 25.0
                                  CONDUCTIVITY_RAMP='CR',
                                  SPECIFIC_HEAT_RAMP='SHR',
                                  HEAT_OF_COMBUSTION=27100 /  FYI= 'http://www.klausbruckner.com/blog/fire-hazards-
of-polyurethane-foam/'

The conductivity and specific heat ramp values are assumed based
on the curve found in http://www.engineeringtoolbox.com/polyurethane-insulation-k-values-d_1174.html

&RAMP ID='CR', T=0,   F=0.15 /
&RAMP ID='CR', T=175, F=0.2 /
&RAMP ID='CR', T=250, F=0.31 /
&RAMP ID='CR', T=350, F=0.7 /
&RAMP ID='CR', T=1000, F=0.8 /

&RAMP ID='SHR', T=0,   F=1.2 /
&RAMP ID='SHR', T=175, F=0.8 /
```

```
&RAMP ID='SHR', T=250, F=0.8  /
&RAMP ID='SHR', T=350, F=1.6 /
&RAMP ID='SHR', T=1000, F=1.6 /

_____FIRE_RAMP_____

DESCRIPTION:SOLID FUEL TEST OF KURIKKA EXPERIMENTS BASED ON INVERSE MQH MODEL

&SURF ID= 'fire', HRRPUA=562.5, COLOR='RED',  TMP_FRONT=98.0, RAMP_Q='PoolRamp' MATL_ID='PUR', THICKNESS=0.01/  A
maximum HRR of approximately 900 kW is assumed.
&RAMP ID=       'PoolRamp'      T=      0       F=      0.0 /
&RAMP ID=       'PoolRamp'      T=      15      F=      0.0 /
&RAMP ID=       'PoolRamp'      T=      30      F=      0.2 /
&RAMP ID=       'PoolRamp'      T=      50      F=      1 /
&RAMP ID=       'PoolRamp'      T=      80      F=      0.585 /
&RAMP ID=       'PoolRamp'      T=      85      F=      0.635 /
&RAMP ID=       'PoolRamp'      T=      95      F=      1 /
&RAMP ID=       'PoolRamp'      T=      105     F=      1 /
&RAMP ID=       'PoolRamp'      T=      135     F=      0.8 /
&RAMP ID=       'PoolRamp'      T=      265     F=      0.0 /
&RAMP ID=       'PoolRamp'      T=      375     F=      0.0 /

_____BURNING_ITEM_____

&VENT XB = 1.2,2.0 , 2.6,4.6 , 0.4,0.4, SURF_ID='fire' /
&OBST XB = 1.2,2.0 , 2.6,4.6 , 0.0,0.4, SURF_ID='INERT' /
&OBST XB = 1.2,2.0 , 2.6,4.6 , 0.4,0.4, SURF_ID='INERT' /
&OBST XB = 1.2,1.2 , 2.6,4.6 , 0.4,0.6, SURF_ID='INERT' /
&OBST XB = 2.0,2.0 , 2.6,4.6 , 0.4,0.6, SURF_ID='INERT' /
&OBST XB = 1.2,2.0 , 2.6,2.6 , 0.4,0.6, SURF_ID='INERT' /
&OBST XB = 1.2,2.0 , 4.6,4.6 , 0.4,0.6, SURF_ID='INERT' /

_____LEAKAGE_____

&ZONE XB=0.0,2.2,0.0,5.8,0.0,3.0, LEAK_AREA(0) =0.005593 /
&ZONE XB=2.2,4.4,0.0,5.8,0.0,3.0, LEAK_AREA(0) =0.005593 /
&ZONE XB=0.0,2.2,0.0,5.8,3.0,6.0, LEAK_AREA(0) =0.005593 /

_____
LEAK RATE       1.5             m3/m2h

Leakage volume flow at 50 Pa, total envelope area, which for the 2.2 x 5.8 x 3.0 m3 cell is
2 * (2.2*5.8 + 2.2*3.0 + 5.8*3.0) = 73.52 m2.
This would give  a leakage area of (1.5*73 / 3600)/(0.6*sqrt(2*50/1.2)) = 0.005593 m2.
_____

_____MATERIALS_____

&MATL ID = 'CONCRETE',
                FYI                                                     = 'Quintiere, Fire Behavior,
Table 7.6'
                CONDUCTIVITY    = 1.0,
  SPECIFIC_HEAT = 0.75,
  DENSITY       = 2200.,
                EMISSIVITY=     .92/

&SURF ID = 'CONCRETE',
                MATL_ID = 'CONCRETE',
                THICKNESS = 0.2,
                COLOR = 'BEIGE',
                DEFAULT=.TRUE./

&SURF ID = 'CONCRETE_1_0',
                MATL_ID = 'CONCRETE',
                THICKNESS = 0.2,
                COLOR = 'BEIGE',
                LEAK_PATH=1,0/
```

```
&SURF ID = 'CONCRETE_2_0',
                    MATL_ID = 'CONCRETE',
                    THICKNESS = 0.2,
                    COLOR = 'BEIGE',
                    LEAK_PATH=2,0/

&SURF ID = 'CONCRETE_3_0',
                    MATL_ID = 'CONCRETE',
                    THICKNESS = 0.2,
                    COLOR = 'BEIGE',
                    LEAK_PATH=3,0/


_____SUPPLPY_____
```

The ducts are described next. steel ducts with roughness 0.045, 225mm = 0.049 m2, 160mm = 0.020106 m2

```
&HVAC ID='FAN1', TYPE_ID='FAN', MAX_FLOW=0.13, MAX_PRESSURE=400./

&HVAC ID = 'ENTRANCE_OUT1'          TYPE_ID='NODE'    DUCT_ID='ENTRANCE_DUCT1'          VENT_ID='ENTRANCE_OUT1'

                    LOSS=0,0/
&HVAC ID = 'ENTRANCE_OUT2'          TYPE_ID='NODE'    DUCT_ID='ENTRANCE_DUCT2'          VENT_ID='ENTRANCE_OUT2'

                    LOSS=0,0/
&HVAC ID = 'ENTRANCE_OUT3'          TYPE_ID='NODE'    DUCT_ID='ENTRANCE_DUCT3'          VENT_ID='ENTRANCE_OUT3'

                    LOSS=0,0/
&HVAC ID = 'ENTRANCE_OUT4'          TYPE_ID='NODE'    DUCT_ID='ENTRANCE_DUCT1'          'ENTRANCE_DUCT2'
                                    'ENTRANCE_DUCT3' 'ENTRANCE_DUCT4', XYZ=1.0          -1                  6
                                    LOSS=0,0/

&HVAC ID = 'ENTRANCE_INTERMEDIATE'                    TYPE_ID='NODE'    DUCT_ID='ENTRANCE_DUCT4'
                    'ENTRANCE_DUCT5' XYZ=1.0          -2                6                                     LOSS=0,0/

&HVAC ID = 'ENTRANCE_IN1'           TYPE_ID ='NODE'   DUCT_ID='ENTRANCE_DUCT5'          AMBIENT=.TRUE.
                                    XYZ=1.0           -2                11                                    LOSS=0,0/



&HVAC ID='ENTRANCE_DUCT1'           TYPE_ID='DUCT'    NODE_ID='ENTRANCE_OUT4'           'ENTRANCE_OUT1'
                    AREA = 0.020106 LENGTH=3.0        ROUGHNESS=0.045, DAMPER=.TRUE.    DEVC_ID='DEV1'/ When the
control or device is .TRUE. the damper will be open.

&HVAC ID='ENTRANCE_DUCT2'           TYPE_ID='DUCT'    NODE_ID='ENTRANCE_OUT4'           'ENTRANCE_OUT2'
                    AREA = 0.020106 LENGTH=3.0        ROUGHNESS=0.045, DAMPER=.TRUE.    DEVC_ID='DEV2'/

&HVAC ID='ENTRANCE_DUCT3'           TYPE_ID='DUCT'    NODE_ID='ENTRANCE_OUT4'           'ENTRANCE_OUT3'
                    AREA = 0.020106 LENGTH=3.0        ROUGHNESS=0.045, DAMPER=.TRUE.    DEVC_ID='DEV3'/

&HVAC ID='ENTRANCE_DUCT4'           TYPE_ID='DUCT'    NODE_ID='ENTRANCE_INTERMEDIATE'   'ENTRANCE_OUT4'
                    AREA = 0.049    LENGTH=1.0        ROUGHNESS=0.045/



&HVAC ID='ENTRANCE_DUCT5'           TYPE_ID='DUCT'    NODE_ID='ENTRANCE_IN1'            'ENTRANCE_INTERMEDIATE'
                    AREA = 0.049    LENGTH=5.0        ROUGHNESS=0.045, FAN_ID='FAN1', LOSS =0,0/ IV-kanava 225 mm 3
m/s
```

&VENT ID='ENTRANCE_OUT1', XB = 0.4,0.6 , 0.0,0.0 , 2.4,2.6, SURF_ID='HVAC', COLOR='GREEN' /

&VENT ID='ENTRANCE_OUT2', XB = 2.6,2.8 , 0.0,0.0 , 2.4,2.6, SURF_ID='HVAC', COLOR='GREEN' /

&VENT ID='ENTRANCE_OUT3', XB = 0.4,0.6 , 0.0,0.0 , 5.6,5.8, SURF_ID='HVAC', COLOR='GREEN' /

_____EXHAUST_____

The ducts are described next. steel ducts with roughness 0.045, 225mm = 0.049 m2, 160mm = 0.020106 m2

&HVAC ID='FAN2', TYPE_ID='FAN', MAX_FLOW=0.13, MAX_PRESSURE=400./

&HVAC ID = 'WC_IN1' TYPE_ID='NODE' DUCT_ID='WC_DUCT1' VENT_ID='WC_IN1' LOSS=0,0/
SELLI1
&HVAC ID = 'WC_IN2' TYPE_ID='NODE' DUCT_ID='WC_DUCT2' VENT_ID='WC_IN2' LOSS=0,0/
SELLI2
&HVAC ID = 'WC_IN3' TYPE_ID='NODE' DUCT_ID='WC_DUCT3' VENT_ID='WC_IN3' LOSS=0,0/
SELLI3
&HVAC ID = 'WC_IN4' TYPE_ID='NODE' DUCT_ID='WC_DUCT1' 'WC_DUCT2'
'WC_DUCT3' 'WC_DUCT4', XYZ=2.0 -1
6 LOSS=0,0/

&HVAC ID = 'WC_INTERMEDIATE' TYPE_ID='NODE' DUCT_ID='WC_DUCT4' 'WC_DUCT5' XYZ=2.0
-2 6 LOSS=0,0/ EXHAUST
INTERMEDIATE NODE
&HVAC ID = 'WC_OUT1' TYPE_ID ='NODE' DUCT_ID='WC_DUCT5' AMBIENT=.TRUE.
XYZ=2.0 -2 11 LOSS=0,0/
IV-HUONE

&HVAC ID='WC_DUCT1' TYPE_ID='DUCT' NODE_ID='WC_IN1' 'WC_IN4'
AREA = 0.020106 LENGTH=3.0 ROUGHNESS=0.045/

&HVAC ID='WC_DUCT2' TYPE_ID='DUCT' NODE_ID='WC_IN2' 'WC_IN4'
AREA = 0.020106 LENGTH=3.0 ROUGHNESS=0.045/

&HVAC ID='WC_DUCT3' TYPE_ID='DUCT' NODE_ID='WC_IN3' 'WC_IN4'
AREA = 0.020106 LENGTH=3.0 ROUGHNESS=0.045/

&HVAC ID='WC_DUCT4' TYPE_ID='DUCT' NODE_ID='WC_IN4' 'WC_INTERMEDIATE'
AREA = 0.045 LENGTH=1.0 ROUGHNESS=0.045/

&HVAC ID='WC_DUCT5' TYPE_ID='DUCT' NODE_ID='WC_INTERMEDIATE' 'WC_OUT1' AREA =
0.049 LENGTH=5.0 ROUGHNESS=0.045 FAN_ID='FAN2', LOSS=0,0/

&OBST XB = 2.0,2.2 , 0.0,0.8 , 2.6,2.8, COLOR='MAGENTA', TRANSPARENCY=0.5/

&VENT ID='WC_IN1', XB = 2.0,2.2 , 0.8,0.8 , 2.6,2.8, SURF_ID='HVAC', COLOR='MAGENTA' /

```
&VENT ID='WC_IN2', XB = 4.6,4.6 , 0.6,0.8 , 2.6,2.8, SURF_ID='HVAC', COLOR='MAGENTA' /

&VENT ID='WC_IN3', XB = 2.2,2.2 , 0.6,0.8 , 5.8,6.0, SURF_ID='HVAC', COLOR='MAGENTA' /



_____GEOMETRY_____

&OBST XB=0.0,2.2, 5.7,5.9, 0.0,3.0,      RGB=91.0,      91,      91,
SURF_ID6='INERT','INERT','CONCRETE_1_0','CONCRETE_1_0','INERT','INERT', TRANSPARENCY=0.5/
&OBST XB=2.4,4.6, 5.7,5.9, 0.0,3.0,      RGB=91.0,      91,      91,
SURF_ID6='INERT','INERT','CONCRETE_2_0','CONCRETE_2_0','INERT','INERT', TRANSPARENCY=0.5/
&OBST XB=0.0,2.2, 5.7,5.9, 3.2,6.2,      RGB=91.0,      91,      91,
SURF_ID6='INERT','INERT','CONCRETE_3_0','CONCRETE_3_0','INERT','INERT', TRANSPARENCY=0.5/

&OBST XB=2.2,2.4, 0.0,6.4, 0.0,3.2,      RGB=91.0,      91,      91,      SURF_ID='CONCRETE',
TRANSPARENCY=0.5/
&OBST XB=0.0,2.4, 0.0,6.4, 3.0,3.2,      RGB=91.0,      91,      91,      SURF_ID='CONCRETE',
TRANSPARENCY=0.5/


&OBST XB=    0.95    2.2    0.6    0.6    0    3.5
             RGB=    91     91     91     SURF_ID=    'CONCRETE',
TRANSPARENCY=0.8/                Sisäseinä MESH1
&OBST XB=    0.95    0.95   0      0.6    0    3.5
             RGB=    91     91     91     SURF_ID=    'CONCRETE',
TRANSPARENCY=0.8/                Sisäseinä MESH1
&OBST XB=    0.95    2.2    0.6    0.6    3.5  7
             RGB=    91     91     91     SURF_ID=    'CONCRETE',
TRANSPARENCY=0.8/                Sisäseinä MESH1
&OBST XB=    0.95    0.95   0      0.6    3.5  7
             RGB=    91     91     91     SURF_ID=    'CONCRETE',
TRANSPARENCY=0.8/                Sisäseinä MESH1
&OBST XB=    1.24    1.34   2.2    2.2    0    3.5
             RGB=    91     91     91     SURF_ID=    'CONCRETE',
TRANSPARENCY=0.8/                Sisäseinä MESH1
&OBST XB=    1.34    2.2    2.5    2.5    0    3.5
             RGB=    91     91     91     SURF_ID=    'CONCRETE',
TRANSPARENCY=0.8/                Sisäseinä MESH1
&OBST XB=    1.24    1.24   2      2.2    0    3.5
             RGB=    91     91     91     SURF_ID=    'CONCRETE',
TRANSPARENCY=0.8/                Sisäseinä MESH1
&OBST XB=    1.34    1.34   2.2    2.5    0    3.5
             RGB=    91     91     91     SURF_ID=    'CONCRETE',
TRANSPARENCY=0.8/                Sisäseinä MESH1


&OBST XB=    1.24    1.34   2.2    2.2    3.5  7
             RGB=    91     91     91     SURF_ID=    'CONCRETE',
TRANSPARENCY=0.8/                Sisäseinä MESH3
&OBST XB=    1.34    2.2    2.5    2.5    3.5  7
             RGB=    91     91     91     SURF_ID=    'CONCRETE',
TRANSPARENCY=0.8/                Sisäseinä MESH3
&OBST XB=    1.24    1.24   2      2.2    3.5  7
             RGB=    91     91     91     SURF_ID=    'CONCRETE',
TRANSPARENCY=0.8/                Sisäseinä MESH3
&OBST XB=    1.34    1.34   2.2    2.5    3.5  7
             RGB=    91     91     91     SURF_ID=    'CONCRETE',
TRANSPARENCY=0.8/                Sisäseinä MESH3
&OBST XB=    0.95    1.05   0.7    0.7    0    3.5
             RGB=    91     91     91     SURF_ID=    'CONCRETE',
TRANSPARENCY=0.8/                Sisäseinä MESH3
```

```
&OBST XB=     0.95      0.95      0.6       0.7       0         3.5
               RGB=      91        91        91        SURF_ID=  'CONCRETE',
TRANSPARENCY=0.8/                          Sisäseinä MESH3
&OBST XB=     1.05      1.05      0.7       1.2       0         3.5
               RGB=      91        91        91        SURF_ID=  'CONCRETE',
TRANSPARENCY=0.8/                          Sisäseinä MESH3
&OBST XB=     0.95      1.05      0.7       0.7       3.5       7
               RGB=      91        91        91        SURF_ID=  'CONCRETE',
TRANSPARENCY=0.8/                          Sisäseinä MESH3
&OBST XB=     0.95      0.95      0.6       0.7       3.5       7
               RGB=      91        91        91        SURF_ID=  'CONCRETE',
TRANSPARENCY=0.8/                          Sisäseinä MESH3
&OBST XB=     1.05      1.05      0.7       1.2       3.5       7
               RGB=      91        91        91        SURF_ID=  'CONCRETE',
TRANSPARENCY=0.8/                          Sisäseinä MESH3


&OBST XB=     3.36      4.6       0.6       0.6       0         3.5
               RGB=91.0  91        91        SURF_ID='CONCRETE', TRANSPARENCY=0.8/
                                   Sisäseinä MESH2
&OBST XB=     3.36      3.36      0         0.6       0         3.5
               RGB=91.0  91        91        SURF_ID='CONCRETE', TRANSPARENCY=0.8/
                                   Sisäseinä MESH2
&OBST XB=     3.65      3.74      2.2       2.2       0         3.5
               RGB=91.0  91        91        SURF_ID='CONCRETE', TRANSPARENCY=0.8/
                                   Sisäseinä MESH2
&OBST XB=     3.74      4.6       2.5       2.5       0         3.5
               RGB=91.0  91        91        SURF_ID='CONCRETE', TRANSPARENCY=0.8/
                                   Sisäseinä MESH2
&OBST XB=     3.65      3.65      2         2.2       0         3.5
               RGB=91.0  91        91        SURF_ID='CONCRETE', TRANSPARENCY=0.8/
                                   Sisäseinä MESH2
&OBST XB=     3.74      3.74      2.2       2.5       0         3.5
               RGB=91.0  91        91        SURF_ID='CONCRETE', TRANSPARENCY=0.8/
                                   Sisäseinä MESH2
&OBST XB=     3.35      3.45      0.7       0.7       0         3.5
               RGB=91.0  91        91        SURF_ID='CONCRETE', TRANSPARENCY=0.8/
                                   Sisäseinä MESH2
&OBST XB=     3.35      3.35      0.6       0.7       0         3.5
               RGB=91.0  91        91        SURF_ID='CONCRETE', TRANSPARENCY=0.8/
                                   Sisäseinä MESH2
&OBST XB=     3.45      3.45      0.7       1.2       0         3.5
               RGB=91.0  91        91        SURF_ID='CONCRETE', TRANSPARENCY=0.8/
                                   Sisäseinä MESH2

_____MEASUREMENT_____

&DEVC ID='PRESS1',                          QUANTITY='PRESSURE', XYZ=0.5,0.5,2.0 /
&DEVC ID='PRESS2',                          QUANTITY='PRESSURE', XYZ=2.7,2.7,2.0 /
&DEVC ID='PRESS3',                          QUANTITY='PRESSURE', XYZ=0.5,0.5,5.5 /

&DEVC ID='PRESS1AVG',          QUANTITY='PRESSURE', XYZ=0.5,0.5,2.0, TIME_AVERAGED=.FALSE. /
&DEVC ID='PRESS2AVG',          QUANTITY='PRESSURE', XYZ=2.7,2.7,2.0, TIME_AVERAGED=.FALSE. /
&DEVC ID='PRESS3AVG',          QUANTITY='PRESSURE', XYZ=0.5,0.5,5.5, TIME_AVERAGED=.FALSE. /


&DEVC ID='VEL_WC_DUCT1', QUANTITY='DUCT VELOCITY', DUCT_ID='WC_DUCT1' /
&DEVC ID='VEL_WC_DUCT2', QUANTITY='DUCT VELOCITY', DUCT_ID='WC_DUCT2' /
&DEVC ID='VEL_WC_DUCT3', QUANTITY='DUCT VELOCITY', DUCT_ID='WC_DUCT3' /

&DEVC ID='VEL_E_DUCT1', QUANTITY='DUCT VELOCITY', DUCT_ID='ENTRANCE_DUCT1' /
&DEVC ID='VEL_E_DUCT2', QUANTITY='DUCT VELOCITY', DUCT_ID='ENTRANCE_DUCT2' /
&DEVC ID='VEL_E_DUCT3', QUANTITY='DUCT VELOCITY', DUCT_ID='ENTRANCE_DUCT3' /

&DEVC ID='O2',                                  QUANTITY='MASS FRACTION', SPEC_ID='OXYGEN',    XYZ=0.5,4.0,0.5 /
&DEVC ID='O2vol',              QUANTITY='VOLUME FRACTION', SPEC_ID='OXYGEN', XYZ=0.5,4.0,0.5/
&DEVC ID='COvol',              QUANTITY='VOLUME FRACTION', SPEC_ID='CARBON MONOXIDE',  XYZ=0.5,4.0,0.5 /
```

```
&DEVC ID='CO2vol',                                    QUANTITY='VOLUME FRACTION', SPEC_ID='CARBON DIOXIDE',
XYZ=0.5,4.0,0.5 /
&DEVC ID='COvolppm',                  QUANTITY='VOLUME FRACTION', SPEC_ID='CARBON MONOXIDE',
   UNITS='ppm', CONVERSION_FACTOR=1000000, XYZ=0.5,4.0,0.5 /

&DEVC ID='O2_2',                                      QUANTITY='MASS FRACTION', SPEC_ID='OXYGEN',    XYZ=2.7,4.0,0.5 /
&DEVC ID='O2vol_2',                                   QUANTITY='VOLUME FRACTION', SPEC_ID='OXYGEN', XYZ=2.7,4.0,0.5/
&DEVC ID='COvol_2',                                   QUANTITY='VOLUME FRACTION', SPEC_ID='CARBON MONOXIDE',
XYZ=2.7,4.0,0.5 /
&DEVC ID='CO2vol_2',                                  QUANTITY='VOLUME FRACTION', SPEC_ID='CARBON DIOXIDE',
XYZ=2.7,4.0,0.5 /
&DEVC ID='COvolppm_2',                QUANTITY='VOLUME FRACTION', SPEC_ID='CARBON MONOXIDE',
   UNITS='ppm', CONVERSION_FACTOR=1000000, XYZ=2.7,4.0,0.5 /

&DEVC ID='O2_3',                                      QUANTITY='MASS FRACTION', SPEC_ID='OXYGEN',    XYZ=0.5,4.0,3.7 /
&DEVC ID='O2vol_3',                                   QUANTITY='VOLUME FRACTION', SPEC_ID='OXYGEN', XYZ=0.5,4.0,3.7/
&DEVC ID='COvol_3',                                   QUANTITY='VOLUME FRACTION', SPEC_ID='CARBON MONOXIDE',
XYZ=0.5,4.0,3.7 /
&DEVC ID='CO2vol_3',                                  QUANTITY='VOLUME FRACTION', SPEC_ID='CARBON DIOXIDE',
XYZ=0.5,4.0,3.7 /
&DEVC ID='COvolppm_3',                QUANTITY='VOLUME FRACTION', SPEC_ID='CARBON MONOXIDE',
   UNITS='ppm', CONVERSION_FACTOR=1000000, XYZ=0.5,4.0,3.7 /


&DEVC ID='Temp_Node_WC_IN1', QUANTITY='NODE TEMPERATURE', NODE_ID='WC_IN1' /
&DEVC ID='Temp_Node_WC_IN2', QUANTITY='NODE TEMPERATURE', NODE_ID='WC_IN2' /
&DEVC ID='Temp_Node_WC_IN3', QUANTITY='NODE TEMPERATURE', NODE_ID='WC_IN3' /
&DEVC ID='Temp_Node_WC_INTER', QUANTITY='NODE TEMPERATURE', NODE_ID='WC_INTERMEDIATE' /
&DEVC ID='Temp_Node_WC_OUT1', QUANTITY='NODE TEMPERATURE', NODE_ID='WC_OUT1' /

&DEVC ID='Temp_Node_ENT_OUT1', QUANTITY='NODE TEMPERATURE', NODE_ID='ENTRANCE_OUT1' /
&DEVC ID='Temp_Node_ENT_OUT2', QUANTITY='NODE TEMPERATURE', NODE_ID='ENTRANCE_OUT2' /
&DEVC ID='Temp_Node_ENT_OUT3', QUANTITY='NODE TEMPERATURE', NODE_ID='ENTRANCE_OUT3' /
&DEVC ID='Temp_Node_ENT_INTER', QUANTITY='NODE TEMPERATURE', NODE_ID='ENTRANCE_INTERMEDIATE' /
&DEVC ID='Temp_Node_ENT_IN1', QUANTITY='NODE TEMPERATURE', NODE_ID='ENTRANCE_IN1' /


&DEVC ID='TEMP_WC_DUCT1', QUANTITY='DUCT TEMPERATURE', DUCT_ID='WC_DUCT1' /
&DEVC ID='TEMP_WC_DUCT2', QUANTITY='DUCT TEMPERATURE', DUCT_ID='WC_DUCT2' /
&DEVC ID='TEMP_WC_DUCT3', QUANTITY='DUCT TEMPERATURE', DUCT_ID='WC_DUCT3' /
&DEVC ID='TEMP_E_DUCT1', QUANTITY='DUCT TEMPERATURE', DUCT_ID='ENTRANCE_DUCT1' /
&DEVC ID='TEMP_E_DUCT2', QUANTITY='DUCT TEMPERATURE', DUCT_ID='ENTRANCE_DUCT2' /
&DEVC ID='TEMP_E_DUCT3', QUANTITY='DUCT TEMPERATURE', DUCT_ID='ENTRANCE_DUCT3' /

&DEVC ID='FLOW_WC_DUCT1', QUANTITY='DUCT VOLUME FLOW', DUCT_ID='WC_DUCT1' /
&DEVC ID='FLOW_WC_DUCT2', QUANTITY='DUCT VOLUME FLOW', DUCT_ID='WC_DUCT2' /
&DEVC ID='FLOW_WC_DUCT3', QUANTITY='DUCT VOLUME FLOW', DUCT_ID='WC_DUCT3' /
&DEVC ID='FLOW_E_DUCT1', QUANTITY='DUCT VOLUME FLOW', DUCT_ID='ENTRANCE_DUCT1' /
&DEVC ID='FLOW_E_DUCT2', QUANTITY='DUCT VOLUME FLOW', DUCT_ID='ENTRANCE_DUCT2' /
&DEVC ID='FLOW_E_DUCT3', QUANTITY='DUCT VOLUME FLOW', DUCT_ID='ENTRANCE_DUCT3' /


&DEVC ID='LEAKAGE_1_0_MASS_FLUX_IN_Y_DIRECTION_AREA_INTEGRAL', QUANTITY='MASS FLUX Y', SPEC_ID='AIR',
STATISTICS='AREA INTEGRAL', XB=0.0,2.2, 6.2,6.2, 0.0,3.0/                    kg_s
&DEVC ID='LEAKAGE_2_0_MASS_FLUX_IN_Y_DIRECTION_AREA_INTEGRAL', QUANTITY='MASS FLUX Y', SPEC_ID='AIR',
STATISTICS='AREA INTEGRAL', XB=4.6,2.4, 6.2,6.2, 0.0,3.0/                    kg_s
&DEVC ID='LEAKAGE_3_0_MASS_FLUX_IN_Y_DIRECTION_AREA_INTEGRAL', QUANTITY='MASS FLUX Y', SPEC_ID='AIR',
STATISTICS='AREA INTEGRAL', XB=2.2,0.0, 6.2,6.2, 3.2,6.2/                    kg_s

&DEVC ID='LEAKAGE_1_0', QUANTITY='DUCT VOLUME FLOW', DUCT_ID='LEAK 0 1' /
&DEVC ID='LEAKAGE_2_0', QUANTITY='DUCT VOLUME FLOW', DUCT_ID='LEAK 0 2' /
&DEVC ID='LEAKAGE_3_0', QUANTITY='DUCT VOLUME FLOW', DUCT_ID='LEAK 0 3' /

_____DAMPER_ACTIVATION_____

&DEVC ID='DEV1',                      QUANTITY='DUCT TEMPERATURE',       DUCT_ID='ENTRANCE_DUCT1',
                  SETPOINT=72.0, INITIAL_STATE=.TRUE. /
```

```
&DEVC ID='DEV2',                    QUANTITY='DUCT TEMPERATURE',    DUCT_ID='ENTRANCE_DUCT2',
                SETPOINT=72.0, INITIAL_STATE=.TRUE. /

&DEVC ID='DEV3',                    QUANTITY='DUCT TEMPERATURE',    DUCT_ID='ENTRANCE_DUCT3',
                SETPOINT=72.0, INITIAL_STATE=.TRUE. /

_____OUTPUT_____

&DEVC ID='TEMP1',                                   QUANTITY='TEMPERATURE',   XYZ=0.5,4.0,0.5 /

&DEVC ID='TEMP2',                                   QUANTITY='TEMPERATURE',   XYZ=2.7,4.0,0.5 /

&DEVC ID='TEMP3',                                   QUANTITY='TEMPERATURE',   XYZ=0.5,4.0,3.7 /


&SLCF QUANTITY='PRESSURE', PBY  =3.0 /
&SLCF PBY=3.0,QUANTITY='DENSITY' /

&SLCF QUANTITY='TEMPERATURE', PBX=1.0 /
&SLCF QUANTITY='TEMPERATURE', PBY=3.0 /

&SLCF QUANTITY='HRRPUV', PBX=1.8 /

&SLCF QUANTITY='VISIBILITY', PBZ=2.0/
&SLCF QUANTITY='VISIBILITY', PBZ=5.2/

&SLCF QUANTITY='VELOCITY', PBZ=2.6/
&SLCF QUANTITY='VELOCITY', PBZ=5.6/

&SLCF QUANTITY='U-VELOCITY', PBZ=2.6/
&SLCF QUANTITY='V-VELOCITY', PBZ=2.8/

&SLCF QUANTITY='carbon monoxide', PBZ=2.0/
&SLCF QUANTITY='carbon dioxide', PBZ=2.0/
&SLCF QUANTITY='oxygen', PBZ=2.0/

&SLCF QUANTITY='carbon monoxide', PBY=1.0/
&SLCF QUANTITY='carbon dioxide', PBY=1.0/
&SLCF QUANTITY='oxygen', PBY=1.0/

&TAIL/
```

REFERENCES

1. Kallada,R. 2016. Fire induced flow in building ventilation system. Master's thesis. 69 s. Aalto Yliopisto.
2. McGrattan, K., McDermott, R., Hostikka, S. & Floyd, J. 2016. Fire Dynamics Simulator (Version 6). User' Guide. Gaithersburg: National Institute of Standards and Technology (National Institute of Standards and Technology Special Publication 1019).
3. McGrattan, K., Hostikka, S., Floyd, J., Baum, H., Rehm, R. Mell, W. & McDermott, R. 2016. Fire Dynamics Simulator (Version 6). Technical Reference Guide. Volume 1: Mathematical Model. Gaithersburg: National Institute of Standards and Technology (National Institute of Standards and Technology NIST Special Publication 1018-1).
4. McDermott, R., McGrattan, K., Hostikka, S. & Floyd, J. 2016. Fire Dynamics Simulator (Version 6). Technical Reference Guide. Volume 2: Verification. Gaithersburg: National Institute of Standards and Technology (National Institute of Standards and Technology Special Publication 1018-2).
5. McGrattan, K., Hostikka, Floyd, J. & McDermott, R.. 2016. Fire Dynamics Simulator (Version 6). Technical Reference Guide. Volume 3: Validation. Gaithersburg: National Institute of Standards and Technology (National Institute of Standards and Technology Special Publication 1018-3).
6. Quintiere, J. 2016. Principles of Fire Behaviour. Second edition. Crc Press. ISBN: 1-4987-3562-2
7. NKB 1994:07. 1994. Funktionsbestemte brandkrav og Teknisk vejledning for beregningsmæssig eftervisning. NKB Utskotts- og arbetsrapporter.
8. Information provided by the Criminal Sanctions Agency (Rikosseuraamuslaitos) in spring 2016.
9. Stroup, D.W., DeLauter, L., Lee, J. &. Roadarmel, G. 2001. Fire Tests of Men's Suits on Racks. Gaithersburg, MD: National Institute of Standards and Technology. Building and Fire Research Laboratory. Report of Test FR 4013.Safety. NISTIR 6030, vol. 1, pp. 187 – 199.
10. Babrauskas, V. 2008. Heat Release Rates. Teoksessa: The SFPE Handbook of Fire Protection Engineering. 4. Painos. Quincy: National Fire Protection Association. s. 3-1 - 3 59.
11. Hietaniemi, J., Baroudi, D., Korhonen, T., Björkman, J., Kokkala, M. & Lappi, E. Yksikerroksisen teollisuushallin rakenteiden palonkestävyyden vaikutus paloturvallisuuteen. Riskianalyysi ajasta riippuvaa tapahtumapuumallia käyttäen (Fire safety impact of the fire resistance of the structures of a single-storey industrial building: risk analyisi using a time-dependent event tree method). Espoo: Technical

Research Centre of Finland, 2002. 95 p. + App. 51 p. (VTT Tiedotteita – Meddelanden – Research Notes 2123.) ISBN 951-38-5935-5. In Finnish.

12. Hietaniemi, J, Korhonen, T., Joyeux, D. & Ayme, N. 2004. Risk-based Fire Safety Engineering Approach to Obtain Balanced Structural Fire Resistance Requirements. In: Bradley, D., Drysdale, D. & Molkov, V. Fire and Explosion Hazards, Proceedings of the Fourth International Seminar. Londonderry, Northern Ireland, UK, September 8-12, 2003. Belfast, Northern Ireland, UK: University of Ulster. S. 505-514

13. Hietaniemi, J., Hostikka, S., & Korhonen, T. 2004. Probabilistic Fire Simulation. In: Almand, K. H. (Ed.). Proceedings of the 5th International Conference on Performance-Based Codes and Fire Safety Design Methods. October 6-8, 2004. Luxembourg. Bethesda, MD. USA. 2004. Society of Fire Protection Engineers. Pp. 280 291.

14. Joyeux, D., Bonnot, S., Hietaniemi, J & Korhonen, T. 2004. Risk-Based Fire Safety Engineering Approach Applied to a Public Building. In: Almand, K. H. (Ed.). Proceedings of the 5th International Conference on Performance-Based Codes and Fire Safety Design Methods. October 6-8, 2004. Luxembourg. Bethesda, MD. USA. 2004. Society of Fire Protection Engineers. Pp. 397 – 408.

15. Hietaniemi, J., Cajot, L.-G., Pierre, M., Fraser-Mitchell, J. Joyeux, D. & Papaioannou, K. 2005. Risk-Based Fire Resistance Requirements. Final Report. Luxembourg: Office for Official Publications of the European Communities. 528 p. ISBN 92-894-9871-4 (EUR 21443 EN)

16. Hietaniemi, J. 2007. Probabilistic simulation of fire endurance of a wooden beam. Structural Safety. Volume 29, Issue 4, October 2007, Pages 322-336

17. Hietaniemi, J., Hostikka, S. & Keski-Rahkonen, O. 2008. Computation of Quantitative Fire Risks Using Two-Model Monte Carlo Simulation and CFD Fire Model. Proceedings of the PSAM 9 Conference . International Conference on Probabilistic Safety Assessment & Management, PSAM 9. Hong Kong, China, May 18 – 23, 2008. www.psam9.org

18. Hostikka, S., Keski-Rahkonen, O. & Korhonen, T. Probabilistic Fire Simulator. Theory and User's Manual for Version 1.2, VTT Building and Transport. VTT Publications 503, 2003. 72 p. + app. 1 p.

C. Apartment case study article

Simo Hostikka, Rahul Kallada Janardhan, Umar Riaz and Topi Sikanen

Submitted for review to the *12th International Symposium of Fire Safety Science*, to be organized in Lund in June 2017.

Fire-induced pressure and smoke spreading in mechanically ventilated buildings with air-tight envelopes

SIMO HOSTIKKA[1], RAHUL KALLADA JANARDHAN[1], UMAR RIAZ[1], and TOPI SIKANEN[2]
[1]Aalto University
Espoo, Finland
[2]VTT Technical Research Centre of Finland Ltd.
Espoo, Finland

ABSTRACT

Fire-induced pressures have not been considered dangerous in building fires, but the situation may be changing as the building envelopes are becoming much more air-tight than before. In this study, we wanted to investigate if this can change the fire development and pose new risks for structural and evacuation safety. We used experiments to validate the numerical models, and models to simulate the fire development in buildings with different air-tightness levels. The results showed that transitioning from traditional and modern buildings to Near-Zero buildings can increase the peak overpressures high enough to cause structural damage. Conditions for avoiding the too high overpressures, while preventing the smoke spread through the ventilation system were identified.

KEYWORDS: pressure, modeling, CFD, smoke, near-zero buildings, high-rise buildings

NOMENCLATURE

A	crossectional area of the duct (m^2)
A_L	leakage area (m^2)
c_p	spesific heat capacity ($kJkg^{-1}K^{-1}$)
C_d	discharge coefficient (-)
Δp	pressure difference (Pa)
h	enthalpy of fluid ($Wm^{-2}K^{-1}$)
K	loss coefficient (-)
P	pressure (Pa)
Q	heat release rate (HRR) (kW)
t_g	growth time (s)
q_{50}	leakage flow at ΔP=50 Pa ($m^3h^{-1}m^{-2}$)
S	compartment surface area (m^2)
T	temperature (K)
u	duct flow speed (ms^{-1})
V_{leak}	leakage flow (m^3s^{-1})
$\dot{V}_{50}$	volumetric leakage flow at ΔP=50 Pa (m^3s^{-1})
Greek	
ρ	density (kgm^{-3})
subscripts	
i,k	nodes
j	duct segments

INTRODUCTION

Fire-induced pressures have been studied in fire science mainly from the viewpoint of their capability to drive the flows between the compartments. The role of the pressure as a potential risk for structural damage has been identified, but limited to explosions or gas deflagrations, i.e. mainly industrial scenarios. Our understanding of the potential threats for fire compartmentation has been dominated by the thermal impact and the load-bearing capacity of structures.

An indication of the evacuation-related risks was reported by a group of Finnish firemen in 2014: They observed that they could not open the inwards-opening door of the fire apartment during the growth stage of the fire. This means that the overpressure must have been well above 100 Pa, and possible occupants would not have been able to use the door to escape. If we combine this observation with the fact that the construction requirements and practices are rapidly moving towards more air-tight building envelopes, as demanded by the energy efficiency and high-rise construction trends, we can expect that the pressure related risks may be coming more significant, unless the preventive measures can be found and justified. Fourneau et al. [1] identified the increased fire pressure as one of the consequences of the better energy efficiency, concluding that the high pressure can lead to a reverse flow in the supply ventilation system. They did not recognize the pressure rise as a risk for escape or structural integrity.

The calculation of compartment fire pressure requires knowledge of the gas temperature development and leakage flows [2]. As pointed out in [2], numerical integration is usually needed as the leakage flows depend on the pressure. The situation is even more complex if the ventilation is mechanically controlled, as is the case in most modern, energy efficient buildings. The pressure calculation has been a part of most numerical fire models capable of solving the flows between several compartments. Among them is the Fire Dynamics Simulator (FDS) [3], for which a dedicated HVAC module was developed by Floyd [4]. The current FDS validation database for fire-induced pressures consists of three experimental campaigns, and the peak overpressures range from a few Pa to 1300 Pa [5]. A detailed validation of the FDS' HVAC modelling capability was recently reported by Wahlqvist and van Hees [6].

The aim of the current study was to investigate how the improving air tightness of the building envelopes will change the fire development, and should we expect new risks for the structural and evacuation safety. First we use existing [7,8] and new [9] experiments to validate the modelling capability of fire-induced pressures in residential buildings. Then we use the models to simulate the fire development in buildings with different air-tightness levels, focusing on pressure and smoke spread outcomes.

METHODS

Numerical method

FDS is a Large Eddy Simulation (LES) based Computational Fluid Dynamics sofware which solves the low-Mach number combustion equations on a rectilinear grid over time. The simulations in this study were performed using version 6.3.2 of FDS.

FDS has a dedicated module for modelling Heating, Ventilation and Air-conditioning (HVAC) systems connected to the gas phase solver. The ventilation network is described as a series of ducts and nodes. The nodes are placed at points where ducts intersect each other or the CFD computational domain. The ducts are uninterrupted domains of fluid flow which can encompass elbows, expansion/contraction fittings and various other fittings. The losses due to friction and various other duct fittings are assigned as dimensionless loss numbers to the ducts. The node losses are also attached to the ducts as loss terms only appear in the duct equation 3. The module does not presently store any mass. Therefore, mass flux into a duct is equal to the mass flux out of the duct. The nodal conservation equations for mass, energy and momentum equations are as follows:

$$\sum_j \rho_j u_j A_j = 0 \tag{1}$$

$$\sum_j \rho_j u_j A_j h_j = 0 \tag{2}$$

$$\rho_j L_j \frac{du}{dt} = (P_i - P_k) + (\rho g \Delta z)_j + \Delta P_j + 0.5 K_j \rho_j |u_j| u_j \tag{3}$$

Leakage modelling

Leakage refers to the amount of air flowing through the building envelope due to the pressure difference between the inside and outside. A standardized method for measuring the leakage (e.g. SFS EN: 13829) makes use of a variable-speed fan mounted to a door in the envelope being tested [10]. All the ventilation paths are sealed during the test. The building interior is then pressurized or depressurized using the fan and the leakage flows are determined by monitoring the flow through the fan. In energy efficiency studies, the leakages are commonly measured at 50 Pa underpressure. Overpressures would be more suitable for fire analyses, although both directions can appear. The leakage can be reported as a volumetric flow $\dot{V}_{50}$, air permeability q_{50} or air exchange rate n_{50}.

From the viewpoint of fire CFD, leakage is a sub grid -scale phenomenon which means that a leak path boundary condition cannot be directly specified. In FDS simulations, the leaks are modelled as a finite area

Table 1. FOA Test configurations. Test 15 had constant pool area of 0.5 m^2.

Test	Fire type	Opening D (m)	Exhaust Network	Supply Network
FOA series 1				
1	1	0.2m	-	-
2	2	0.2m	-	-
3	3	0.2m	-	-
FOA series 2				
11	1	0.2	-	-
12	1	0.15	-	-
13	2	0.2	-	-
14	2	0.15	-	-
15	-	0.2	-	-
21	2	0.2	Exhaust network 1	-
22	2	0.15	Exhaust network 1	-
23	2	0.15	Exhaust network 2	-
31	1	0.10	Exhaust network 1	Supply network 1
32	2	0.15	Exhaust network 1	Supply network 1
33	2	0.2	Exhaust network 1	Supply network 1

using vents on the domain boundaries. FDS utilizes the HVAC module to solve the leakage flow

$$\dot{V}_{leak} = A_L \text{sign}(\Delta p) \left(\frac{2\Delta p}{\rho} \right)^{1/2} \tag{4}$$

Validation experiments

The FDS validation studies are performed using three sets of experiments. Two first sets [7,8] were conducted by the Swedish FOA Defence Research Establishment, and the third set by Aalto University [9].

The first series consists of three tests with t^2 fires of different growth rates specified in Table 1 [7]. The fire room was 4.0 m × 5.5 m × 2.6 m (high) and the fire source was a heptane pan of 0.73 m × 1 m (c.f. Fig. 1a). These tests did not include actual ventilation network, but the fire room had a circular opening (D = 0.2 m) connected to a 2.2 m long tube. Temperature and flow speed were measured at the end of the tube. The opening was located at 0.6 m from the floor. The fire room was divided in two parts with a wall, and the wall had a 1.9 m wide opening from floor to ceiling. The t^2 behaviour of the HRR was achieved using a lid that was moved over the pan at a given rate thereby increasing the heptane burning area. Assuming a value 1600 kW/m^2 for the HRR per unit area, the movement speeds were adjusted to yield three different growth rates:

Type 1: $\dot{Q} = 0.035t^2$ kW (between fast and medium)

Type 2: $\dot{Q} = 0.075t^2$ kW (between ultra-fast and fast)

Type 2: $\dot{Q} = 0.085t^2$ kW (between ultra-fast and fast)

The second series consists of three groups of experiments with the same room and same fire types as the first set, but with different ventilation configurations, as shown in Table 1 [8]. The leakage openings of different diameters were connected to a 0.32 m diameter and 3.2 m long tube connecting to the ambient. The opening was located at 0.6m height from the floor on one wall of the room. In the first group, there was not ventilation system, only leakage opening. In the second group, the room was equipped with an exhaust system, shown in the top part Fig.2. (Test 23 had slightly different exhaust ventilation. See [8] for details.). A supply network (Fig.2) was added in the third group.

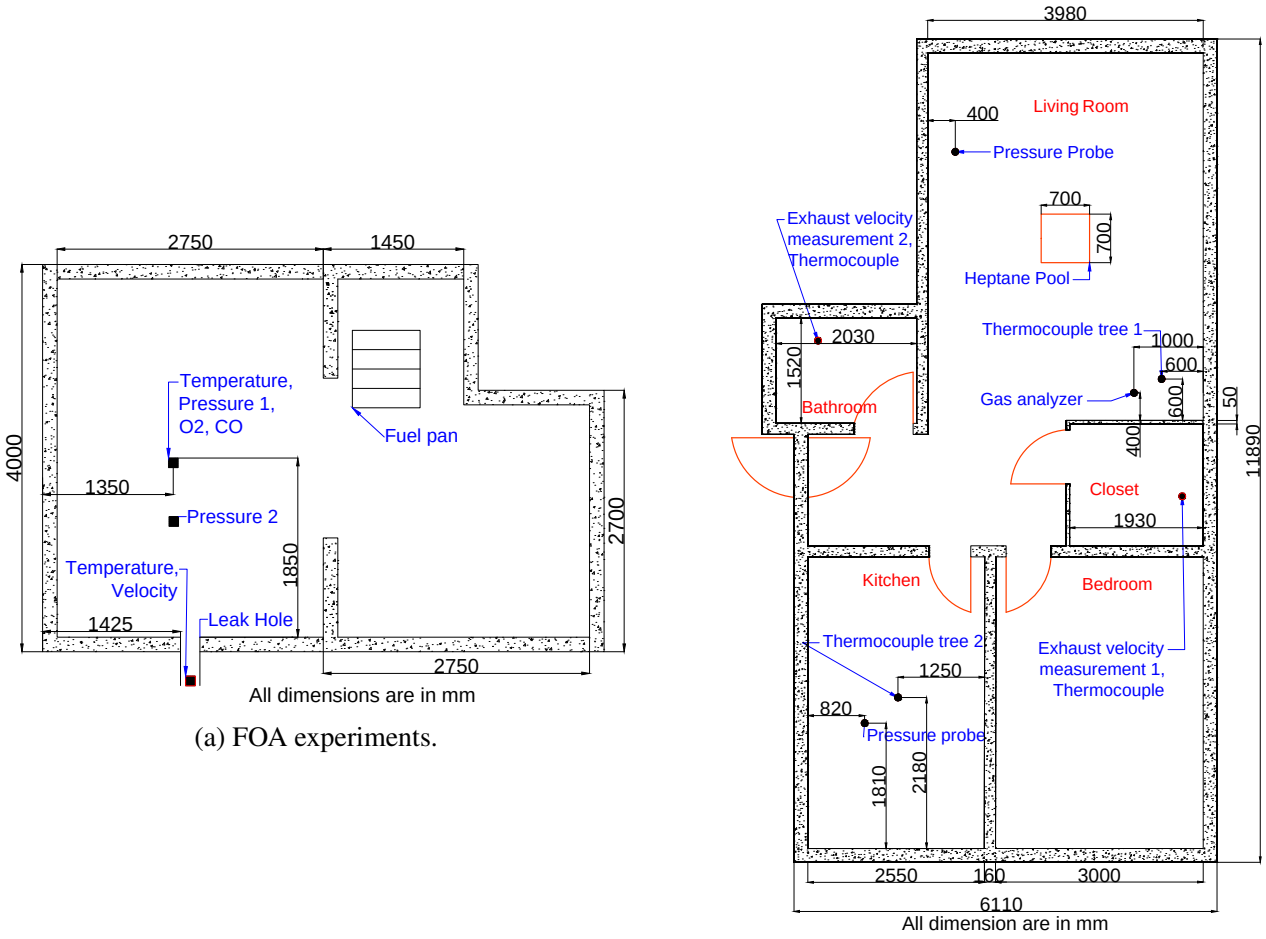

(a) FOA experiments.

(b) Aalto experiments.

Fig. 1. Plan drawins and measurements of the validation experiments.

The main components of the HVAC models for FOA tests are nodes, ducts, and a fan. The other components such as dampers and expansion/contraction fittings are accounted for in the loss terms. Multiple ducts have been combined into a single duct with appropriate loss coefficients for further simplification. Dampers do not completely block the smoke flow, they only limit the volume flow through the ducts to 25 l/s.

The exhaust network in Fig. 2 is modelled using 8 nodes, starting from Node 1 which connects the computational domain to the main duct which is also connected to three fictive compartments maintained at ambient pressure. The total length of the duct from Node 1 to 5 was about 7.5 m. Nodes 5,6,7 and 8 are maintained at ambient pressure. The exhaust fan that drives the flow is placed in the last duct connecting nodes 4 and 5. The fan curve was defined by specifying the flow rates (0, 60 and 120 Ls) at three static pressures (310, 190 and 18 Pa), respectively.

In theory, it would be possible to determine the loss coefficients for all the duct sections from the individual losses of the components and the friction. As all the details cannot be found out at this stage, effective loss coefficients were estimated first defining a constant roughness of 1 mm for ducts, and then adjusting the loss of the first duct to match the known volume flow of 25 L/s. The losses from the damper and the 90 degree bend were thus combined into a single loss coefficient. Identical losses are used for forward and reverse flow.

The third series of validation experiments consists of experiments carried out in 2015 in a 1970's apartment building in western Finland. A detailed explanation of the experiments is given in [9], and only a brief summary is presented here. The apartment (see Fig. 1b) had two exhaust ventilation ducts leading to the roof. All the other ventilation paths were closed during the experiments. The originally natural ventilation had been enforced by post-installed fan in the bathroom exhaust. Two different fires and three exhaust damper configurations were used. Open configuration means that the dampers were removed completely. The experiments are listed in Table 2. For heptane tests, several repeats were performed.

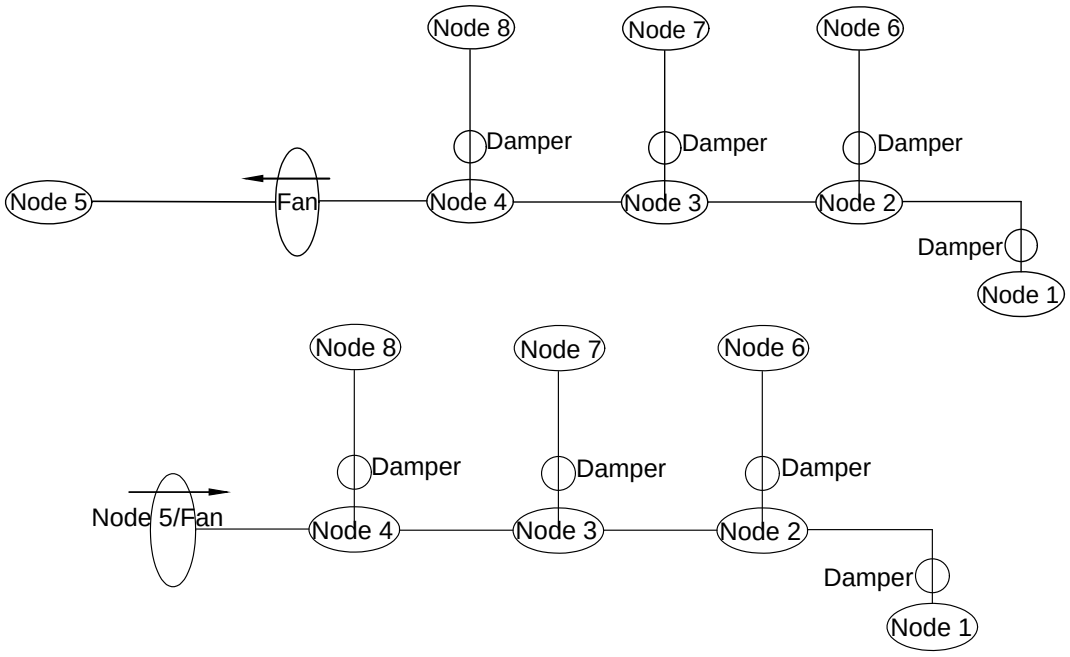

Fig. 2. Ventilation networks used in FOA experiments. Top: Exhaust network 1. Bottom: Supply network 1

The ventilation ducts were modelled as combinations of two or three duct segments. The first duct was installed for the measurements, and the third segment of the bathroom duct was used for including the fan. The ventilation model parameters for these tests are given in Table 3.

In addition to the quantitative results to be used for validation, the experiments of the third series provided two interesting qualitative results. First, we were able to confirm the hypothesis that the fire-induced pressure can prevent one from opening the inwards-opening door. A fireman staying inside the fire could not open the door without help from outside. Second observation was that the pressure resulting from a polyurethane foam fire was sufficient to break a light-weight external wall of the apartment. The critical pressure was in the range 1400-1650 Pa.

Table 2. Kurikka test configurations

Test	Fuel	Ducts	Roof fan
1	Heptane 3.0 L	Open	OFF
2	Heptane 3.0 L	Normal	ON
3	Heptane 3.0 L	Closed	ON
4	Polyurethane foam 3.82 kg	Normal	ON

Table 3. HVAC model inputs [9].

Ventilation configuration	L_1 (m)	L_2 (m)	L_3 (m)	A_1, A_2 (m^2)	A_3 (m^2)	K_1	K_2	K_3
Bathroom duct								
Open	0.4	10	1.0	0.01227	0.049	0	3	1
Normal	0.4	10	1.0	0.01227	0.049	0	38	1
Closet duct								
Open	0.4	10		0.01227		0	2	
Normal	0.4	10		0.01227		0	70	

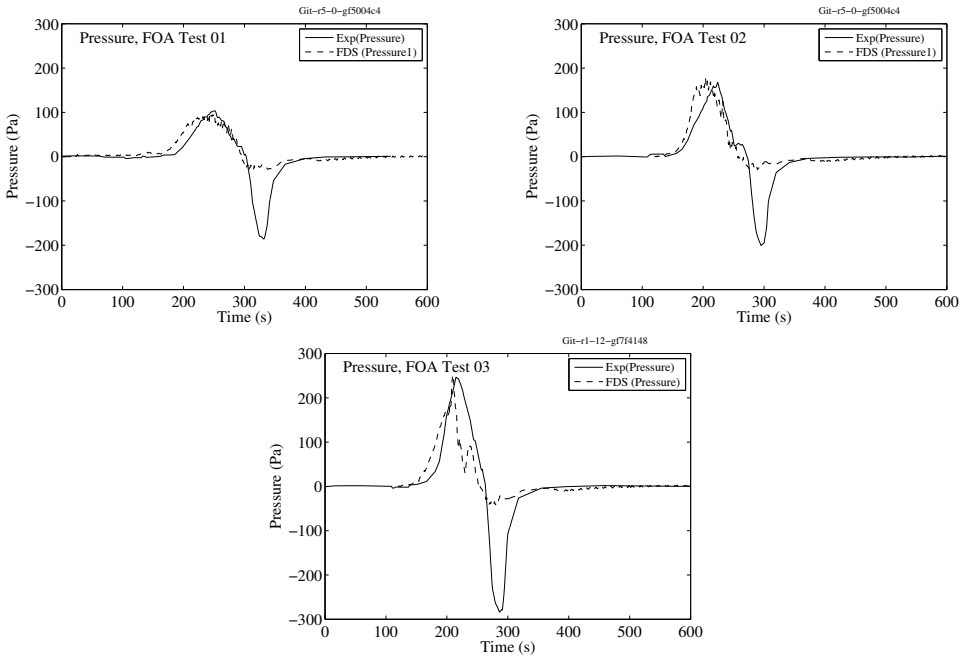

Fig. 3. FOA Series 1: Measured and simulated fire pressures

VALIDATION RESULTS

The experimental and simulated fire room pressures in FOA Series 1 are shown in Figure 3. The positive pressures during the fire growth stage are reproduced by the simulation model with good accuracy. The negative pressures after the fire suppression, in turn, are not captured as well. The same behaviour was observed in all three validation series.

A summary of the gas temperature and peak overpressure predictions is shown in Fig. 4. Gas temperature comparisons were made for all the individual temperature measurements, not for the averaged layer temperatures as in [5]. The temperatures are overpredicted by 11 % in average. Overall, the temperature uncertainties are satisfactory, and increase our confidence on the accuracy of the estimated model inputs for HRR. The peak overpressures are underpredicted by 7 % in average. The model relative standard deviation is dominated by the combined experimental uncertainty.

RESIDENTIAL CASE STUDY DESCRIPTION

Building description

The influence of the envelope air-tightness on the fire-induced pressures and smoke spreading in the ventilation network was studied through the fire simulations in a hypothetical residential building. The simulation geometry for the case study consists of a single floor of a multi storey apartment building. There are 11 apartments with 50 m^2 or 100 m^2 floor areas and a corridor. The model does not include a staircase connecting the domain to the other floors of the building, and the corridor pressure conditions are not studied here. The ceiling height is 2.5 meters. The room walls and ceiling are made of 15 cm thick concrete. The fire is assumed to ignite in one of the smaller apartments. Within this apartment, the structures dividing the apartment into rooms are included, but the doors are assumed to be open. Fig. 5 shows the geometry.

Modern ventilation systems

The traditional ventilation systems in residential buildings have been based on mechanical or buouyancy driven exhaust, with the supply air provided through the building envelope either as an uncontrolled leakage or through valves. In modern HVAC systems, there are usually separate networks for supply and exhaust air. Both networks are typically equipped with a fan unit to control the flow rate and to implement the heat-

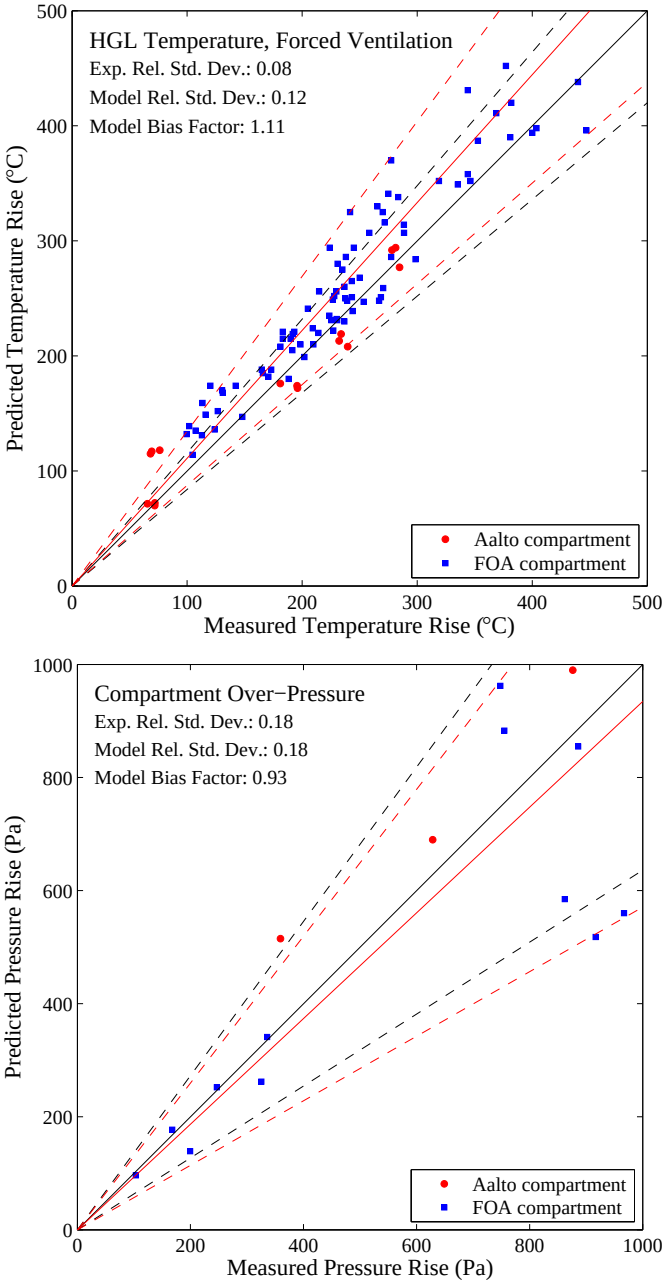

Fig. 4. Uncertainty of peak overpressure predictions.

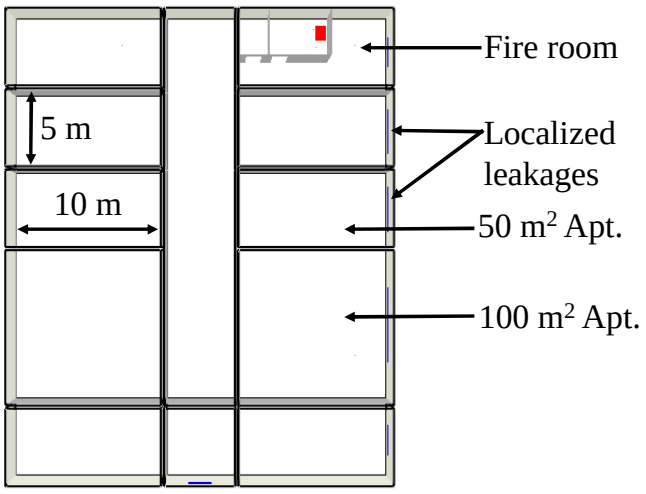

Fig. 5. Geometry for the apartment case study

ing/cooling, as well as heat recovery and air filtration for indoor air quality control. Single fan unit may serve entire building or a single floor of a multi-storey apartment building. The coils and filters introduce drag to the flow. As a result, the fan unit will cause pressure losses even when the fans are turned off. For fire compartmentation and smoke control, fire and/or smoke dampers are typically installed to the ducts entering and leaving the apartments. In addition, the modern ventilation fans are often equipped with dampers that automatically close the ambient connection when the fan is turned off. In fire situation, turning off the fan can therefore lead to complete closing of the ventilation system.

Simulation model

Each room in the model has a designated mesh. The discretization is 10 cm for the fire room and 50 cm elsewhere. Each room is considered its own pressure zone with an individual solution for the background pressure. There is no heat transfer through the walls between the rooms and all leakages are to the ambient. The ventilation system consists of independent inlet and exhaust networks, both equipped with a fan with stalling pressure of P_{max} = 550 Pa and a zero-pressure flow rate of V_{max} = 650 l/s. The fan unit model parameters were tuned to produce 150 Pa pressure loss to the flow. Each network consists of a central duct (⌀=250 mm) and smaller (⌀=125 mm) ducts for each individual apartment. Two inlet and exhaust connections are used for the fire apartment, but only one for all the other apartments. Loss coefficients K for the inlet and exhaust ducts are adjusted in non-fire conditions to achieve 40 l/s ventilation rate and slightly negative pressure for the apartment.

In total, 34 simulations were performed, varying the damper configuration, envelope air-tightness level and the fire growth rate. The influence of the fire/smoke dampers installed in the ventilation ducts was studied by studying three different compartmentation damper configurations:

Damper=Off Both inlet and outlet remain open during the fire.

Damper=Inlet The inlet duct of the fire apartment is closed by a damper 10 s after the ignition.

Damper=Both Both inlet and outlet are closed by dampers 10 s from the ignition.

Additionally the effect of the dampers located at the inlet and outlet fans was investigated.

Three different levels of the building envelope air-tightness were investigated. These levels were defined using the air permeability values q_{50}, listed in Table 4. The class "Traditional" represents an average of the required and reference value (for heat loss calculations) in the current Finnish building code (Part D3: Energy efficiency, 2012, Ministry of Environment). The "Modern", in turn, corresponds to the measured air-tightness in the concrete element multistorey buildings [10] and the "Near-zero" represents the current, technically achievable target level.

The volumetric leakage flow rate $\dot{V}_{50}$ at 50 Pa can be calculated from the air permeability values using equation 5.

$$\dot{V}_{50} = \frac{q_{50}}{3600} S \, [\mathrm{m}^3/\mathrm{s}] \tag{5}$$

and the air exchange rate as $n_{50} = V_{50}/V$, where V is the building volume. The leakage areas A_L, through which these air-tightness levels are spesified into the FDS models, are then calculated from the volumetric flow rates as

$$A_\mathrm{L} = \frac{\dot{V}_{50}}{C_d \left(\frac{2\Delta p}{\rho_\infty} \right)^{1/2}} \, [\mathrm{m}^2] \tag{6}$$

In the models, these leakage areas are distributed equally at the locations of doors and windows.

Three different fire scenarios were used in the simulations. Two of them were defined as typical t^2 fires with prescribed maximum HRR, and the third one was based on the experimental heptane pool burning rate in the Aalto experiments:

Table 4. Envelope specifications

Envelope Type	q_{50} ($m^3m^{-2}h^{-1}$)	V_{50} (m^3/s)	n_{50} (h^{-1})	A_L (m^2)
Traditional	3	0.146	4.2	0.02690
Modern	1.5	0.073	2.1	0.01345
Near-zero	0.75	0.036	1.05	0.006725

Medium: $\dot{Q} = Q_0(t/t_g)^2$, t_g = 300 s, $\dot{Q}_{max}$ = 4 MW

Fast: $\dot{Q} = Q_0(t/t_g)^2$, t_g = 150 s, $\dot{Q}_{max}$ = 4 MW

Ultra-fast: $\dot{Q}$ experimental, $t_g \approx 70$ s, $\dot{Q}_{max}$ = 1 MW

In above, Q_0 = 1 MW. The targeted peak HRR of the t^2 fires was set 4 MW which was considered realistic value for apartment fires [11] and sufficiently high to consume the O_2 in the compartment and hence yield a physically relevant duration and yield of combustion products.

RESIDENTIAL CASE STUDY RESULTS AND DISCUSSION

Pressure in the fire apartment

Figure 6 presents the simulation results for the fire compartments pressure in the most severe conditions, i.e. when the building envelope is very air-tight and the dampers are closed on both supply and exhaust ducts. Overpressure peak is shown to depend very strongly on the fire growth rate: While the pressure in the medium fire remains below 1000 Pa, the fast and ultra-fast fires reach 3000 Pa and 7000 Pa pressures. It is obvious, that the structure would not withstand such pressures. The negative peaks are much more modest. They are, however, associated with much higher uncertainty than the overpressures.

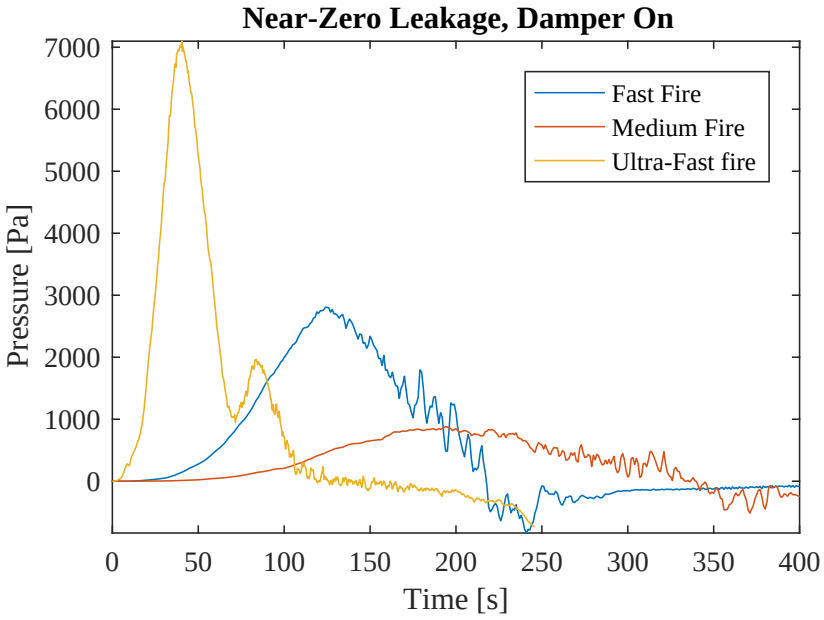

Fig. 6. Effect of fire type on pressures

The observed peak pressures are summarized in Fig. 7. These results were not corrected for the estimated model bias of - 7 %. The trends in the results are clear and consistent. All the three parameters - fire growth rate, damper configuration and air-tightness - are found to be important for the expected peak pressure. Interestingly, the sensitivity of the pressure to the parameter values seems to increase when moving towards a scenario with higher pressure. For instance, the damper configuration is not very important in traditional and normal buildings, but can become crucially important very air-tight buildings. The results of Fig. 7 were found to be independent of the fan operation (on or off) and the position of the fan unit's damper. This means

that the leakages through the other apartments can compensate for the fan pressure differences and complete closing of the ventilation system. Of course, this means that smoke will spread to the other apartments through the network.

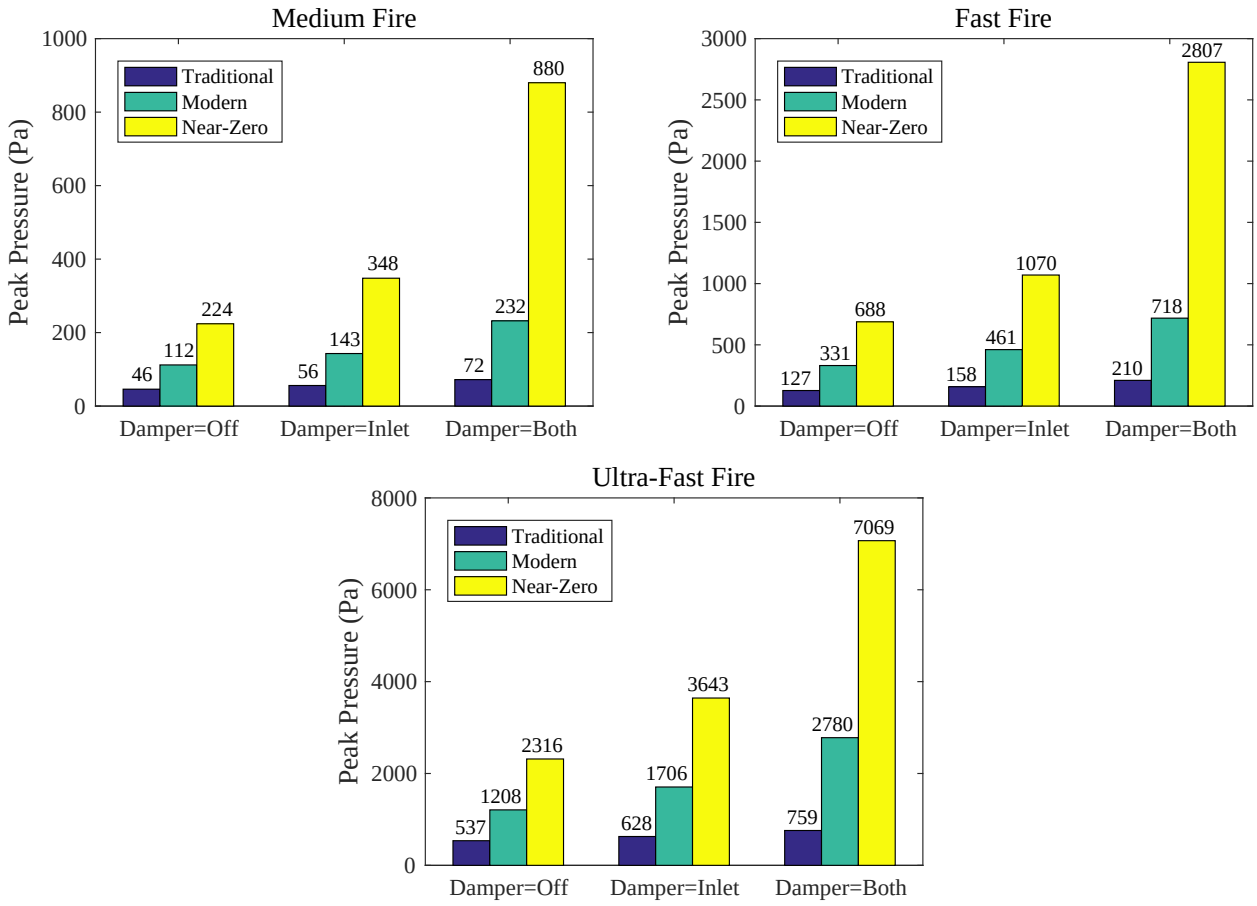

Fig. 7. Simulations Peak Pressures Bar Plots

From the viewpoint of the occupants possibility to escape from the fire apartment, we want ot compare the overpressure against an appropriate threshold. Here we assume that the door opening is not possible if the overpressure is more than 100 Pa. In design purposes, the pressure difference limit is usually 50 Pa, but for the risk analysis we choose a less conservative value. Based on the observed peak pressures, the door opening is possible in traditional buildings if the fire growth rate is medium. For more air-tight buildings and faster fires, the door opening would be challenging. It is, however, important to notice that these were just the momentary peak pressures, and do not tell much about the time duration when (how soon and how long) the door opening would be difficult.

Challenges for the structural integrity can be expected in fast or ultra-fast fires. If we choose the failure criterion based on our own experimental observation (1500 Pa), the fast fires could pose a risk when the dampers are closed and the envelope is very airtight. This could be the situation in Near-Zero or high-rise buildings. In fires that develop even faster, problems would be expected in all modern buildings whenever dampers are used. In very air-tight buildings, the capacity of the ventilation network is not sufficient to relief the pressures even if no dampers are used. Possible means for pressure relief should be investigated there.

Smoke spreading through the ventilation network

Based on the above pressure results it seems that open ventilation ducts could be used as a potential path of pressure relief at least in the buildings built according to the current air-tightness expectations, and in very air-tight buildings with modifications. The possibility of smoke spread to the other apartments and the resulting loss of compartmentation becomes then an issue. Figure 8 visualizes the smoke concentration in the neighbouring apartments 170 s from the ignition. If no dampers are used, the smoke spreads to the neighbours

regardless of the fan operation. The third figure corresponds to a situation where the damper is used only on the inlet side and the exhaust ventilation fan is kept running. Interestingly, the smoke is not spreading to other apartments in this case. Obviously, the cases with both dampers operating can be expected to be safe in this respect.

A more quantitative presentation of the same results is given in Fig. 9 showing the minimum visibility over the entire fire duration in the different combinations. The red horizontal bars show the median values from all the neighbouring apartments, and the boxes indicate a “typical range”. The visibility values get down to few meters in all cases without any dampers, and closing the fan reduces the visibility down to about two meters. Making the building more air-tight increases the amount of soot in the neighbours and reduces the visibility. In the simulations with fan operating and damper only on the inlet side, smoke is not observed in the neighbours. If the inlet side is open, the operating fan makes the situation worse as the fan pressure head prevents smoke from escaping through the inlet branch.

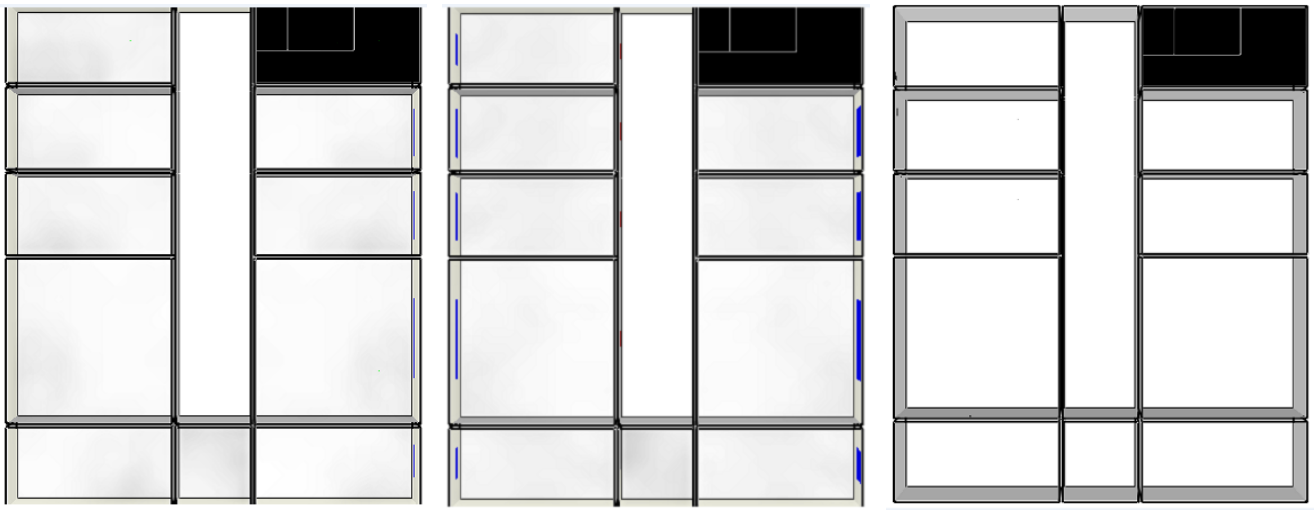

(a) Fan = Off, Dampers = Off (b) Fan = On, Dampers = Off (c) Fan = On, Dampers = Inlet

Fig. 8. Visualization of smoke concentration 170 s after ignition.

CONCLUSIONS

We used previously published experimental results and carried out new fire experiments to understand the pressure development in fires taking place within closed but mechanically ventilated compartments. We then used the experimental data to validate fire modelling, including the modelling of HVAC systems and building envelope leakages. Using the validated modelling, we investigated the influence of the damper configuration, envelope air-tightness and fire growth rate on the pressures and smoke spreading to neighbouring apartments in a mechanically ventilated building with many apartments.

Experimental overpressure peaks as high as 900 Pa were observed in a heptane pool fires and 1650 Pa in a polyurethane fires. The overpressure was found to decrease when the gas temperature stopped increasing. Based on the experimental results we can make the following conclusions:

1. High overpressure can prevent the apartment occupants from escaping through an inwards-opening door. This risk has not been identied before, and should be taken into account when designing the evacuation safety.

2. Fire induced pressures were found to damage a light-weight structure of the apartment. This possibility should be considered in the future as well.

The numerical simulations of the apartment building fire scenarios showed that the peak overpressure is sensitive to the damper configuration, envelope air-tightness and fire growth rate, but practically independent

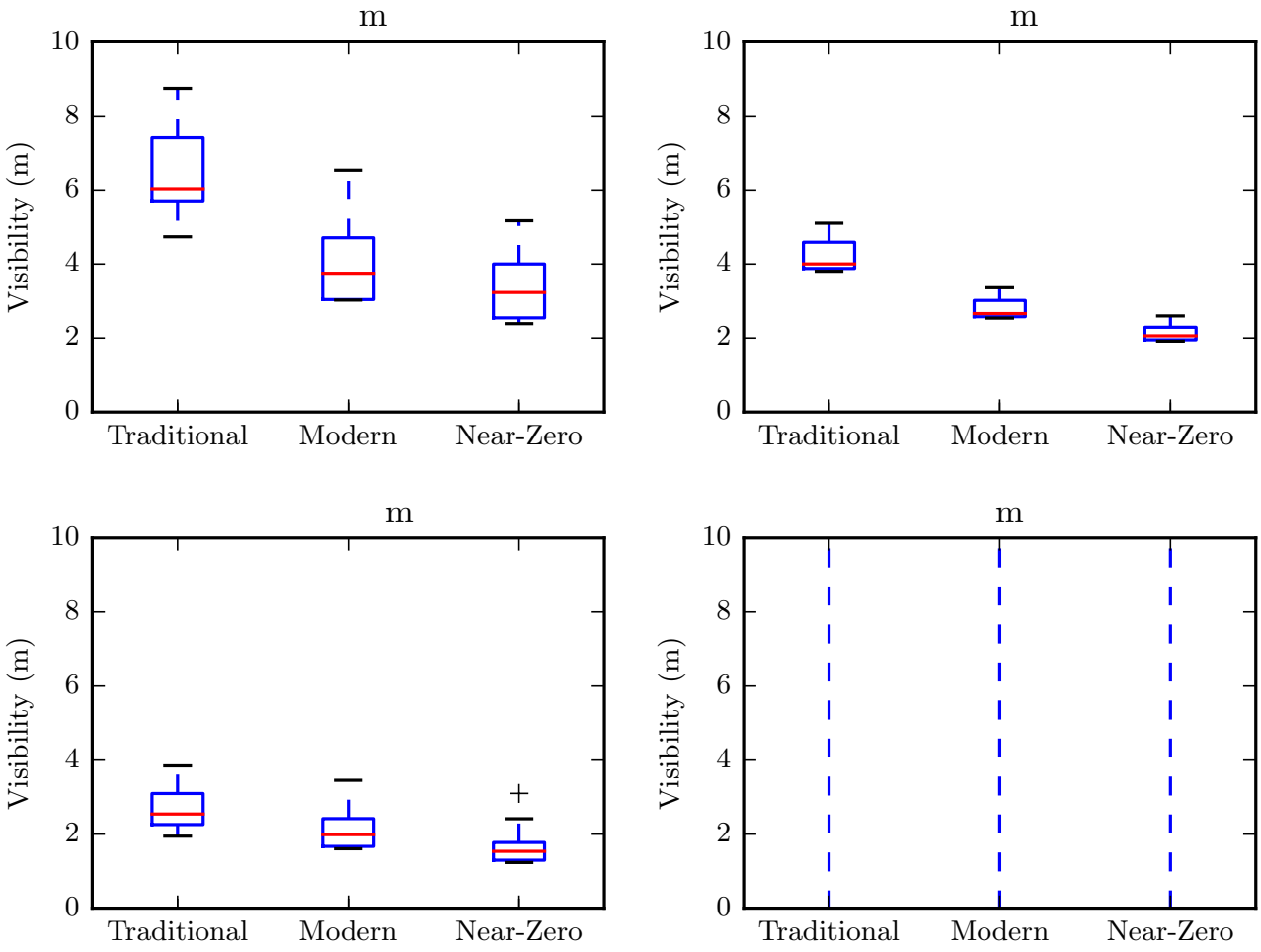

Fig. 9. Minimum visibility in neighbouring apartments

on the fan operation. The pressure was found to increase with improving air-tightness (reduced leakage), increased use of fire or smoke dampers, and the increased rate of fire growth. The peak pressures were found to be sufficiently high to prevent escape through an inwards-opening door in modern, air-tight buildings. However, more work is needed to quantify the actual risk by comparing the evacuation time-line with the timing of the dangerously high pressures. The risk of structural damage was found to exist with fast and ultra-fast growth rates. With fast fire development, the risk of structural damage was limited to the very air-tight buildings with dampers installed in both inlet and exhaust ducts. With ultra-fast fires, such as the heptane pool fire, the very air-tight building would be at risk regardless of the damper configuration, and the buildings according to the current practice whenever even one of the ventilation ducts is closed by a damper.

The simulations of the different damper configurations and fan operation modes showed that the smoke spreading to the neighbouring apartments can be avoided if only the inlet ventilation branch is closed with a damper and exhaust fan is kept at running. This mode of operation was found to be the only combination where the smoke spread can be prevented, simultaneously maintaining the pressure at acceptable level. The situation can of course be improved by introducing additional technical means of pressure management. These should be among the future applications of the newly developed simulation capability.

References

[1] Forneau, C., Delvosalle, C., Breulet, H., Desmet, S., and Brohez, S., (2012) "Comparison of fire hazards in passive and conventional houses," *Chemical engineering Transactions*, 26:375-380, http://dx.doi.org/10.3303/CET1226063

[2] Mowrer, F.W. "Enclosure Smoke Filling and Fire-Generated Environmental Conditions," *The SFPE Handbook of Fire Protection Engineering, Fifth ed.*, Hurley, M.J. (ed.), Society of Fire Protection Engineers, 2016. pp. 1066-1101. http://dx.doi.org/10.1007/978-1-4939-2565-0

[3] McGrattan, K.B., McDermott, R., Floyd, J., Hostikka, S., Forney, G. and Baum, H., (2012) "Computational fluid dynamics modelling of fire," *International Journal of Computational Fluid Dynamics*, 113.

[4] Floyd, J. "Coupling a Network HVAC Model to a Computational Fluid Dynamics Model Using Large Eddy Simulation." *Fire Safety Science – Proceedings of the Tenth International Symposium*, International Association for Fire Safety Science, 2011, pp. 459-470.

[5] McGrattan, K., Hostikka, S., McDermott, R., Floyd, J., Weinschenk, C., and Overholt, K., "Fire Dynamics Simulator, Technical Reference Guide, Volume 3: Validation," National Institute of Standards and Technology, Gaithersburg, Maryland, USA, and VTT Technical Research Centre of Finland, Espoo, Finland, sixth edition, November 2015.

[6] Wahlqvist, J. and van Hees, P., (2013) "Validation of FDS for large-scale well-confined mechanically ventilated fire scenarios with emphasis on predicting ventilation system behavior," *Fire Safety Journal*, 62 B:102-114.

[7] Hgglund, B., Nireus, K., and Werling, P., "Pressure rise due to fire growth in a closed room. Description of three full-scale tests," FOA Defence Research Establishment, FOA-R-96-00347-2.4-SE, 1996. 27 p.

[8] Hgglund, B., Nireus, K., and Werling, P., "Pressure rise due to fire growth in a closed room. An experimental study of the smoke spread via ventilation ducts," FOA Defence Research Establishment, FOA-R-98-00870-311-SE, 1998. 97 p.

[9] Janardhan, R.K. and Hostikka, S. (2016) Experiments and numerical simulations of pressure effects in apartment fires, *Fire Technology*, submitted for review, http://www.arxiv.org/.

[10] Vinha, J., Manelius, E., Korpi, M., Salminen, K., Kurnitski, J., Kiviste, M. and Laukkarinen, A. (2015) *Building and Environment* 93:128-140. http://dx.doi.org/10.1016/j.buildenv.2015.06.011

[11] Blomqvist, P., Rosell, L., Simonson, M., "Emissions from Fires Part II: Simulated Room Fires," SP Swedish National Testing and Research Institute, Bors, Sweden.

D. PFS Simulations of the apartment case study

Tomas Fagergren

Project name	Apartment case studies – Aalto University	**Project number**	-
Document author	Tomas Fagergren	**Document reviewer**	-
Project owner	-	**Date**	2016-10-31

Apartment case studies – Aalto University

PFS program

The PFS program flow system can calculate almost any static flow system. The flow system is described with a simple sketch. Double lines are used describe flow paths. Short texts connected to the double lines define different flow path properties. Single lines are used to describe volumes connecting a number of flow paths. A flow path can be rather general and does not have to be a proper duct or pipe. The media can be air, water, other fluids or compressed gases.

A main idea with the program is that the sketch as a text file should be self-documenting. The result text file is equal to the input text file with added result print outs. Another idea is that different components such as fans, pumps, dampers, valves or heaters should be defined by a single line.

The program has been documented in a number of manuals and reports about the program language, the operation of the program and a large number of application examples. All manuals and reports except two are however in Swedish.

The program can be run under Windows. The program consists of a user interface for Windows pfs.exe written in C++ by Jonny Roos (2001) as a master thesis work and a solver sfs.dll written in Fortran by Lars Jensen (1995) (professor at LTU) and developed ever since assisted by Kurt Källblad.

Conditions – case studies

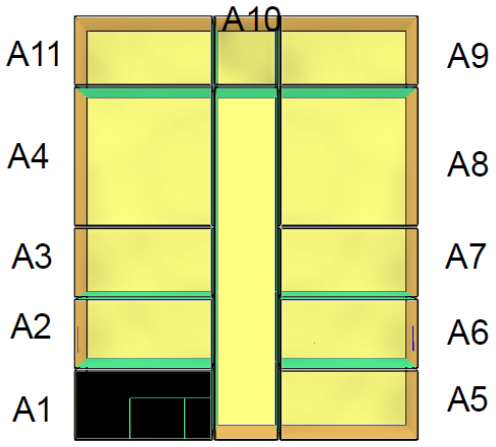

Box 9196 Långholmsgatan 27 10 tr 102 73 Stockholm 08-588 188 00 brandskyddslaget.se
info@brandskyddslaget.se Org nr: 556634-0278 Innehar F-skattebevis

- ***Rum A1*** is the fire room. 50 m^2, h 2,5 m.
  Leak for 50 m^2 room, 0.036, 0.073 and 0.146 m^3/s – 50 Pa. Assumed the same leakage for each room, A1, A2, A3, A4, A5, A6, A7, A8, A9, A10, A11.
  Small rooms 50 m^2, large room 100 m^2.
- Mechanical ventilation, 40 l/s (balanced) in each room, A1, A2, A3, A4, A5, A6, A7, A8, A9, A10, A11.
  Ductings, circular 125 mm to the rooms and circular 250 mms in the corridor.
  The internal pressure losses for AHU, 150 Pa – 440 l/s.
  Fan curve, 750 Pa - 0 flow, 450 Pa - 300 l/s, 0 Pa - 650 l/s
- Fire
  Medium 0,012 kW/s^2, fast 0,047 kW/s^2, average temperature assumed to +250 degree Celsius

Cases – fire in room A1

Medium 0,012 kW/s^2, leak - 0.036 m^3/s

1. Normal conditions, fan is on (no fire).
2. Fan is on, fire.
3. Fan is on, a small gap of the window in room A10 is open.
4. Fan is on, dampers are closed in the supply air to room A1.
5. Fan is off, dampers are open in the AHU.
6. Fan is off, dampers are closed in the AHU.
7. Fan is off, dampers are closed in the AHU, and a small gap of the window in room A10 is open.
8. Fan is off, dampers are closed in both supply air and exhaust air to room A1.

Fast 0,047 kW/s^2, leak 0.036 m3/s

9. Normal conditions, fan is on (no fire), the same result as in case 1.
10. Fan is on, fire.
11. Fan is on, a small gap of the window in room A10 is open.
12. Fan is on, dampers are closed in the supply air to room A1.
13. Fan is off, dampers are open in the AHU.
14. Fan is off, dampers are closed in the AHU.
15. Fan is off, dampers are closed in the AHU, and a small gap of the window in room A10 is open.
16. Fan is off, dampers are closed in both supply air and exhaust air to room A1.

All cases in the same PFS model

17. All cases above in the same model with a table function, made by Lars Jensen.

Summery

Medium

Case	Pressure, room A1	Exhaust fan, operating point	Supply fan, operating point	Exhaust flow, room A1	Supply flow, room A1	Exhaust flow, room A10	Supply flow, room A10	Smoke spreading to other rooms
1	0 Pa	283 Pa, 440 l/s	283 Pa, 440 l/s	40 l/s	40 l/s	40 l/s	40 l/s	-
2	770 Pa	207 Pa, 454 l/s	283 Pa, 349 l/s	129 l/s	148 l/s reverse direction	33 l/s	50 l/s	Yes
3	769 Pa	208 Pa, 453 l/s	294 Pa, 350 l/s	129 l/s	148 l/s reverse direction	34 l/s	50 l/s	Yes
4	1683 Pa	215 Pa, 457 l/s	256 Pa 397 l/s	186 l/s	0 l/s	27 l/s	40 l/s	No
5	736 Pa	78 l/s	93 l/s reverse direction	120 l/s	161 l/s reverse direction	5 l/s reverse direction	6 l/s	Yes
6	749 Pa	0 l/s	0 l/s	120 l/s	161 l/s reverse direction	13 l/s reverse direction	15 l/s	Yes
7	746 Pa	0 l/s	0 l/s	120 l/s	160 l/s reverse direction	35 l/s reverse direction	25 l/s	Yes worst case - medium
8	4673 Pa	0 l/s	0 l/s	0 l/s	0 l/s	0 l/s	0 l/s	No

Fast

Case	Pressure, room A1	Exhaust fan, operating point	Supply fan, operating point	Exhaust flow, room A1	Supply flow, room A1	Exhaust flow, room A10	Supply flow, room A10	Smoke spreading to other rooms
9	Same as case 1							
10	2411 Pa	161 Pa, 476 l/s	316 Pa, 282 l/s	219 l/s	280 l/s reverse direction	56 l/s	26 l/s	Yes
11	2407 Pa	167 Pa, 469 l/s	313 Pa, 286 l/s	220 l/s	280 l/s reverse direction	60 l/s	15 l/s reverse direction	Yes
12	5491 Pa	166 Pa, 474 l/s	250 Pa, 379 l/s	329 l/s	0 l/s	15 l/s	38 l/s	No
13	2364 Pa	140 l/s	168 l/s reverse direction	215 l/s	288 l/s reverse direction	12 l/s reverse direction	8 l/s	Yes
14	2404 Pa	0 l/s	0 l/s	214 l/s	286 l/s reverse direction	27 l/s reverse direction	24 l/s	Yes
15	2395 Pa	0 l/s	0 l/s	215 l/s	287 l/s reverse direction	63 l/s reverse direction	44 l/s	Yes worst case - fast
16	15034 Pa	0 l/s	0 l/s	0 l/s	0 l/s	0 l/s	0 l/s	No
17	All cases , 1- 16, in the same model with a table function, made by Lars Jensen							